# A FAST ATOM BOMBARDMENT MASS SPECTROMETRY STUDY OF TRIS(3,6-DIOXAHEPTYL)AMINE-ALKALI METAL HALIDE COMPLEXES AND HYDROGEN BONDED COMPLEXES

Roger Théberge, B. Sc.

A thesis submitted to the
Department of Chemistry
in partial fulfillment of the requirements
for the degree of
Master of Science

Brock University,
St. Catharines, Ontario
July, 1987

To my parents for their love and
unrelenting support
And in the memory of those who passed away tragically
on october 19, 1986 (especially France)

## Abstract

The objective of this thesis was to demonstrate the potential of fast atom bombardment mass spectrometry (FABMS) as a probe of condensed phase systems and its possible uses for the study of hydrogen bonding. FABMS was used to study three different systems. The first study was aimed at investigating the selectivity of the ligand tris(3,6-dioxaheptyl) amine (tdoha) for the alkali metal cations. FABMS results correlated well with infrared and nmr data. Systems where a crown ether competed with tdoha for a given alkali metal cation were also investigated by fast atom bombardment. The results were found to correlate with the cation affinity of tdoha and the ability of the crown ether to bind the cation.

In the second and third studies, H-bonded systems were investigated. The imidazole-electron donor complexes were investigated and FABMS results showed the expected H-bond strength of the respective complexes. The effects of concentration, liquid matrix, water content, deuterium exchange, and pre-ionization of the complex were also investigated. In the third system investigated, the abundance of the diphenyl sulfone-ammonium salt complexes (presumably H-bonded) in the FABMS spectrum were found to correlate with qualitative considerations such as steric hindrance and strength of ion pairs.

## Acknowledgements

I would like to express my deep gratitude to Dr J.M. Miller for his guidance, help, and advice. His supervision has made my stay at Brock fruitful and enriching. My heartfelt thanks to Tim jones for his patience (with me and the mass spectrometer), and willingness to help. Thanks to Dr M.F. Richardson for some helpful discussions on coordination chemistry.

I cannot forget my very good friends, Steve and Benny, for our 'scanning' forays and discussion of other enthralling topics (including chemistry). Jim, I thank you for your time, patience, compassion, and wisdom at a time when it was most needed. Bea, the fights, bites, and chases were most appreciated. Thank you Chris, for your love, support, and cheerfulness at all times. You made it a lot easier.

Grand merci à Boris Vian pour avoir écrit 'Vercocquin et le plancton' (surtout le chapitre 4) qui m'a donné le goût de rire quand je ne m'en pensais plus capable.

'Fluctuat mercmurgitur'

## Table of Contents

## List of Tables

## List of Figures

# I. INTRODUCTION

## A. FAB and SIMS

In the past, a chemist studying thermally labile, involatile, and polar molecules had to regard mass spectrometry as a technique whose success was limited. This was due mainly to the fact that achievement of optimal results in mass spectrometry is highly dependent on the method of ionization and on the method of sample introduction.

However, the advent of new ionization techniques has greatly enhanced the scope of mass spectrometry to compounds previously not amenable to study by it. Fast atom bombardment mass spectrometry (FABMS)[1] is probably the most important of the new ionization techniques because of its simplicity, adaptability, versatility, and relatively low cost. FAB involves the bombarding of a sample in a liquid matrix, with a neutral beam of atoms having energies of 2-8 KeV to obtain sputtered negative and positive ions. The ionization process and inlet techniques are combined. FAB can be considered an outgrowth of Secondary Ion Mass Spectrometry (SIMS) which uses 2-8 KeV ions without a matrix liquid.

Although the techniques rely on the same principle, the extension of SIMS to solid organic samples proved to be difficult owing to extensive radiation damage. Benninghoven[2] provided the first solution to this problem by reducing the

flux of the primary ions (bombarding particles) and adjusting the angle of incidence on the target. However, the use of a low beam flux means that the sample ion current is reduced to the point where integration of the signal over 5-30 minutes is necessary to produce analytically useful results.

Fundamentally, the use of a neutral atom beam is a minor difference since Benninghoven[3] has demonstrated that the charge (+ve, 0ve, or -ve) of the bombarding particle has no effect on secondary ion emission. Furthermore, a neutral beam had previously been used for organic and inorganic analysis[4].

The second and most significant difference resides in sample preparation. In FAB, the sample is usually dissolved in a liquid matrix of low vapour pressure (glycerol is the most common and versatile). When this solution is exposed to the bombarding particles, the sputtered sites on the matrix surface are continually replenished with analyte by the process of diffusion.

The terminological polemics concerning FAB and SIMS have not ended. Although the term FAB is somewhat a conveyor of misinformation[5], the root of the problem is the lack of a definite convention with respect to the meaning of the term FAB. The term liquid SIMS has been proposed as an alternative.

## B. The FAB Method

The FAB method involves, first and foremost, providing a mass spectrometer with an atom gun. A beam of fast atoms is produced by ionizing the atoms, accelerating them through a potential (typically 2-8 KeV), and finally allowing the fast ions to be neutralized through resonant gas phase charge exchange.

The remaining ions can be eliminated by an electrostatic deflecting plate. (There are many designs of atom guns[6], but the concern here is with the most common and widespread types which use rare gases [Ar, Xe] as their source of atoms.)

The fast atom beam is then intercepted by the sample which is mounted on a metal target attached to a direct insertion probe. The position of the probe tip is such that the beam produces a 60 degree angle with respect to the normal of the probe tip surface and maximizes sputtering into the mass spectrometer. The various geometrical requirements for different target configurations have been examined by Perel.[7]

The resulting ions sputtered from the sample are then extracted by collimating and focussing electrodes to the mass spectrometer. The angle of incidence is critical as it is sensitivity related[8]. The collision of bombarding atoms with the sample imparts energy to the sample atom which recoils with sufficient energy to generate a collection of low energy

secondary recoil molecules. It is the concerted movement of these recoil molecules which provides enough energy to overcome the surface barrier. This is the so-called linear collision cascade mechanism. In light of this mechanism, another factor enhancing the sputter yield (sensitivity) is the mass of the bombarding atom[8]. An increase in the mass of the bombarding atom increases the amount of energy imparted to the sample by the beam. Xenon, for example, offers a sensitivity that is approximately three times greater than Argon which is the most routinely used bombarding atom. Mercury[9], siloxane fragments[10] (a diffusion pump fluid), and cesium[11] are amongst a wide variety of bombarding particles that have been experimented with in the need to achieve high sputtering yield with high signal to noise ratio. The use of liquid metal ion sources[12] has been experimented with but the impact of these devices cannot be assessed at this time because of their limited use.

## C. Instrumentation.

Although a variety of primary ion sources are available for FABMS, by far the most widespread gun designs are the gas fed sources based on the saddle field[13] and the capillaritron[14]. The advantage of the FAB source is that it can be retrofitted to old or new instrument designs provided a suitable port onto which the atom gun can be mounted is available while still providing for a direct insertion probe.

It is also possible to have the gun mounted on the direct insertion probe.

The main modifications necessary concern a more efficient ion source pumping system (to remove gas from the atom gun and evaporated matrix) and wide spacing of the collimating and focusing electrodes to allow for the greater dispersion of the sputtered ions. A high mass magnet is generally desirable to exploit the high mass ions generated by FAB.

Secondary ion mass spectrometer design considerations[15a] and FABMS guns[15b] are discussed in a recent ACS symposium series volume. The author discussing the former topic states that the field is "still in its infancy [and that] most of the instrumental features outlined in this paper... have yet to be incorporated into present day machines, [that] most instruments currently being used have capabilities for SIMS [and FAB] far below those which are potentially available if currently available ion optical techniques were used."

The advantages of focussed primary ion beams and immersion lenses[16] for more efficient secondary ion extraction have been reported. The usefulness of a neutral atom beam (despite the fact that it is not entirely neutral) is still controversial as Magee stated that "for reasons that are unclear, the makers of magnetic sector organic SIMS instruments promulgate the mystique that it is difficult to direct a focussed ion beam into the sample region due to the

high electric fields present..."

## D. Matrix Liquids

Notwithstanding the potential misinformation imparted by the term FAB, the matrix liquid is the crucial innovative component of the technique. The fact that sensitivity can be changed by orders of magnitude by modifying the chemical environment of the matrix shows how crucial matrix chemistry is in FABMS. The publication of two recent reviews[17,18] on the subject signifies the importance of this component of FAB. Generally, there are a number of requirements which the matrix should fullfill to optimize FABMS results. The matrix should:

(1) Dissolve the sample

(2) Remain relatively involatile at ion source pressure and temperature

(3) Allow the sample to replenish the sites from which sputtering occurs i.e. the viscosity of the matrix should be low enough to ensure the diffusion of solutes to the surface.

(4) Be chemically unreactive toward the sample unless the reaction is one which is known or desired or which promotes simple ionization.

It was clear in the earliest FAB results[19] that optimal results were obtained with pre-formed ions. Watson et al [20] have used UV in conjunction with FAB to show this. A

good correlation was observed between the degree of protonation indicated by the appropriate absorption bands of porphyrins and the abundance of the quasi-molecular ions $[M+H]^+$ in the FAB spectrum of the corresponding solution.

Pre-ionization in the matrix can be promoted in a number of ways. The addition of various agents such as acids or alkali metal salts can increase the secondary ion current. An example would be the cationization of the sample with alkali metal salts in the study of carbohydrates[21]. Silver complexes[22] have also been used because of their easily identifiable isotopic pattern.

Classical organic reactions can be used to produce cationic sample molecules. Quaternization of molecules containing a heteroatom has been used for amino, telluro, seleno, and thio derivatives[23]. Girard's p reagent can be reacted with ketones and aldehydes to form a pyridinium salt. Primary amines can be converted into pyridium salts by pyrillium[24] derivatives. The limitations of these methods are the same as those of a classical derivatization reaction, those being a good yield and a relatively easy experimental procedure. The means of promoting anion formation have received little attention so far. This type of reverse derivatization is opposite to derivatization procedures of conventional mass spectrometry which seeks to produce more volatile and non-polar compounds. To efficiently sputter these pre-formed ions, a liquid matrix possessing a high dielectric constant seems logical since it will seperate these

ion pairs. Thus, where pre-formed ions are present, a high dielectric constant matrix might be a general requirement.

Many liquid matrices are mixtures using a co-solvent to remedy solubility problems encountered. For example, glycerol/dimethylformamide mixtures were used as a liquid matrix to obtain spectra of 4,4'-disubstituted 2,2'-bipyridine tetracarbonylmetal complexes of molybdenum and tungten[25].

For maximum sensitivity, the sample should form a perfect monolayer at the surface of the matrix liquid. Under monolayer conditions, ions due to the matrix liquid should be totally suppressed.

There are two drawbacks to the use of a matrix liquid. First, where monolayer conditions cannot be achieved, the liquid matrix may generate peaks which could complicate spectrum interpretation. In this case, peaks due to the matrix and to adducts formed by the matrix may appear in the spectrum. The second complication involves chemical interaction between the sample and the matrix where the sample may be decomposed by matrix. Finding compatible matrix-sample combinations can require substantial experimentation.

Apart from glycerol (the most common and versatile matrix liquid) many other matrix liquids have been experimented with. for example, crown ethers, 2-nitrophenyl octyl ether, meta-nitrobenzyl alcohol, thioglycerol, diethanol amine, tetramethylene sulphone, and polyphenyl ethers (diffusion pump oil) to name a few. Their efffectiveness is intrinsically related to their ability to fulfill the general

requirements mentionned earlier. The development of a FABMS continuous flow probe[26] has allowed a significant increase in the water content of the matrix (80% water/20% glycerol). It has been shown that the more aqueous nature of the matrix leads to a significant increase in the sensitivity of detection of some bio-organic compounds[27].

## E. FABMS Aplications to Solution Chemistry

One of the key features of the FAB method is the use of a liquid matrix, most commonly glycerol or glycerol/solvent mixtures. Despite this, the potential of FABMS as a technique for the study of condensed phase systems has been underestimated and relatively unexplored. Thus, the second advantage (though some see it as a disadvantage) of a liquid matrix is that it allows solution chemical reactions and equilibria to be studied as part of the analytical process.

In one of the first solution chemistry applications of FABMS, Caprioli was able to determine the apparent dissociation constants of weak acids in solution[28]. Despite some inherent limitations compared to published values in pure aqueous systems (the presence of glycerol, a lower dielectric constant component), the results are significant. Caprioli also monitored the progress of an enzyme-catalyzed reaction by measuring the relative abundances of selected ions present in

the FAB mass spectra of reaction solutions[29]. Johnstone and co-workers have correlated ion abundances in FAB spectra with changes in solution concentrations of cation-crown ether complexes[30]. A mixture of macrocyclic ligand, glycerol, and water was used as the liquid matrix. It was found that the variations in ion abundances corresponding to metal cation-ligand complexes closely paralled published stability constants. This study is of particular importance since the methods used for the investigation of complexation between macrocyclic or acyclic polyethers and metal cation tend to be cumbersome and usually require calorimetry, potentiometry, or absorption spectroscopy for the determination of stability constants.

The authors also measured the cation affinity of the macrotetralide antibiotic nonactin for $Na^+$ and $K^+$. The measured complex ratio of [ligand-$Na^+$]/[ligand-$K^+$] was 1:17 which closely matched the published value of 1:19 (30°C in methanol).

Kalinoski et al [31] have investigated the use of FABMS as a probe of condensed phase chemistry. In their study, FABMS was used in conjunction with their synthetic efforts to elucidate complex organometallic reactions of aryl and hetrocyclic mercuric acetates with chiral furanoid and pyranoid glycals (cyclic enol ethers). The direct reaction mixture FABMS analysis showed that the principal ions in the FAB spectra accorded closely with species postulated on the basis of product isolation studies and mechanistic

considerations. The authors were cautious as to the significance of their results but nonetheless acknowledged that FABMS is full of promises as an effective tool for the elucidation of complex organometallic reaction mechanisms.

Saito and Kato[32] detected short-lived glutathione conjugates of an aryl nitroso carcinogen by performing the reaction in a glycerol matrix with subsequent FABMS analysis. Negative ion FABMS was used to study the reaction of boronic acids with triols, sugars, and nucleosides *in situ* on the probe of the mass spectrometer[33]. Boronic acids react with trifunctional compounds having the appropriate configuration to give 5 to 8 membered ring boronate cage compounds that are negatively charged.

Benzene boronic acid was dissolved with glycerol, thioglycerol, 3-aminopropane-1,2-diol, and triethanol amine, then analysed by FABMS to give the negatively charged cage complex. Because the stability of the complex depends on the orientation of the reacting functional groups, it was concluded that the method has use for configurational analysis of the appropriate polyfunctional natural products and in increasing the sensitivity with which such compounds can be detected (a case of reverse derivatization).

Smith *et al* [34] have demonstrated that enzymes could remain active in glycerol/water mixtures on the probe tip within the mass spectrometer provided exposure to the fast atom beam was limited to 6X30 seconds stints over a period of 30 minutes. The hydrolysis of p-toluenesulphonyl-L-arginine

methyl ester (TAME) by the enzyme trypsin was monitored by FABMS. The course of this reaction was followed over 24 minutes and the peak due to the reactant diminished in favour of the free acid with time.

FABMS was used to measure accurately the rates of enzymatic reactions and these rates were then used to calculate kinetic parameters of the reaction[35]. In these studies, the removal of aliquots from the batch reaction with time for FABMS analysis was preferable since it circumvented the problem of variations in the reaction mixture if it stayed in the high vacuum environment of the mass spectrometer as in 'real time' analysis. The recent advent of FAB flow probes will now permit continuous sampling of reaction solutions.

Pedzer and De Pauw[36] have reported redox processes in LSIMS (liquid SIMS) and FABMS of glycerol solutions. They point out that the relative intensity of ions due to the reduction of $Fe^{+3}$, $Cr^{+3}$, and $Cu^{+2}$ (as glycerol adducts) reflects their relative redox potentials. Of particular interest was the reduction of cationic organic dyestuffs form a quinoid to semi-quinoid species. The experimental results were qualitatively interpreted in terms of the standard redox potential scale. A further study[37] with other dyestuffs confirmed the results of the previous study.

The development of a continuous-flow FABMS probe will allow the use of matrix liquids much more volatile than are currently used. This could go a long way in alleviating the problems that arise from the limited number of liquid matrices

available. The main advantage of the technique is that it will allow the use of matrix liquids with a high aqueous character (up to 90% water).

To conclude, the most significant sign to date for the acceptance of FABMS as a probe for the study of condensed phase systems is the latest specialists periodical report on mass spectrometry[38] which briefly discusses the FABMS applications to solution chemistry.

## ELECTROHYDRODYNAMIC IONIZATION

The only other mass spectrometry technique that has been applied to solution chemistry is EHMS (electrohydrodynamic mass spectrometry)[39]. Electrohydrodynamic ionization is another modification of the field ionization technique. Electrohydrodynamic ionization extracts preformed ions directly from solution using a strong applied electric field imparting little or no internal energy to the sampled ions. Thus EHMS spectra are usually devoid of fragmentation.

A first study involved $(bipyridyl)_3$ M ($M=Ru^{+2}$, $Cr^{+2}$) complexes sampled from glycerol solutions. As expected on the basis of relative lability, only the $(bpy)Cr^{+2}$ complex gave evidence of oxidation and ligand exchange (with chloride counter ion and glycerol solvent).

The formation of metal ion complexes of 18-crown-6 were investigated with EHMS. The relative abundances

adduct ions followed expectations based on adduct stabilities reported provided that competing ions were of the same charge. For example, divalent metal ions were more strongly solvated, indicating greater solvent interactions and hence a larger potential barrier to field evaporation. A similar case was the $Li^+$ complex, for which EHMS had a low sensitivity. This was probably due to the lithium ion's high charge density and thus its strong ion-pairing and solvent interaction potential. This low EHMS sensitivity was interpreted as consistent with solution behavior rather than gas phase chemistry.

Thus, EHMS can be complicated by the difficulty in obtaining reproducible emission for some solutions and by the variability of ion sampling anddetection efficiencies(sensitivity). Limitations in this respect are due to ion-pairing and charge density effects. Furthermore, EHMS requires solutions with low volatility and high conductivity.

## G. Mass spectrometry and hydrogen bonding

Hydrogen bonding has been studied by both spectroscopic and non-spectroscopic techniques[42]. However, the use of spectroscopic techniques has become dominant in recent years and infra-red, nuclear magnetic resonance, ultra violet, and photoelectron spectroscopy have been used successfully for the study of hydrogen bonding. Save for high

pressure methods[43] and ion cyclotron resonance[44], mass spectrometry has been largely ignored for the study of hydrogen bonding.

The traditional ionization method of electron impact requires volatilization of the sample and bombardment with a 70eV beam of electrons, the combination of which rules out the use of EI for the study of hydrogen bonded complexes. In general, the hydrogen bonded complexes studied by ICR and high pressure mass spectrometry are the result of ion-molecule reactions. This limits those methods to compounds volatile enough to create the pressure required for the ion-molecule reactions to occur.

Despite the routine appearance in FAB spectra of glycerol (or any other matrix capable of inter molecular H-bonding) dimers and oligomers, presumably held by H-bonding, the potential of FABMS for the study of H-bonding has been virtually ignored. Miller and Clark[45] have observed the H-bonded complex of imidazole and trimethyl phosphate with FABMS. IR, $^{15}N$ nmr, and X-ray crystallographic data support a strong, easily polarizable H-bond in the complex. The nature of the information obtained by FAB is complementary to that obtained with other 'fast' analytical techniques such as nmr and IR. The authors suggest that the application of FABMS to the analysis of hydrogen bonded complexes may well become a routine analytical method for the study of strong hydrogen bonding.

## 7. Scope of the thesis

The objective of this thesis is to demonstrate the ability of FAB to monitor the solution behavior of condensed phase systems and its uses for the study of hydrogen bonding. The work performed can be seperated in three parts; the last two being somewhat intrinsically related.

### i) Tris(3,6-dioxaheptyl)amine alkali metal cation complexes

Complexes formed in solution between polyethers and metallic cations have been widely studied because of their excellent selective transport properties. We have studied the complex formation between tris(3,6-dioxaheptyl)amine (tdoha, industrial name TDA-1) and alkali metal cations using FABMS. In light of the controversy surrounding the ability of FABMS to give an accurate picture of solution behavior, we have obtained IR and NMR data supporting our FABMS results. Systems in which a crown ether and tdoha competed for an alkali metal cation were also investigated.

### ii) Hydrogen bonded complexes of imidazole with various electron donors

As mentionned earlier the FABms of the H-bonded complex of imidazole and trimethyl phosphate was reported and an ion corresponding to the complex observed. A further study of H-bonding to imidazole with a range of electron donors of

varying strength using FABMS was carried out. The effect of matrix liquid, concentration, and water content on the H-bond were investigated.

iii) Multiply H-bonded cationic complexes

In hope of increasing the strenght of H-bonded complexes as well as their FABMS sensitivity, multiply H-bonded cationic complexes were studied. It was hoped that complexes with multiple H-bonds would be more stable and thus increase the likelyhood of detection using FABMS. The effect of cationization is well documented and did enhance FABMS sensitivity as expected. The H-bonded complexes of protonated secondary amines and phenyl sulfones formed the bulk of this study. Other systems were investigated though not as extensively.

# II. Experimental

## A. Instrumental

The FABMS mass spectra were obtained using a Kratos AEI MS-30 double beam mass spectrometer (Kratos Ltd, Manchester, U.K.) retrofitted with a saddle field fast atom bombardment gun (Ion tech, Teddington, U.K.) and a Kratos FAB source in beam 1. Xenon and argon were the bombarding atoms and the energy of the beam was 6-8 Kev. Stainless steel probe tips were used. All spectra were acquired at a scan speed of 10 seconds per decade at full gain.

The accelerating voltage and resolution were kept at 4Kv and 1000 throughout, respectively. Data were collected as peak time centroid and mass convertion was done offline based on a tris(perfluoroheptyl)-s-triazine calibration. An interfaced Kratos DS-55 data system was used for data collection and manipulation. The PLOT program was used to obtain pictorial representation of the mass spectra. The QUAN program gave quantitative reports including peak masses and intensities in terms of % of base peak and % total ion current.

Infrared spectra were obtained using an Analect FX-6260 FT-IR at a resolution of $4cm^{-1}$. $^{1}H$ nmr were obtained using a Buker WP-80 and a Bruker AC 200 spectrometer.

## B. Tris(3,6-dioxaheptyl)amine

The saturated solutions of alkali metal halides were prepared and left to stand at 45 °C for at least 24 hours. The solution were then analysed by FABMS without a liquid matrix as tdoha is a liquid with a low vapor pressure. All spectra were peak averaged from a minimum of ten scans. The bombarding atom was xenon.

Infra-red spectra were recorded as thin films of the neat samples between KBr disks. The crude NaI-tdoha infra-red spectrum was obtained as a nujol mull. The $^{1}H$ nmr spectrum of tdoha and the NaI-tdoha complex were obtained in $[^{2}H_{6}]$DMSO on a Bruker WP-80. $^{19}F$ nmr spectra were obtained from the neat sample on a Bruker WP-60 (external lock). $CFCl_3$ was the external reference. $^{1}H$ nmr, $^{19}F$ nmr, and infra red spectra (except RbI-tdoha spectrum) were run by Dr S.J. Brown.

Crown ether-tdoha-alkali metal chloride solutions were prepared in approximately 1:1:1 molar ratio. This was done by weighing 0.5-1.0g of the alkali metal halide salt and adding equimolar amounts of the crown ether and tdoha in that order. FABMS spectra were obtained after standing for a minimum of 24 hours at 40 °C.

The crude NaI-tdoha complex was prepared from a saturated solution of NaI in tdoha. Precipitation of a brown solid was observed after heating the mixture to about 130 °C and allowing it to cool at room temperature. The dark brown

solid was washed with cyclohexane and diethyl ether. The resulting pale brown solid was hygroscopic and dried under vacuum (0.1 torr) at room temperature. Complex formation also appeared to occur when tdoha and NaI were mixed in a 1:1 molar ratio and left to stand for more than 48 hours. After 48 hours, the 1:1 NaI-tdoha mixture crystallized to a brown solid. $^{15}N$ nmr was attempted on a 1:1 molar solution of LiBr-tdoha with a Bruker AC 200 at a frequency of 20.287 MHz. The INEPT (insensitive nucleus enhancement by polarization transfer) sequence was used with $^{2}J_{(N-H)}$. The $^{2}J_{(N-H)}$ was estimated from literature data on aliphatic amines.

The tdoha/alkali metal halide and glycerol/water systems were prepared by dissolving about 0.10g of salt in 2 mL of 50/50 (v/v) glycerol/water solution. A molar equivalent of tdoha was then added to the mixture. The solutions were left to stand for a minimum of 24 hours prior to FABMS analysis. The competitive system, where equimolar amounts of alkali metal iodides competed for one molar equivalent of tdoha, was set up in a similar manner. The amounts of LiI, NaI, KI, RbI, and tdoha added were molar equivalents of 0.12g of CsI ($4.6X10^{-3}$ moles) dissolved in 5mL of 50/50 (v/v) glycerol/water solution.

The ligand tdoha was obtained from May and Baker. 18-crown-6, 15-crown-5, and 12-crown-4 were obtained from Aldrich. LiF, LiCl, LiBr, LiI, NaF, NaCl, NaI, KF, KCl, KBr, KI, RbF, RbI, CsF, CsCl, and CsI were obtained from BDH, Alfa, and Fisher scientific. All the above compounds were of

reagent grade and were used unpurified.

## C. Imidazole-electron donor complexes

The neutral hydrogen bonded complexes were prepared by dissolving 1.0g (0.015 moles) of imidazole in 150-200mL of diethyl ether. A molar equivalent of the electron donor was then added. The resulting mixture was subjected to rotary evaporation to remove the bulk of the solvent. The remainder of the mixture was then pumped dry (0.1 torr) to leave the crystalline complex. All solvent removal was carried out as described above.

The 2:1 (molar ratio of electron donor to imidazole) complexes were prepared by dissolving 1.0g of imidazole in 150-200 mL of acetonitrile. A molar equivalent of concentrated HBr (47% in water) was added to generate the protonated imidazole. Two molar equivalents of electron donor were next added and the solvent removed as previously outlined. Deuteroimidazole was prepared by warming imidazole in $D_2O$ followed by removal of the $D_2O$ under vacuum. Deuterium content was confirmed by $^1H$ nmr in $CDCl_3$. Deuterium content was found to be about 90%. The deuteroimidazole-diphenyl sulphoxide 1:1 complex was prepared in the same manner as other 1:1 imidazole-electron donor complexes.

The 1:1 imidazolium bromide-triphenyl phosphine oxide complex was prepared by dissolving 1.0g of imidazole in 100mL in acetonitrile. Addition of a molar equivalent of

concentrated HBr (47% in water) followed by removal of the solvent gave the imidazolium bromide salt. One gram of the salt was dissolved in 100 mL of acetonitrile and a molar equivalent of triphenyl phosphine oxide was added to the solution. Solvent removal yielded the crystalline complex.

FABMS samples were prepared by dissolving the sample in the chosen liquid matrix. Slight heating was applied to the mixture in some cases to facilitate dissolving the sample. All samples were left to stand a minimum of 24 hours before obtaining the FABMS spectra. The MIKE spectrum of the imidazolium bromide-triphenyl phosphine oxide was obtained from a VG ZAB-E.

Infrared spectra were obtained as hexachlorobutadiene mulls. All $^{1}H$ nmr spectra were obtained in $CDCl_3$ on Bruker WP-80(courtesy of Dr S.J. Brown). The $^{31}P$ nmr of the imidazolium bromide-triphenyl phosphine oxide complex, imidazole-triphenyl phosphine oxide complex, triphenyl phosphine oxide, and triphenyl phosphine oxide-tetrabutyl ammonium iodide solution were obtained with a Bruker AC 200 at 81.015 MHz. All spectra were run in acetonitrile at a concentration of 0.18 moles per litre in 0.5 mm tubes. Each spectrum was obtained from 16 scans. $H_3PO_4$ was used as an external reference.

Diphenyl sulphoxide, triphenyl phosphine oxide, benzophenone, diphenyl ether, and triphenyl methanol were from Aldrich. Imidazole was from BDH. Sulfolane, glycerol, and meta-nitro benzyl alcohol were from Aldrich.

Ortho-nitrophenyl octyl ether was obtained from Fluka AG. All the compounds were reagent grade and were used unpurified.

Multiple donors

Ortho-phenanthroline was prepared from the monohydrate. The monohydrate (2.00g) was dissolved in 150 mL of toluene. KF dried at 350 $^{o}$C for 24 hours was added to the mixture. The mixture was next heated until the solvent was refluxing up the condenser and into the Dean-Stark apparatus. Refluxing was carried out until there was no more water collected. The remainder of the mixture was filtered to remove the KF. The remainder of the solvent was then removed as outlined before ( rotary evaporation followed by drying under 0.1 torr vacuum). The infrared spectrum of the white crystalline product indicated the absence of water.

The ammonium halide salts were obtained by reacting the amines with concentrated HBr or HI (both 47% in water). Ammonium halide salts were obtained in this way for imidazole, pyridine, triethyl amine, diethyl methyl amine, and di-isopropyl amine. Dimethyl ammonium chloride and diethyl ammonium chloride were obtained from Aldrich. Dimethyl ammonium iodide was obtained by ion exchange of dimethyl ammonium chloride. A column of anion exchange resin ( Amberlyst A-26) was loaded with iodide by eluting one Liter of 1.1 M KI through the column. The column was then washed with 50 mL of acetonitrile. Finally, 100 mL of 0.2 M dimethyl

ammonium chloride in acetonitrile was eluted through the column. The eluant was subjected to rotary evaporation to remove the bulk of the solvent. A pale yellow crystalline solid precipitated and was dried under vacuum (0.1 torr). The infra red spectrum of the product (as KBr disk) showed a shift to lower wavenumber of the N-H stretch vibration compared to the dimethyl ammonium chloride salt. The band shifts from the chloride salt to the iodide salt were 2439 $cm^{-1}$ to 2415 $cm^{-1}$ and 2782 $cm^{-1}$ to 2752 $cm^{-1}$, respectively. The infra red spectrum of the product also indicated the absence of water. The FABMS spectrum of the product in NBA showed the m/z 219 which corresponds to $(Me_2NH_2^+)_2I^-$. No cluster ions with the chloride ion were observed.

The infrared solution spectra of diphenyl sulfone, dimethyl ammonium chloride, and the diphenyl sulfone-dimethyl ammonium chloride were obtained in dry acetonitrile at a concentration of approximately 0.2 M with KBr windows (0.5mm path length). The positive ion ammonia chemical ionization spectra of sulfolane and diphenyl sulfone were obtained on a ZAB-E.

Diphenyl sulfone, sulfolane, dimethyl ammonium chloride, diethyl ammonium chloride, dimethyl sulfone, triphenyl phosphine oxide, quinuclidine, dimethyl ethyl amine, di-isopropyl amine, and ortho-phenanthroline were obtained from Aldrich. Imidazole, amberlyst-26, and triethyl amine were obtained from BDH. All the above were of reagent grade and were used unpurified.

## III. Results and Discussion

### A. Tris(3,6-dioxaheptyl)amine-alkali metal complexes

#### A1. Introduction

Saturated solutions of LiF, LiCl, LiBr, LiI, NaF, NaCl, NaI, KF, KCl, KBr, KI, RbF, CsF, CsCl, and CsI in tris(3,6-dioxaheptyl)amine (tdoha) were prepared and analysed by FABMS. Since tdoha is a liquid with a high boiling point (>330C), a liquid matrix was not required for FABMS analysis. This property of tdoha enabled recording of scans for 15 minutes without significant change. The potential of tdoha as a matrix was briefly investigated but did not seem promising. The compound diphenyl tin chloride dissolved well in tdoha but the FABMS spectrum was virtually identical to that of neat tdoha. The same results were obtained with tetraphenyl phosphonium bromide which should have exhibited a high FABMS sensitivity.

Sharp *et al*[46] have used 18-crown-6 mixed with 10% tetraglyme to depress its melting point as a FAB matrix for the analysis of rhodium, platinum, and iridium organometallics. The advantage of tdoha over crown ethers is its relatively low toxicity (LD50=4.5g/Kg) and lack of mutagenic activity as well as comparatively low price given the simpler synthetic procedures[47]. Unfortunately, the effectiveness of tdoha as a FABMS matrix seems limited.

The FABMS spectrum of tdoha (figure 1) showed no molecular ion. The quasi molecular ion $[M+H]^+$ was at m/z 324. The peak at m/z 322 can be rationalized as arising from protonation at the nitrogen with subsequent cyclization involving loss of a hydrogen molecule. The base peak in the spectrum at m/z 234 corresponds to the fragment $C_{11}H_{24}NO_4$. Other intense peaks occur at m/z 59 (92%) base and m/z 248 (38% base) corresponding to $C_3H_7O$ and $C_{12}H_{26}NO_4$, respectively. The electron impact mass spectrum of tdoha showed a small molecular ion at m/z 323 (less than 1% base intensity). Interestingly, loss of a hydrogen molecule from the molecular ion was observed. The main ions m/z 59 and 234 were also observed.

Weber *et al* [48] believe that variations of complex stability and ion selectivity can often be accomplished more readily than with their cyclic counterparts. Complexation and decomplexation are generally faster in acyclic systems as the pseudo cavity has greater conformational flexibility. The acyclic ligands offer the advantage of facile synthesis. Contrary to crown and cryptand compounds, the acyclic ligands do not suffer the drawback of more involved synthetic procedures necessary to generate cyclic compounds. This results in inexpensive, versatile synthesis. The first non-cyclic cryptates were first introduced by Voegtle *et al* [49]. A first index of cryptand analoguous complexation behavior was provided by the phase transfer of solid $KMnO_4$ and

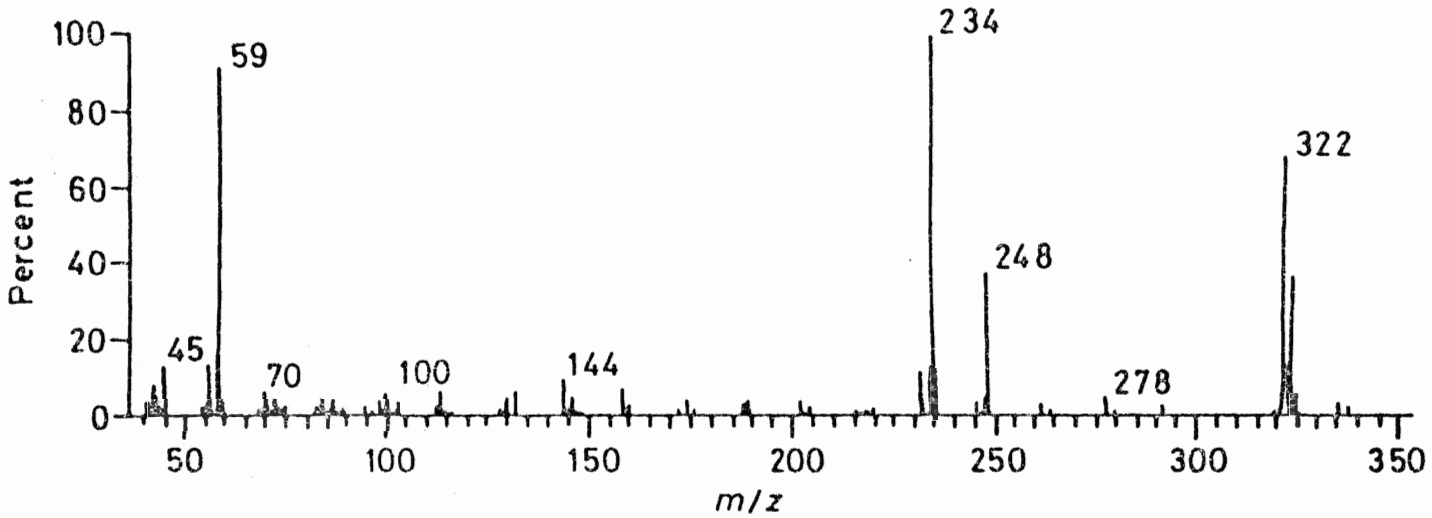


Figure 1. FABMS spectrum of neat tdoha

Figure 2. Tris(3,6-dioxaheptyl)amine

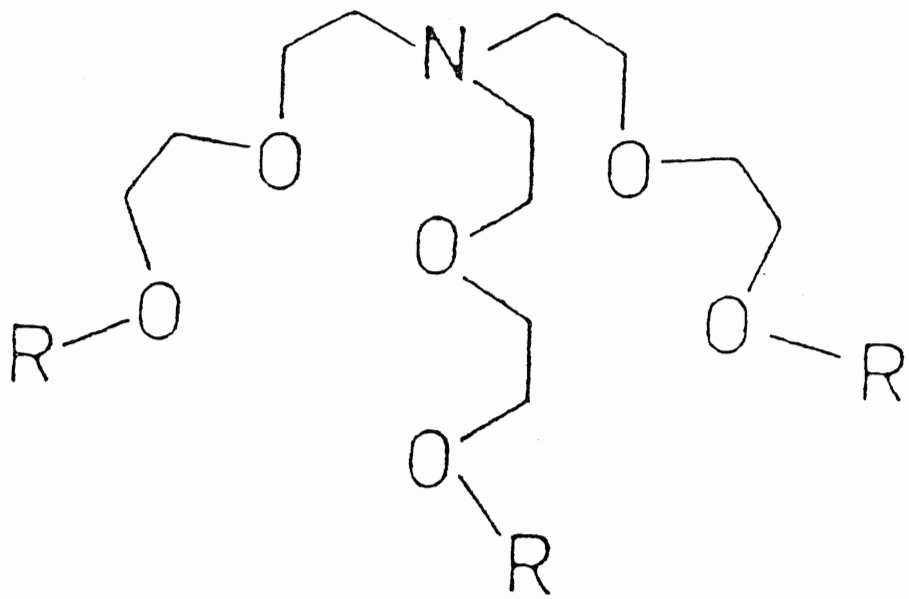


R= Methyl

alkali metal picrates into non-aqueous phase. This phase transfer capacity[50] was found to exceed that of dibenzo-18-crown-6.

The initial aim of our research was to investigate the potential of tdoha as a phase transfer catalyst for KF or $CaF_2$. The idea, as in the 18-crown-6-KF system, is to generate a naked fluoride ion[51]. This is achieved by the polyether strongly complexing the cation. In analoguous fashion, tdoha has been used in solid-liquid phase transfer catalyst for the preparation of alkyl thiocyanates by nucleophilic displacement[47].

In the presence of a catalytic amount of tdoha, solid NaSCN (in chlorobenzene) becomes gradually solubilized and the reaction with the alkyl bromide takes place; sodium bromide precipitates. The equilibria 1 and 3 are considerably displaced to the right and the catalyst is released after each reaction.

Figure 3. tdoha in the preparation of R-SCN

$$NaSCN + tdoha \rightleftharpoons tdoha[Na]^+SCN^- \quad (1)$$

$$R\text{-}Br + tdoha[Na]^+\text{---}SCN^- \longrightarrow R\text{-}SCN + tdoha[Na]^+\text{---}Br^- \quad (2)$$

$$tdoha[Na]^+\text{---}Br^- \rightleftharpoons \underline{NaBr} + tdoha \quad (3)$$

## A.2. Neat tdoha-Alkali metal Halide systems

The features of the FABMS spectra of the saturated alkali metal halide/tdoha solutions depended on the complexation affinity of tdoha for the alkali metal cations.

If the affinity of tdoha was high, as in the case of the lithium cation, the peaks due to tdoha were suppressed compared to the tdoha-cation complex peak. The strength of the interaction was reflected by the presence of a metal containing fragment of tdoha, $Li(C_6H_{13}NO_2)^+$, at m/z 138 (figure 4).

As can be seen in table 1, our results show there is no apparent periodic trend in terms of cation-tdoha complex abundances as obtained with FABMS. The lack of periodic trend is obvious when comparing KI and NaI. No explanation can be offered for this anomalous result at this point. However, because NaI forms a solid complex with tdoha, there is the possibility that some of the NaI precipitates. The potassium salts gave the expected trend with the total ion current due to the complex increasing on changing the anion from fluoride to iodide. For the fluorides, the presence of water would help solubilize the cation or anion. However, aquated complex ions were not observed.

A crude solid NaI-tdoha complex was isolated from the saturated solution. Its FABMS spectrum in glycerol is described in table 3. In contrast to the saturated solution FABMS spectrum, the peak corresponding to the complex was the base peak and a metal containing fragment was observed at m/z 154. This metal containing ion is analoguous to the m/z observed in the lithium-tdoha FABMS spectra. Cesium chloride and iodide showed no complex formation while KF, RbF, and CsF

Figure 4. FABMS spectrum of saturated LiCl-tdoha solution

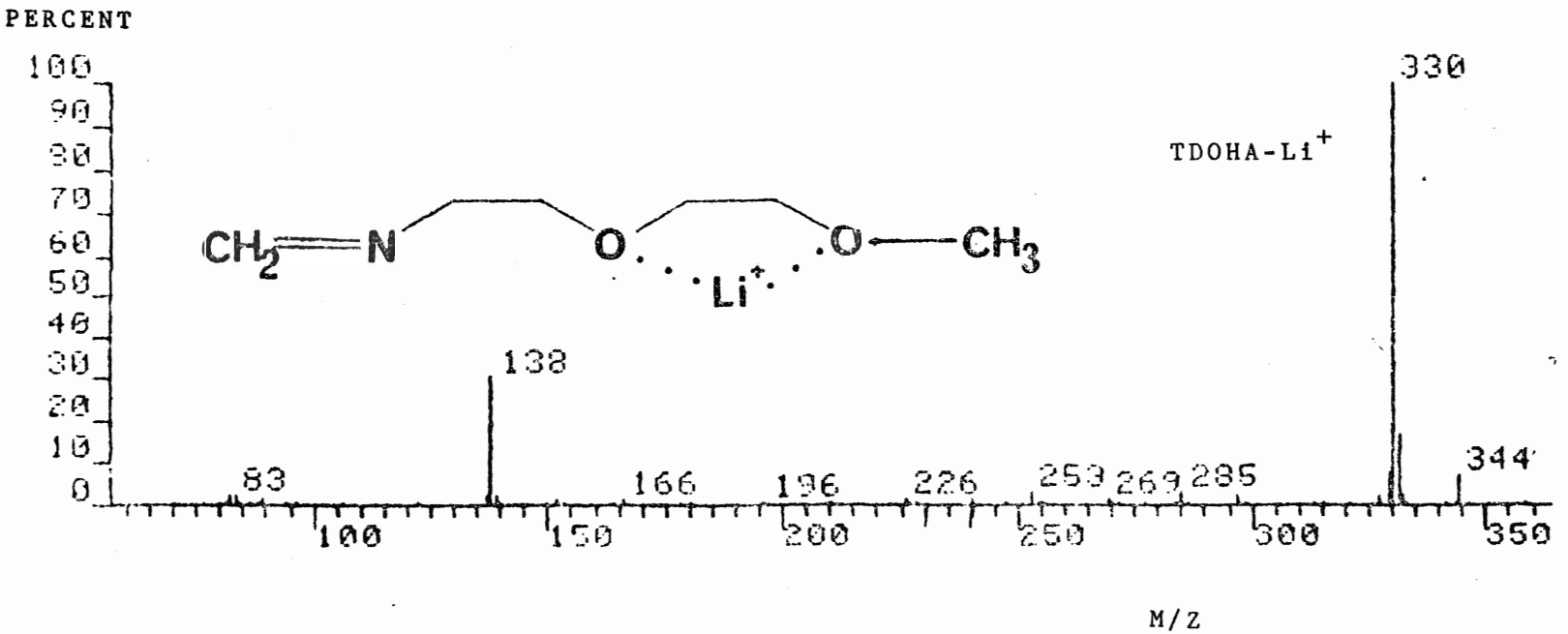

Table 1. FABMS of alkali halide-tdoha saturated solutions

| alkali Halide | m/z 324 $(M+H)^+$ | m/z 234 | Percentage of TIC* (tdoha+cation) peak |
|---|---|---|---|
| LiF | 4.2 | 13.5 | 0.0 |
| LiCl | 0.9 | 5.1 | 27.9 |
| LiBr | 0.0 | 0.0 | 45.1 |
| LiI | 0.0 | 0.0 | 38.8 |
| NaF | 6.8 | 14.0 | 0.0 |
| NaCl | 5.6 | 16.7 | 0.2 |
| NaI | 3.4 | 11.2 | 4.9 |
| KF | 5.8 | 14.8 | 0.2 |
| KCl | 4.8 | 12.4 | 0.3 |
| KBr | 4.1 | 17.8 | 3.2 |
| KI | 0.0 | 0.4 | 22.8 |
| RbF | 4.6 | 13.9 | 0.2 |
| CsF | 4.9 | 14.0 | 0.1 |
| CsCl | 4.1 | 13.3 | 0.0 |
| CsI | 5.4 | 14.3 | 0.0 |

Table 2. FABMS of LiCl-tdoha saturated solution

| m/z | % of base peak | Assignment |
|---|---|---|
| 330 | 100.0 | $[tdoha+Li]^+$ |
| 324 | 3.1 | $[tdoha+H]^+$ |
| 322 | 11.3 | $[tdoha-H]^+$ |
| 234 | 18.4 | $[C_{11}H_{24}NO_4]^+$ |
| 138 | 17.0 | $[C_6H_{13}NO_2Li]^+$ |
| 59 | 10.2 | $[C_3H_7O]^+$ |

Figure 5. FAB mass spectrum of the NaI-tdoha complex in glycerol

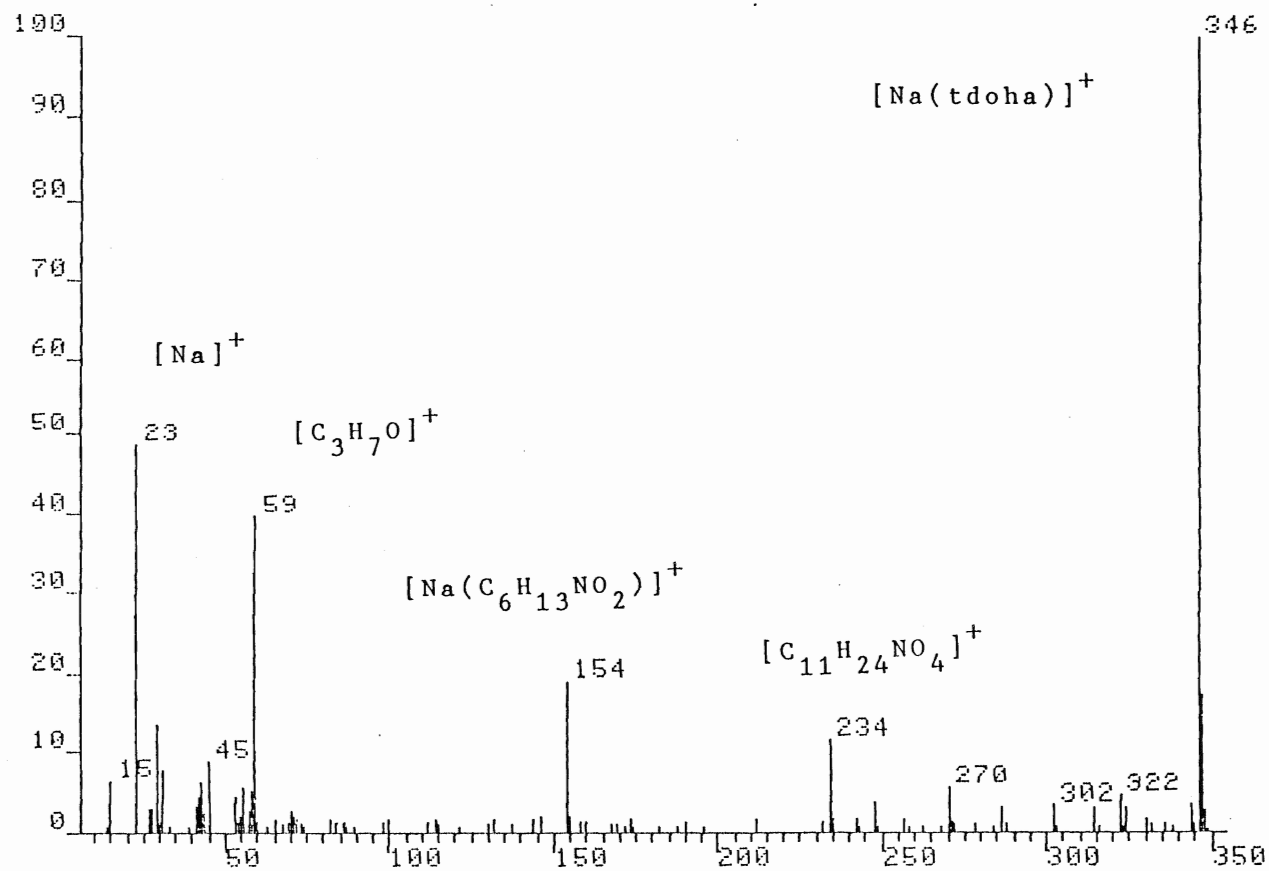

Table 3. FABMS of the crude NaI-tdoha complex in glycerol

| m/z | % of base peak | Assignment |
|---|---|---|
| 346 | 100.0 | $[Na(tdoha)]^+$ |
| 322 | 4.5 | $[M-H]^+$ |
| 234 | 11.6 | $[C_{11}H_{24}NO_4]^+$ |
| 154 | 19.2 | $[Na(C_6H_{13}NO_2)]^+$ |
| 59 | 39.6 | $[C_3H_7O]^+$ |
| 23 | 48.8 | $[Na]^+$ |

showed weak complexation. The high hygroscopicity of these salts may also be responsible for their anomalous behavior. The IR spectra of the RbF and CsF-tdoha solutions did show water contamination. The $^{19}F$ nmr of the saturated tdoha of LiF, NaF, KF, RbF, and CsF were in agreement with FABMS results. LiF and NaF gave no complex peak in the FABMS. The $^{19}F$ nmr of these systems gave no observable signal demonstrating that none of the salts had dissolved. KF, RbF, and CsF which gave weak complex peaks in FABMS, showed a signal corresponding to $F^-$ in $^{19}F$ nmr. The chemical shifts were typical of the fluoride ion (-97 to -117ppm, $CFCl_3$ reference). The signals were unusually broad, with CsF having a linewidth at half peak height of 740Hz. These unusually broad linewidths are analoguous to those observed for the crown ether alkali metal fluoride solutions. The possibility of reverse micelles was postulated for these systems[52].

Given the controversy surrounding the ability of FABMS to reflect solution behavior, IR data was obtained for the tdoha-alkali metal halide systems. The systems which showed complexation in the FABMS experiment also showed significant changes in their IR spectra. As with crown ethers, the greatest change in going from the free ligand to the complex occurs in the 900-1200$cm^{-1}$ region.

The C-O-C asymmetric vibration of tdoha at 1120$cm^{-1}$ was significantly shifted to lower wavenumber upon

complexation (figure 6). The magnitude of the shift to lower wavenumber was cation dependent. The frequency change of the C-O-C asymmetric vibration (table 4) appeared to parallel the strength of the complex.

It should be noted that the exact frequency shift was difficult to determine, given that the width of the bands increased. New bands were observed at about 930 and 750cm$^{-1}$. The intensity of these bands was found to be dependent on the degree of complexation but not on the cation.

The samples were run as thin films between KBr discs. As a result, some complexation of $K^+$ occurred. However, this was not significant enough to affect the spectra in the time needed to obtain it (2-3 minutes). This was demonstrated by obtaining a spectrum using an ATR accessory with a ZnSe crystal.

A complex was isolated only for NaI. The IR spectrum of the crude NaI-tdoha complex was virtually identical to that of the saturated solution. The $^1$H nmr of the NaI-tdoha complex showed slight changes compared to tdoha. The $H_a$ protons were found to shift to 0.15ppm higher field, consistent with an ion-dipole interaction between the oxygen atoms and the sodium ion. The other proton chemical shifts were unchanged.

An attempt was made to analyze a neat solution of LiBr-tdoha (1:1 molar ratio) by $^{15}$N nmr[53]. This was an atempt to show the participation of the nitrogen atom in the

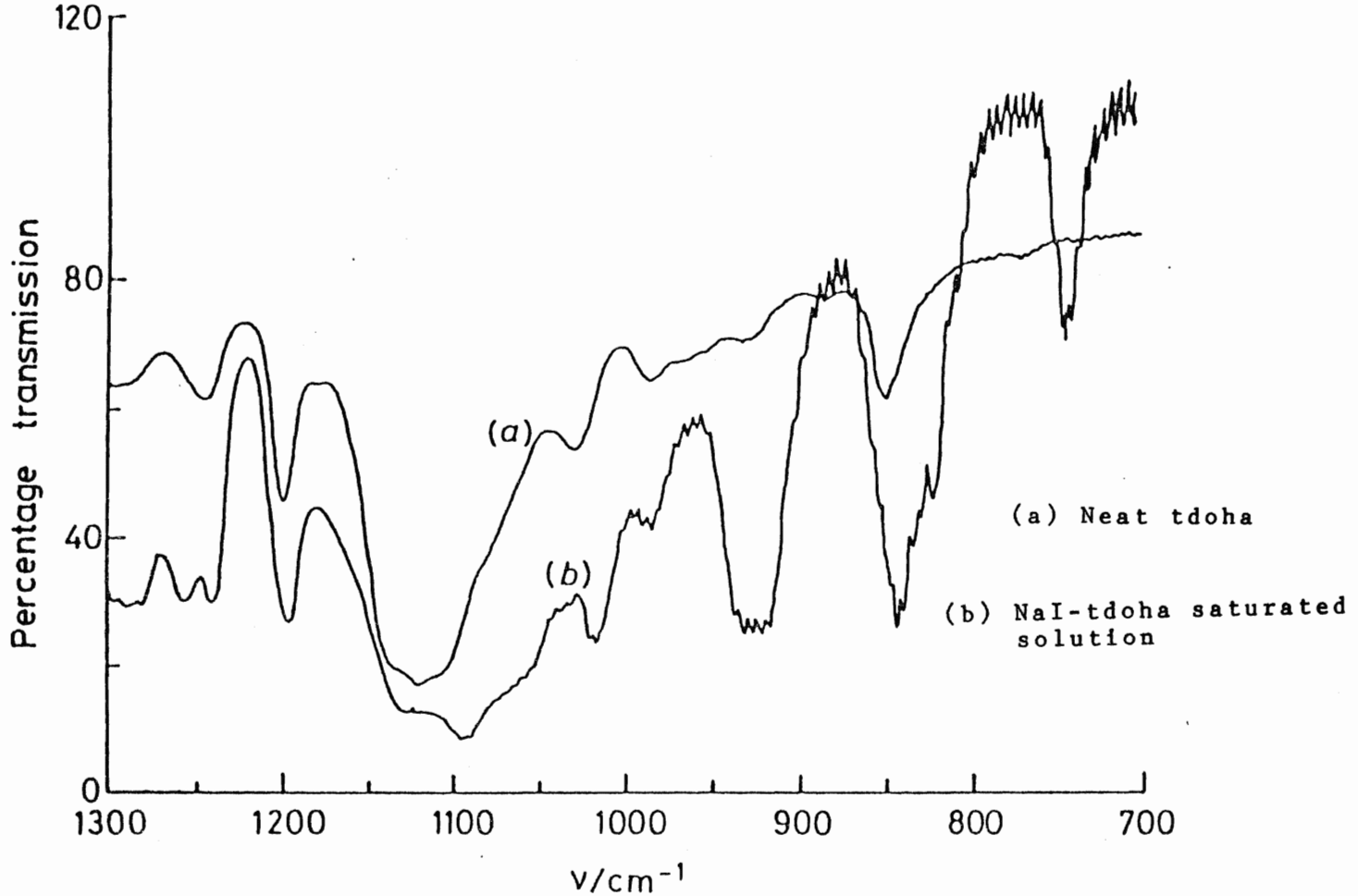


Figure 6. Infrared spectra of (a) tdoha and (b) NaI-tdoha saturated solution

Table 4. C-O-C asymmetric vibration shift in the infrared spectra of saturated tdoha-alkali halide solutions

| Salt | Change in frequency($cm^{-1}$) |
|---|---|
| LiI | 33 |
| NaI | 26 |
| KI | 26 |
| RbF | 10 |
| CsF | 10 |
| CsI | 0 |

complexation of $Li^+$ by tdoha. No signal was observed for the LiBr-tdoha solution. This could be due to the low molar concentration of nitrogen in the sample. The effect of the viscosity of the solution on the relaxation parameters as well as the change in the electrical environment of the $^{15}N$ nuclei are not clear.

### A.3. Crown ether-tdoha competitive systems

Johnstone et al. [54] have shown that the peak heights due to the crown ether-cation complexes in FABMS were proportional to the concentration of those species in solution. However, their attempt to extract quantitative determination of crown ether/metal cation complexes concentrations in solution from FABMS data is a little premature. Their use of published stability constants to calculate the concentration of crown ether-cation complexes in a different solvent can be questioned. Furthermore, comparing the peak intensity ratio of two complexes (valomycin-$K^+$ and valomycin-$Na^+$) with the ratio of the stability constants of those same complexes determined in a different solvent seems erroneous. However, the concept that one can get a relative idea of ligand-cation affinities seems more reasonable.

The competitive systems where a crown ether and tdoha competed for an alkali metal cation were set up and subsequently analysed by FABMS. Since none of the translational energy of the incoming atom was required for

ionization, it was assumed that energy was used to overcome coulombic forces and seperate the ligand-cation complexes from their counter ions. Thus, approximately the same amount of energy was required to desorb the tdoha crown ether complexes. Hence, the relative concentrations of the tdoha and crown ether complexes were assumed to be directly proportional to their respective peak intensities. This assumption implies that differences in desorption efficiencies were small. The crown ethers, tdoha and alkali chloride salts were mixed in a 1:1:1 molar ratio and analysed by FABMS. This type of experiment gave an interesting insight on the relative complexing strengths of the ligands (table 5). Fragment ions due to tdoha were abundant and strong but the ions corresponding to the respective crown and tdoha complexes were significant.

The above results correlate well with respective affinities of the crown ethers for the cations based on the cation size. In the case of the potassium cation, when mixed with 18-crown-6 and tdoha the majority of the $K^+$ was complexed to the crown. This was probably due to the optimum size of the 'cavity' of 18-crown-6 for the $K^+$ cation. With 15-crown-5, an increasing amount of $K^+$ was coordinated to tdoha because of the smaller size of the crown ether cavity. With 12-crown-4, all the potassium was coordinated to tdoha. The sodium series can be rationalized along the same lines i.e in terms of the respective size of the cation and crown ether

Table 5. FABMS of crown ether-tdoha-alkali chloride solution

| Crown ether | Cation | Crown cavity radius[57] (Angs.) | Cation radius (Ang.) | Crown ether complex* | tdoha complex* |
|---|---|---|---|---|---|
| 18-crown-6 | $K^+$ | 1.45 | 1.33 | 88 | 12 |
| 15-crown-5 | $K^+$ | 0.92 | 1.33 | 55 | 45 |
| 12-crown-4 | $K^+$ | 0.72 | 1.33 | 0 | 100 |
| 18-crown-6 | $Na^+$ | 1.45 | 0.98 | 100 | 0 |
| 15-crown-5 | $Na^+$ | 0.92 | 0.98 | 40 | 60 |
| 12-crown-4 | $Na^+$ | 0.72 | 0.98 | 0 | 100 |
| 18-crown-6 | $Li^+$ | 1.45 | 0.78 | 23 | 77 |
| 15-crown-5 | $Li^+$ | 0.92 | 0.78 | 35 | 65 |
| 12-crown-4 | $Li^+$ | 0.72 | 0.78 | 3 | 97 |

* Percentage of metal containing ions only

cavity as well as the affinity of tdoha for the cation.

The competitive crown ether-tdoha-lithium chloride system confirmed the high affinity of tdoha for the lithium cation. With 18-crown-6, 23% of the $Li^+$ was bound to the crown ether and 77% to tdoha. Reducing the cavity size of the crown ether with 15-crown-5 resulted in an increase of the crown ether bound cation complex with 35% of the $Li^+$ coordinated to the crown ether. Finally, a further decrease of the cavity size (12-crown-4) resulted in 97% of the $Li^+$ bound to tdoha.

Although it seems fair to say that the data support the view that small crowns bind small cations better than large ones and vice versa, the severe limitations of this generalization must not be overlooked. One should consider the flexibility of the ligand as well as the possibility that the complex stoichiometry may not necessary be 1:1[55]. For example, 18-crown-6 can fold somewhat around the $Na^+$ cation which is smaller than its cavity size. The effect of ligand flexibility is well illustated by the potassium dibenzo-30-crown-10 complex where the ligand wraps itself completely around the cation (figure 7).

A.4. Structural aspects of tdoha complexes

The structures of the complexes formed by tdoha and alkali metal cations have received little attention. Although some complexes have been isolated [56] only two crystal structures of open chain cryptands (tdoha analogues) appear in

Figure 7. The structures of the complexes of Dibenzo-30-crown-10($K^+$) and 18-crown-6($Na^+$)

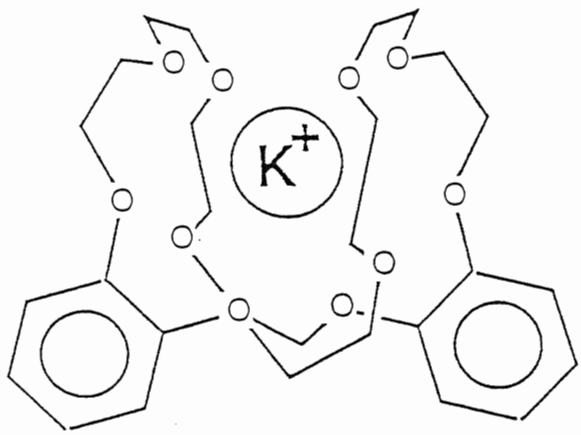


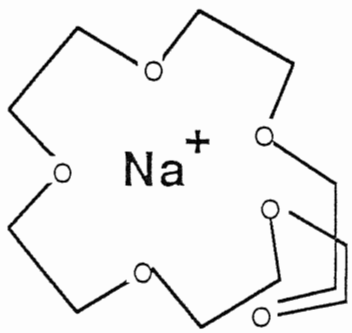

the literature. The crystal structure of the complex formed between the three-armed decadentate ligand and KSCN shows the arms of the tripodand wrapped around the cation in a propeller-like way with all donor atoms coordinated to $K^+$. An interesting fact is that coordination by the anion is totally hindered because of the complete envelopment of the cation. The anion remains outside the lipophilic 'shell' of the complex in analogy to the bicyclic cryptates where the metal cations are also completely enveloped[57]. Whether this envelopment of the cation would significantly affect the desorption efficiency in FABMS of the smaller cation complexes (by reducing coulombic attractions between the anion and cation) compared to that of the larger cation complexes is uncertain. In tdoha, the nitrogen atom probably participates effectively in the coordination of the smaller cations. This is again based on an anology to the cryptands which can assume three conformations according to the configuration of the two nitrogen bridgeheads (figure 8). X-ray studies show the free [2.2.2.] cryptand to exist in the endo-endo conformation in the crystal. In all known cryptand complexes, the configuration is also endo-endo[55].

However reasonable it may seem, one cannot assume that tdoha complexes adopt such a configuration in solution. The flexibility of the open chain cryptand possibly allows for a variety of conformations for different cations. This is supported in part by the crystal structure of the complex

Figure 8. The three different conformations of a cryptand.

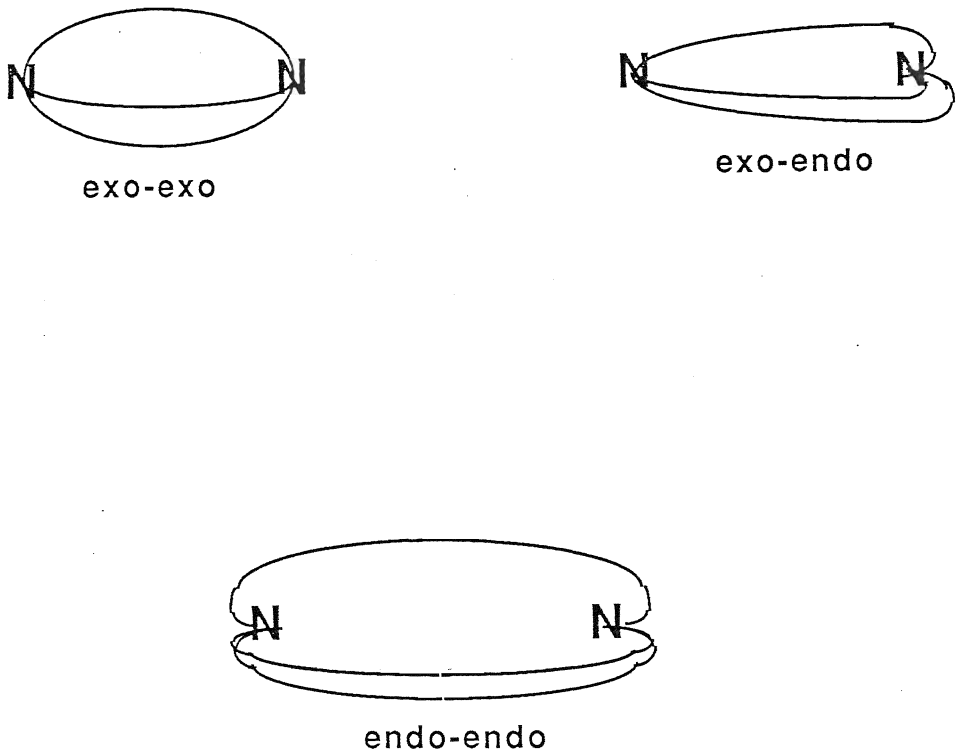

formed between the ligand tris-[(2-methyl-8-quinoyl-oxy)ethyl] amine and rubidium iodide (figure 9 ). It appears the tripodand wraps around the cation in the manner of a linear ligand rather than a cryptand[58]. Nonetheless, one should be aware that conclusions on the real tendency of formation and the stability of a polyether complex as well as the ligand conformation of the complex in solution can only be drawn to a limited extent via the crystal structure[59].

A.5. Complexation order

The complexation order found in this study (neat tdoha) contrasts with results obtained by a potentiometric study[56] in water/methanol where the complexation order was

$Na^+$, $K^+ > Rb^+ > Cs^+$, $Li^+$

The complexation order from the peak intensity of the respective cation-tdoha complex in the FABMS experiment (neat tdoha) was

$Li^+ > Na^+$, $K^+ > Rb^+ > Cs^+$

The low complexation order of the lithium cation in the potentiometric study can be rationalized by the fact that it is strongly solvated by the water/methanol solvent system.

Preliminary FABMS experiments on the tdoha/water/glycerol/alkali halide salts system gave a complexation order close to that of the potentiometric study. The complexation order with the water/glycerol matrix was

$Na^+ > K^+ > Li^+ > Rb^+ > Cs^+$

This order was obtained by submitting to FABMS

Figure 9. Crystal structure of the RbI complex of tris-[(2-methyl-8quinoyl-oxy)ethyl]amine

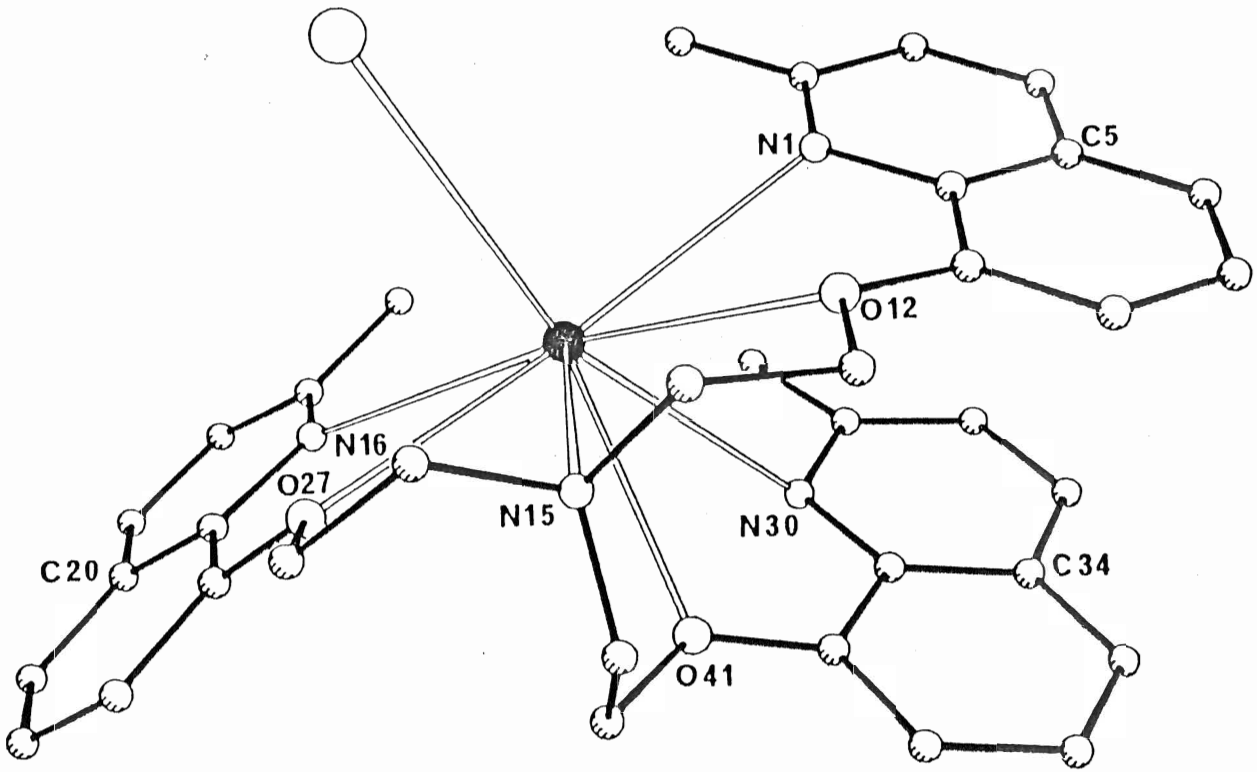

analysis an equimolar mixture of alkali iodides in glycerol/water (2:1 by weight) mixed with 1 molar equivalent of tdoha. The complexing order was defined according to the peak intensities corresponding to the respective tdoha-cation complexes (figure 10).

If one takes into account the abundance of the free metal cations, relative stability constants can be roughly determined. The thermodynamic stability constant[60] $K_{th}$ can be given by equation(4), where $F_c$, $F_L$, and $F_M$ are the activity coefficients of the three species present.

$$K_{th} = \frac{F_c[LM^{n+}]}{F_L[L]F_M[M^{n+}]} \qquad (4)$$

Since the coefficients are generally unknown, the stability constants $K_s$ based on the concentrations are usually employed. $K_s$ is an average stability constant for the system in thermodynamic equilibrium.

$$K_s = K_{th}\,(F_L F_M / F_c) = \frac{[LM^{n+}]}{[L][M^{n+}]} \qquad (5)$$

In the experiment described above, [L], the concentration of the ligand, was a constant since all cation affinities were measured simultaneously. The 'relative' stability constants were obtained by using the respective peak intensities instead of concentrations. In other words, the

figure 10. FAB mass spectrum of the LiI/NaI/KI/RbI/CsI/tdoha/water/glycerol system

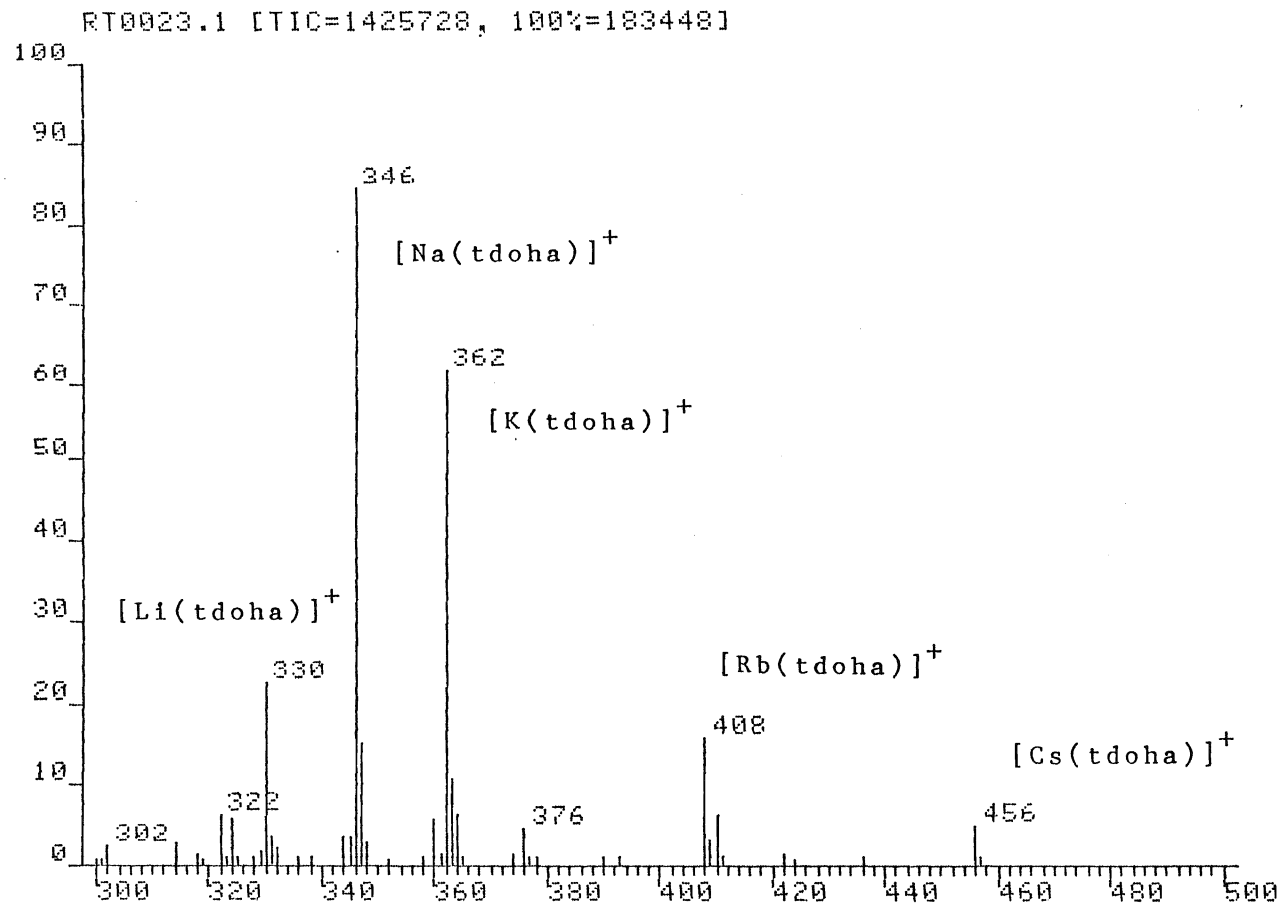

'releative' stability constants were defined as the ratio of the peak intensities corresponding to the ligand-cation complex and the free cation (tdoha-$M^+/M^+$). The data are tabulated in table 6. Corrections were not made for the differences in sensitivity at different m/z values. Johnson et al [30] stated that the corrections were unlikely to invalidate general conclusions provided one was dealing with one ligand and a series of metal cations.

However, the reliability of the value of the lithium-tdoha relative $K_s$ can be questioned. This is due to two factors. First, because the mass spectrometer was only calibrated to m/z 11, the abundance of the lithium cation had to be measured from the ion meter(gauge). Second, the mass spectrometer has an inherently low sensitivity for a mass as low as that of lithium (m/z 7). A third consideration may be that the lithium is strongly solvated by the glycerol/water solvent system which could further diminish its abundance in the FABMS spectrum. Thus, the effect of these three considerations is that the abundance of the uncomplexed lithium cation should be assumed to be higher. This in turn implies a lower relative $K_s$ which is reasonable considering the stability of similar polyether lithium complexes in strongly solvating medium.

If one discards the $K_s$ value for lithium the complexation order from relative $K_s$ values is qualitatively the same as that from the peak intensities of the complexes.

Table 6. Relative stability constants for the $M^+$-tdoha complexes

| Cation | complex abundance as % of base peak | $K_s X10$ | $Log K_s$ |
|---|---|---|---|
| $Li^+$ | 22.6 | 28.1 | 1.5 |
| $Na^+$ | 84.3 | 17.2 | 1.2 |
| $K^+$ | 61.7 | 6.2 | 0.8 |
| $Rb^+$ | 19.2 | 4.6 | 0.7 |
| $Cs^+$ | 5.2 | 2.0 | 0.3 |

Table 7. Log $K_s$ values for tdoha from Voegtle[56]

| | $Li^+$ | $Na^+$ | $K^+$ | $Rb^+$ | $Cs^+$ |
|---|---|---|---|---|---|
| Log $K_s$ | <2.0 | 2.2 | 2.2 | 2.0 | <2.0 |

There has been only one study on the stability constant values for tdoha-alkali metal cations complexes in solution[56]. The $K_s$ values were determined in water/methanol using a pH metric method. The results are reported in table 7.

As can be seen the results do not agree all that well with the FABMS results. This discrepancy could be explained by the difference in solvent systems. However, the authors failed to mention the experimental limitations of the method as determined by Lehn et al [61]. First, only values of $\log K_s > 2$ are considered reliable. Second, the errors resulting from experimental scatter of the $\log K_s$ values are about $2 < \log K_s$, $\Delta K_s \pm 0.4$. This means that there is no 'definitive' data in the literature on the magnitude of the stablity constants of the tdoha-alkali metal cations. Notwithstanding this there is qualitative agreement between the potentiometric and FABMS methods whereby the sodium and potassium complexes are significantly stronger than the lithium, cesium, and rubidium complexes.

A.6. Conclusion

The recent development of continuous flow FAB probes could greatly enhance the scope of solution studies by FABMS altough the pumping speed requirement for such devices are demanding and thus not amenable to many instruments. The use of matrices with a more aqueous character allowed by the continuous flow probe technique should allow more relevant comparison of the FABMS results with data obtained by more

conventional methods. Because different solvent systems are used and due to the fact that such factors as desorption efficiency and surface activity could contribute to the enhancement or depletion of a particular complex ion, interpretation of the results should be cautious.

Because of the possibility of oxidation-reduction processes in FABMS it is probably not possible to extend the use of the technique for the study of transition metal cation selectivity of multidentate ligands. This probably limits the technique to the alkali metals and alkaline earth metals.

Given the fact that the methods used for the investigation of complexation between macrocyclic or acyclic polyethers and various metal cations tend to be cumbersome and usually require calorimetry, potentiometry or absorption spectroscopy, it is hoped that the usefulness of FABMS in this regard has been shown to be a quick and efficient method to obtain qualitative data. The simplicity and time saving aspects of the experiment are great assets. It should be stressed that these results are to be interpreted with caution and should be considered qualitative. The specificity of mass spectrometry confers a great advantage to FABMS with respect to other techniques. However, FABMS is hampered by the limited number of suitable matrices available. This in turn restricts the number of systems amenable to FABMS.

## B. Imidazole-Electron Donor Complexes

### B.1. Basic Considerations and Matrix Selection

Our study of H-bonded systems by FABMS started with an attempt to observe the H-bonded dimer of benzoic acid. This was done by dissolving relatively high amounts of benzoic acid in N-methylpyrrolidone which was used as the matrix liquid. However, the H-bonded dimer of benzoic acid was not observed probably because there is no site where protonation of this species can occur without breakdown of the dimer itself. Polar molecules are usually observed as the protonated quasi-molecular ion in FABMS and the observation of the molecular ion in the spectrum is exceptional unless one is dealing with a salt which generally show the intact cation and anion. Thus, the main problem confronted in FABMS for the study of H-bonded complexes resides in the fact that as a mass spectrometric technique, FABMS requires complexes that are charged in order to be detected. This means the complex must be either pre-ionized (i.e. be a cation or an anion) or provide for a site where protonation can occur to yield the quasi-molecular ion $[M+H]^+$.

The imidazole-electron donor complexes[62] are ideal candidates for the study of H-bonding by FABMS since the

complexes can be protonated at the N3 position of imidazole without breaking the hydrogen bond[63]. In this study, the electron donors used were triphenyl phosphine oxide, diphenyl sulphoxide, benzophenone, triphenyl carbinol, and diphenyl ether.

The second problem in the FABMS study of hydrogen bonded complexes is the selection of a suitable liquid matrix. Glycerol is by far the most used matrix liquid but its strong hydrogen bonding capability (both as a donor and acceptor) would imply that only the complexes possessing quite strong hydrogen bonds[64] would be expected to be observed. Unfortunately, liquid matrices with good H-bonding capability are usually the best FABMS matrices. Preliminary work with glycerol gave the expected results which confirmed that a strong H-bonding matrix interferes with the observation of the complex. Only the imidazole-electron donor complexes having the strongest H-bonds, such as that formed by triphenyl phosphine oxide, were observed with glycerol as the liquid matrix. Glycerol-imidazole and glycerol-triphenyl phosphine oxide H-bonded adducts were also observed.

Ortho nitrophenyloctylether was also used but the complexes were found to have low solubility in this matrix. Because of this low solubility only the stronger H-bonded complexes were observed. For other electron donors, the low concentration of the species probably led to dissociation of

the complex. The use of diffusion pump oil (polyphenyl ether) was also limited by the poor solubility of the complexes.

An extensive study was carried out with sulfolane (tetramethylene sulfone) because of the high solubility of the complexes in this matrix. Initial results were encouraging since complex ion abundances were relatively high. A concentration study was undertaken with the diphenyl sulphoxide-imidazole complex. The results were inconclusive and unreliable due to the high volatility of the matrix in the vacuum of the mass spectrometer at low sample concentration. This meant that only 2-3 scans could be accumulated over a period of less than 2 minutes. Even though at higher sample concentration the FABMS spectra were more long lived, examination of each individual scan showed a rather significant change in the peak intensities of the ions of interest relative to one another over 10 scans (about 5 minutes). Furthermore, the intensity of the complex peak m/z 271 did not seem to follow corresponding decreases in sample concentration.

Another problem with sulfolane was the tendency of the triphenyl phosphine oxide-imidazole complex to crystallize on the probe tip after a short time inside the vacuum system of the mass spectrometer. This resulted in the suppression of the signal due to the H-bonded complex. Thus, after considerable experimentation, the results

indicated that the short lifetime of sulfolane in the mass spectrometer vaccuum made it unsuitable as a liquid matrix for the study of H-bonded complexes if reliable results were to be obtained. The advent of the continuous flow probe may solve the volatility problem of sulfolane. What was a drawback in the 'classical' FABMS experiment could become an asset with the continuous flow probe since the solvent used must have a certain volatility to allow a reasonable flow. The higher intensities of hydrogen bonded complexes observed in sulfolane implies that weaker complexes could be observed using the continuous flow probe.

Meta-nitrobenzyl alcohol (NBA) was the best matrix for the study of hydrogen bonded complexes of imidazole. The use of NBA allowed the accumulation of spectra over a period of 10-15 minutes without loss of ion current. In contrast with sulfolane, the lifetime of NBA in the vacuum system of the mass spectrometer was long and did not require high sample concentration for the ion current to be long lasting. Another advantage of NBA is its relatively low capacity to form H-bonds relative to other protic matrices such as glycerol. However, complex ion abundances observed in NBA were generally somewhat lower than in sulfolane.

## B.2. H-bond strengths

The FABMS of imidazole in NBA (1.3 M ) showed the

imidazole quasi-molecular ion at m/z 69 as the base peak (figure 11) Other significant ions were the imidazole dimer $[2Im+H]^+$ (m/z 137, 13% of base), and a peak at m/z 222 (2% of base) corresponding to NBA presumably H-bonded to imidazole. The FABMS spectra of the complexes typically showed peaks corresponding to the quasi-molecular ion of the hydrogen bonded complex (when it was present), the protonated imidazole, and the protonated electron donor. The FABMS spectrum of the triphenyl carbinol-imidazole complex did not show a quasi-molecular ion for the electron donor. The base peak was usually $Ph_3C^+$, probably arising through loss of water from the protonated triphenyl carbinol. Figure 12 shows the FABMS spectrum of the imidazole-triphenyl phosphine oxide complex in NBA. The ion corresponding to the complex appears at m/z 347 with the protonated triphenyl phosphine oxide dimer at m/z 556. The ion at m/z 201 corresponds to loss of a phenyl from triphenyl phosphine oxide.

The abundance of matrix peaks decreased with an increase in sample concentration. This particular phenomenon is well documented in the earliest FABMS literature and is believed to arise from the formation of a monolayer of sample at the surface of the matrix thus suppressing peaks due to the matrix.

For $Ph_3P=O$, $Ph_2S=O$, $Ph_2C=O$, and $Ph_3COH$ the H-bond formation was confirmed by infra red spectroscopy[63]. The

figure 11. FAB mass spectrum of Imidazole in NBA (1.3 M )

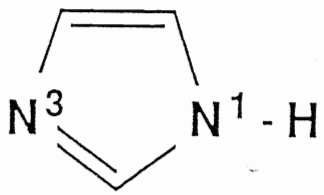


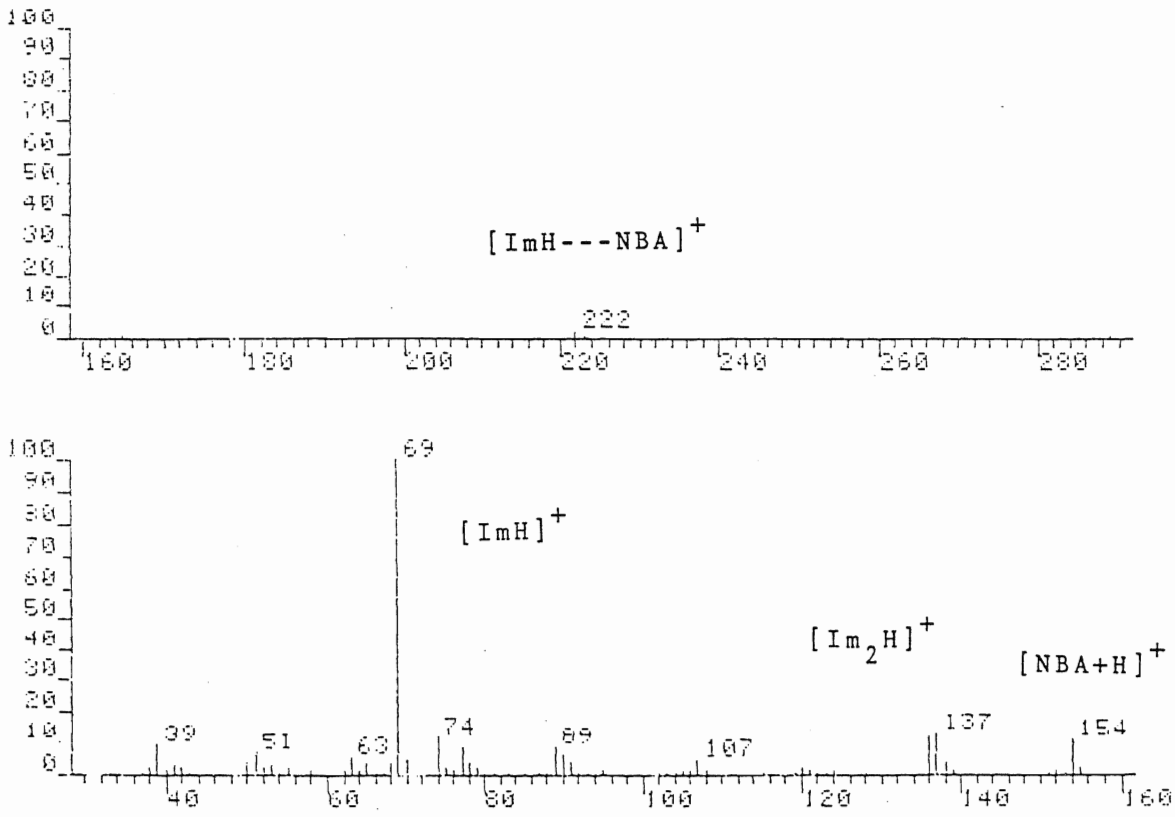

figure 12. FAB mass spectrum of the triphenyl phosphine oxide-imidazole H-bonded complex

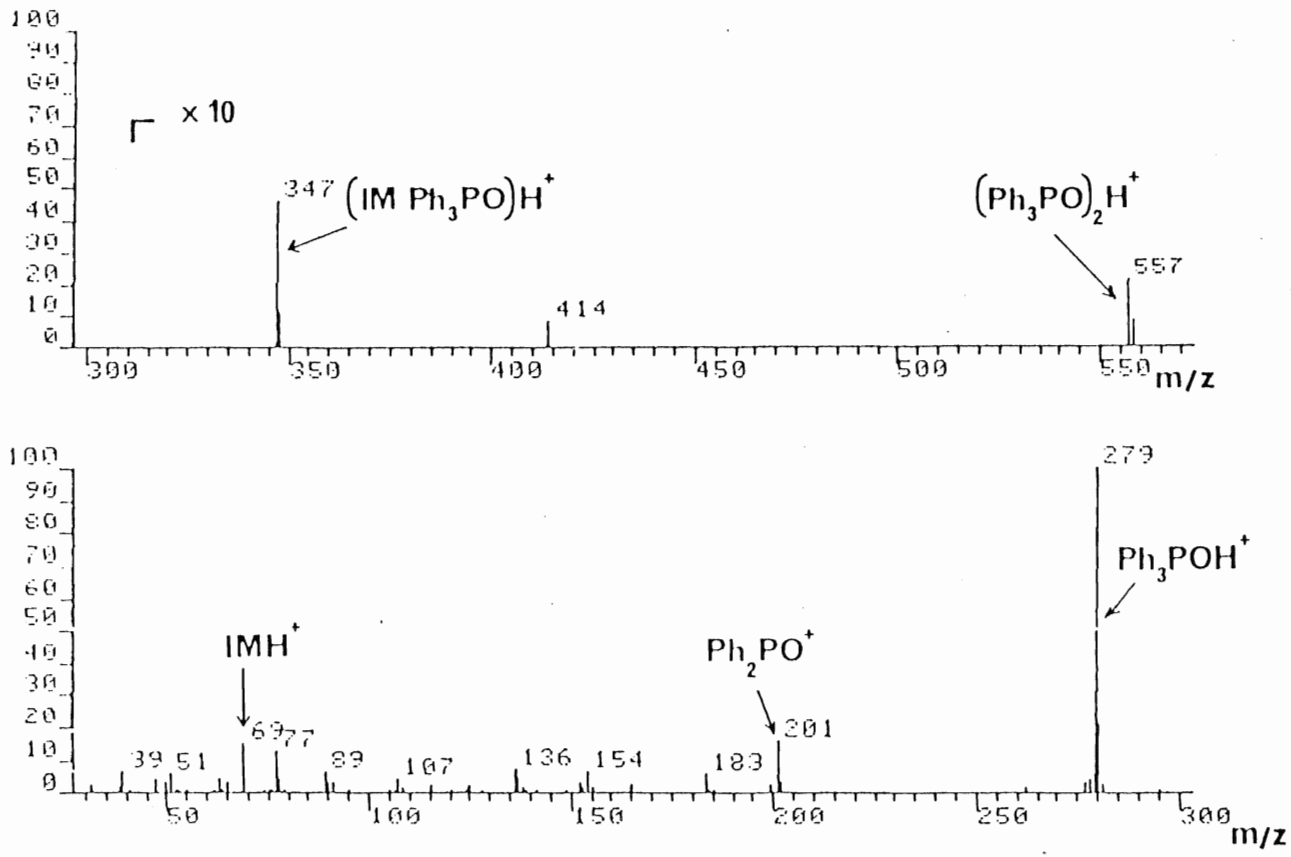

1:1 ratio of the electron donor to imidazole was confirmed by $^{1}H$ nmr. Diphenyl ether did not seem to form a complex. There was no peak corresponding to the hydrogen bonded complex in the FABMS spectrum. For the triphenyl carbinol-imidazole complex, it is possible for the hydrogen bond to have two forms in solution. This arises from the ability of the hydroxy group to act both as a hydrogen bond donor and acceptor. In other words, the triphenyl carbinol could be hydrogen bonded to the imidazole with the hydroxy hydrogen H-bonded to the N3 nitrogen. This complex would not be detectable by FABMS since the N3 position is blocked and ionization would therefore not take place. However, there is a possibility that protonation could occurr at N1 but N3 should be the preferred site. The presence of the triphenyl carbinol-imidazole H-bonded complex in the FABMS mass spectrum cannot be ascertained with definitive certainty as its intensity was rather weak.

The intensity of the peak corresponding to the hydrogen bonded complex of imidazole with the electron donor was not an accurate measure of the complexes' strengths. The use of tetramethyl ammonium iodide as an internal standard at low concentration in the matrix ($6.3X10^{-3}$ M ) failed to give good results presumably because its 'ionization efficiency'is quite different from that of the complex. Furthermore, the use of an internal standard is complicated by possible interactions with analyte and matrix

components[38]. This is why the use of isotopically labeled analogs have become the norm in FABMS quantitation experiment[65]. Thus the 'internal standard' should be chemically similar to the compound of interest if one is to assume that the ionization efficiency of the internal standard and analyte are the same. Riley et al.[66] have reported a good example of FAB quantitation in an industrial context. The same argument holds for measuring the intensity of hydrogen bonded complex relative to the quasi-molecular ion of the electron donor since the ionization efficiency changes from one electron donor to the other. That is to say, the tendency of the electron donors to undergo protonation is not the same throughout the series. Furthermore, the ionization efficiency of the electron donors is not the same as that of the complex. Since ionization of both imidazole and the hydrogen bonded complex involve protonation at the N3 position of imidazole, it was assumed that their ionization efficiencies were similar. Thus, the ratio of the peak abundances corresponding to the complex and protonated imidazole was used as the index of complex strength. This choice was further justified by the similar stabilities of the ion currents corresponding to the protonated imidazole and the hydrogen bonded complex exhibited in the cross scan report (figure 13).

The ionization mechanism of neutral species in

figure 13. Cross-scan report of the imidazole triphenyl phosphine oxide complex in NBA

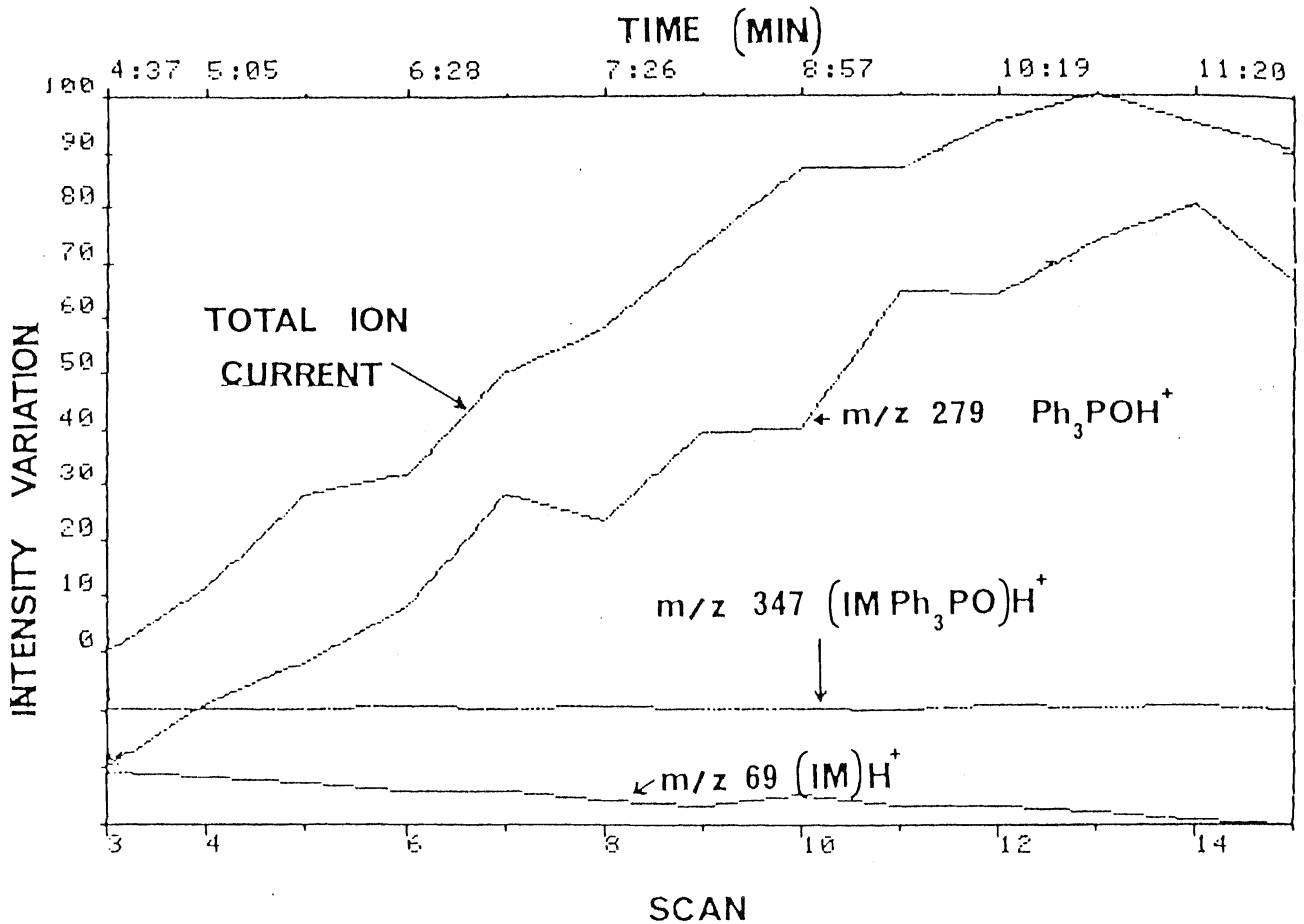

FABMS has been the subject of controversy since the onset of the technique. Clayton and Wakefield[67] have proposed that interaction of the atom beam with the sample or matrix in the condensed phase could cause electron abstraction from the sample or matrix. If a radical cation $[M^{+\cdot}]$ is formed from the sample, a quasi-molecular ion $[M+H]^+$ can arise by hydrogen radical abstraction from a protic matrix. Cooks et al [68] have proposed an ionization mechanism for desorption methods. This mechanism involves ion-molecule reactions (i.e protonation) in the liquid-gas interface (selvedge). In the case of neutral species, the separability of the desorption and ionization events is proposed.

Similarly, Budziekiewicz[69] and co-workers recently proposed that FABMS ionization occurs predominantly in the gas phase. The implication of this postulate is that the function of the matrix, in addition to transport of the neutral substrate into the gas phase, is one similar to a chemical ionization reagent gas. Recent publications by Kebarle[70, 71] point out the contribution of the gas phase basicities of matrices and analytes in the FABMS spectra of simple systems.

Whether the imidazole-electron donor hydrogen bonded complex is ionized in the selvedge or in solution does not deter the fact that the FABMS data shows a good correlation with the expected strength of the hydrogen

bonded complexes. The expected strength of the hydrogen bonded complex is based on the electron density on the electron donor's oxygen atom. The electron density on th oxygen moiety would be expected to rise on going from benzophenone to triphenyl phosphine oxide. The order of H-bond strength as defined in FABMS by the ratio of the ion abundance of the protonated complex over that of the protonated imidazole is listed in table 8.

It can be seen that the FABMS results agree well with the expected hydrogen bond strength which is $Ph_3P=O>$ $Ph_2S=O>$ $Ph_2C=O>$ $Ph_3COH>$ $Ph_2O$.

## B.3. Effect of concentration

The effect of concentration on the abundance of the hydrogen bonded complex with respect to the abundance of imidazole was carried out for the triphenyl phosphine oxide-imidazole complex. As expected, the results (table 9) show the decrease of the complex abundance relative to the imidazole corresponding with the decrease in complex concentration. A plot of the ratio of the complex peak intensity over that of the free imidazole versus the concentration of the complex gives a non-linear relationship (figure 14). The flattening of the upper portion of the plot can easily be rationalized. As the concentration of the complex increases, a monolayer begins to form at the

Table 8. H-bond strength in terms of the [complex]/[free imidazole] ratio

| Complex | Concentration | [complex]/[Im] |
|---|---|---|
| $ph_3P{=}O$/Im | 1.26 | 0.28 |
| $ph_2S{=}O$/Im | 1.26 | 0.15 |
| $ph_2C{=}O$/Im | 1.26 | 0.02 |
| $ph_3COH$/Im | <1.00* | trace |
| $ph_2O$/Im | 1.26 | 0.00 |

* The solubility of the complex in NBA was limited

Table 9. Concentration study on the neutral triphenyl phosphine oxide-imidazole complex in NBA

| Complex | Concentration | Complex/free Im |
|---|---|---|
| $Ph_3P=O/Im$ | 0.08 M | 0.17 |
| $Ph_3P=O/Im$ | 0.42 M | 0.20 |
| $Ph_3P=O/Im$ | 0.84 M | 0.26 |
| $Ph_3P=O/Im$ | 1.26 M | 0.28 |

figure 14. Plot of the concentration of the triphenyl phosphine oxide-imidazole complex against the [complex]/[free imidazole] ratio.

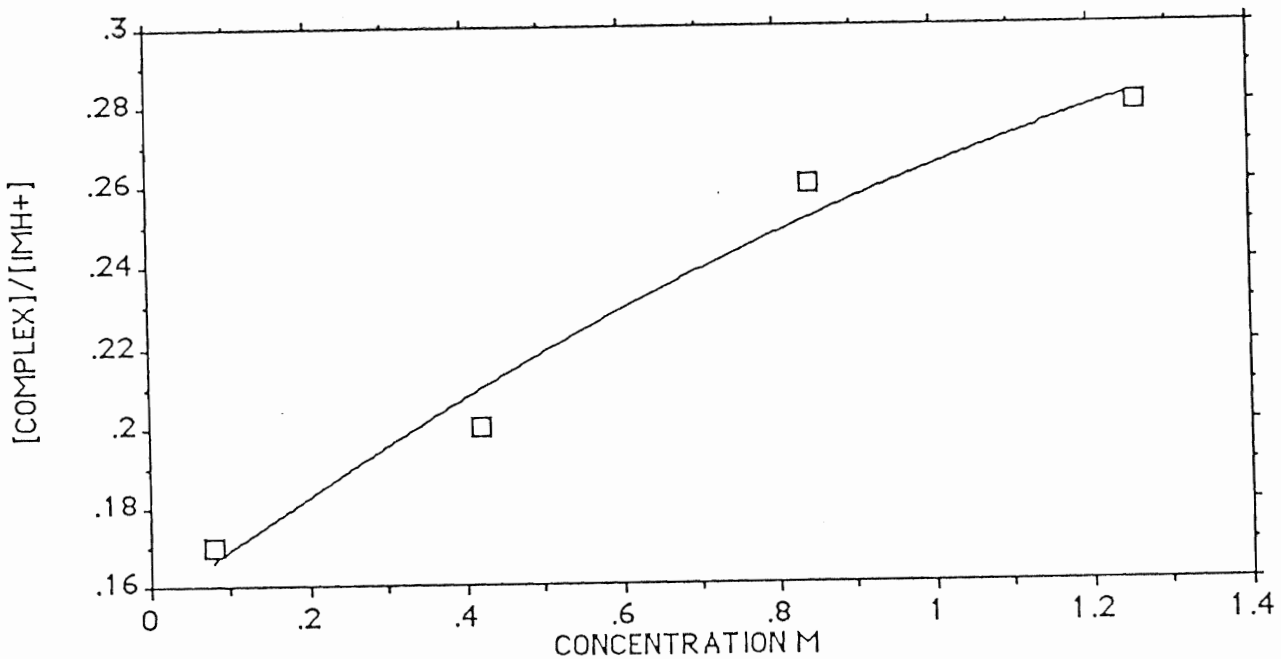

surface of the liquid matrix. This results in increased ion abundances of the analytes and suppression of the matrix spectrum. Further increases in concentration cause a redistribution of the analytes in a more tightly packed form until no further packing can occur. At this point (surface saturation), the measured ion abundances become relatively constant. Whether the ions are sputtered exclusively from the surface[72] or whether there is a contribution from the bulk[73] of the solution has not been firmly established[74]. A surface self-cleaning mechanism has been proposed[75]. The lower [complex]/[imidazole] values at lower concentration can also be understood in terms of more effective competition of the matrix for the imidazole and triphenyl phosphine oxide resulting in more extensive dissociation of the complex.

## B.4. Study of hydrogen-deuterium exchange in the complex

The FABMS analysis of a deuterated imidazole-diphenyl sulphoxide complex showed rapid exchange of the deuterium atom which took part in the hydrogen bond of the complex. The $^{1}H$ nmr of the complex showed approximately 90% deuterium incorporation at the N1 position of the imidazole. FABMS analysis was carried out in normal NBA and dried NBA (4 angstrom molecular sieves

activated at 350°C). The FABMS spectrum of the complex in 'normal'(wet) NBA showed approximately 9% deuterium incorporation in the quasi-molecular ion corresponding to the hydrogen bonded complex. The spectrum also showed that the intensity of m/z 70 was greater than the expected $^{13}C$ contribution from the imidazole quasi-molecular ion. This was probably due to the protonated monodeuterated imidazole. There was also evidence for the presence of imidazole with two deuterium atoms appearing at m/z 71. The M+2 intensity of NBA was slightly greater than the $^{13}C$ contribution to that peak.

The FABMS spectrum in dried NBA was similar to that obtained with normal (wet) NBA. The main difference in the two spectra was a 23% decrease in total ion current when the 'dry' NBA was used. Again, there was only about 9% deuterium incorporation the hydrogen bonded complex as shown by comparing the intensities of m/z 271 and m/z 272. There was no evidence observed in either spectra of the hydrogen bonded complex with two deuterium atoms. The above experiment shows that reduced water content showed no visible effect on the hydrogen-deuterium exchange in the hydrogen bonded complex. This result seems to indicate the possibility that most of the hydrogen deuterium exchange occurred with the liquid matrix. The significant decrease in ion current observed for the 'dry' NBA system indicates that water probably plays a part in the generation of

quasi-molecular ions.

Similar experiments were attempted earlier in undried sulfolane. Doping a mixture of the undeuterated complex and sulfolane with various molar ratios of $D_2O$ showed a higher level of deuterium incorporation in the quasi-molecular ions of the complex, the diphenyl sulphoxide, and the imidazole. This was probably due to the greater number and lability of the $D_2O$ deuteriums. Unfortunately, the sulpholane/$D_2O$ mixture was too volatile in the mass spectrometer and the spectra too transient to provide reliable data. Given the speed and ease of hydrogen exchange in solution of hydrogens involved in hydrogen bonding, it seems reasonable to assume that a large part of the hydrogen-deuterium exchange took place in solution. The contribution of a gas phase mechanism cannot be ruled out, however.

The hydrogen-deuterium exchange most likely occurred with the hydroxy moiety of the NBA (possibly helped by a catalytic amount of water). Contribution from the hydrocarbon hydrogens is unlikely or very small. Ligon[76] has obtained the FABMS spectrum of C-perdeuterioglycerol. A value of 3% deuterium incorporation in the quasi-molecular ion of glycerol (as $[M+D]^+$) was reported. This value is in agreement with that obtained by McCloskey et al[77]. Similarly, the positive ion FABMS of the nucleotide 5'-iodouridine in C-perdeuterioglycerol showed no deuterium

incorporation in the quasi-molecular ion[78].

## B.5. Pre-ionized and 1:2 complexes

Given the higher sensitivity of FABMS for pre-ionized species, a 1:1 imadazole-electron donor complex which bore a formal charge was investigated. This was done simply by making the complex with imidazolium bromide instead of imidazole. The FABMS spectrum of the imidazolium bromide-triphenyl phosphine oxide complex (0.77 M in NBA) was very similar to its 'neutral' counterpart (0.84 M in NBA). At a similar (but lower) concentration, the charged complex spectrum showed seemingly greater suppression of matrix background (figure 15). The total ion currents were comparable. The main difference lied in the considerably higher % total ion current (2.4%) obtained in the pre-charged complex FABMS spectrum for the ion corresponding to the complex (m/z 347). The ion corresponding to the complex carried only 0.4% of the total ion current in the FABMS of the neutral complex. For the charged complex, the [complex]/[imidazole] ratio was 0.46 as opposed to 0.26 for the neutral complex. The reason for the higher abundance of the ion corresponding to the complex in the FABMS spectrum of the pre-ionized complex as opposed to the neutral complex is twofold. First, when the complex is pre-ionized it is bound to exhibit a higher FABMS sensitivity due to the fact

figure 15. FAB mass spectrum of the triphenyl phosphine oxide-imidazole complex in NBA at 0.84 M (top) and of the imidazolium bromide-triphenyl phosphine oxide complex at 0.77 M in NBA (bottom spectrum).

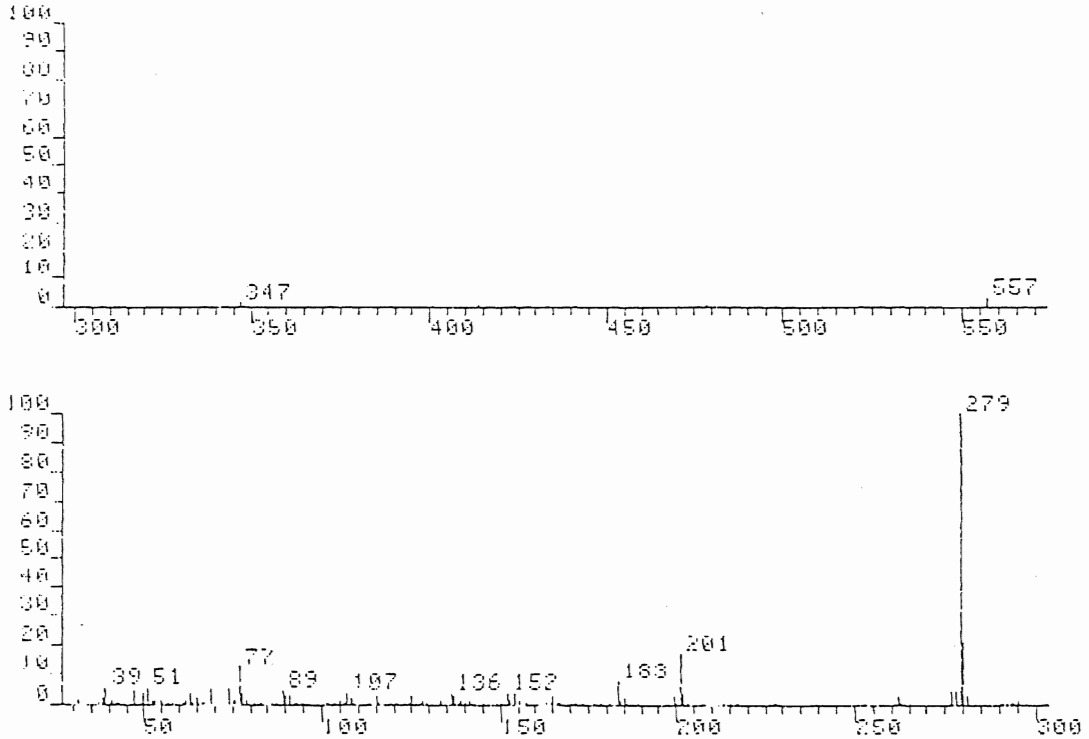

that it only requires to be desorbed to be observed. The efficiency of the ionization event does not really come into consideration. For the neutral complex, a comparatively greater amount of energy is required since its observation in the FABMS spectrum entails ionization and desorption. In this case, the efficiency of the ionization process (whatever it may be) is a governing factor. Second, the pre-ionization (protonation) of the neutral complex undoubtedly changes the strength of the hydrogen bond. The H-bond is probably stronger. This suggestion is substantiated by $^{31}P$ nmr[79] (table 10). The $^{31}P$ chemical shift was 2.8 ppm to lower field for the charged complex compared to that of triphenyl phosphine oxide. For the neutral complex, the difference was slightly more than 1 ppm. To insure that the shift observed for the charged complex was not due simply to the presence of a salt, the $^{31}P$ spectrum of triphenyl phosphine oxide with one molar equivalent of tetra n-butyl ammonium iodide was obtained. No change in the chemical shift was observed. This result clearly shows the stronger H-bonding interaction in the charged complex as opposed to the neutral complex. The respective contributions of these two factors (stronger H-bond and formal charge) to the abundance of the ion corresponding to the complex in the FABMS spectrum of the pre-ionized complex are not clear but are probably more or less additive.

Table 10. $^{31}P$ nmr data of $Ph_3P=O$ complexes (chemical shift in ppm from $H_3PO_4$)

| Compound | Chemical shift |
|---|---|
| $Ph_3P=O$ | 27.04 |
| $Ph_3P=O$-Imidazolium bromide | 29.82 |
| $Ph_3P=O$-Imidazole | 28.06 |
| $Ph_3P=O$-$Bu_4NI$ | 27.08 |

A concentration study was carried out in the same concentration range as that of the neutral complex (table 11 and figure 16). The shape of the line is the same as in figure 14.

Because the observation of the imidazole-electron donor complex depended on protonation of the imdazole (most likely at the N3 position), a study of the complexes of imidazole with two electron donors was undertaken. This can easily be done since protonation of imidazole yields two equivalent hydrogen bonding sites. Thus, the synthesis of the complexes was carried out with imidazolium bromide. The 1:2 complexes for $Ph_2S{=}O$ and $Ph_3P{=}O$ were observed but only at weak intensity. The intensity of the 1:2 complex was very weak but above the background and present in every scan. The intensity of the 1:2 triphenyl phosphine oxide adduct was more intense than that of the diphenyl sulfoxide. The FABMS spectra of the 1:2 complexes were qualitatively similar to the spectra of the 1:1 neutral complexes. The main difference was the enhanced abundance of the 1:1 complex (in terms of [complex]/[imidazole]) of $ph_2S{=}O$ and $ph_3P{=}O$ compared with those obtained in the FABMS of the 1:1 neutral complexes. This is due in part to the higher FABMS sensitivity provided by the pre-formed ions. Also, the greater abundance of electron donor available to hydrogen bond in a 1:1 complex could result in a higher concentration of that complex stoichiometry. The enhancement of the 1:1

Table 11. Concentration study of the $Ph_3P{=}O\text{-}ImH^+Br^-$ complex in NBA

| Concentration | Complex/free Im |
|---|---|
| 0.06 M | 0.13 |
| 0.29 M | 0.23 |
| 0.77 M | 0.46 |
| 1.13 M | 0.56 |

figure 16. Plot of the concentration of triphenyl phosphine oxide imidazolium bromide complex against the [complex]/[free imidazole ratio.

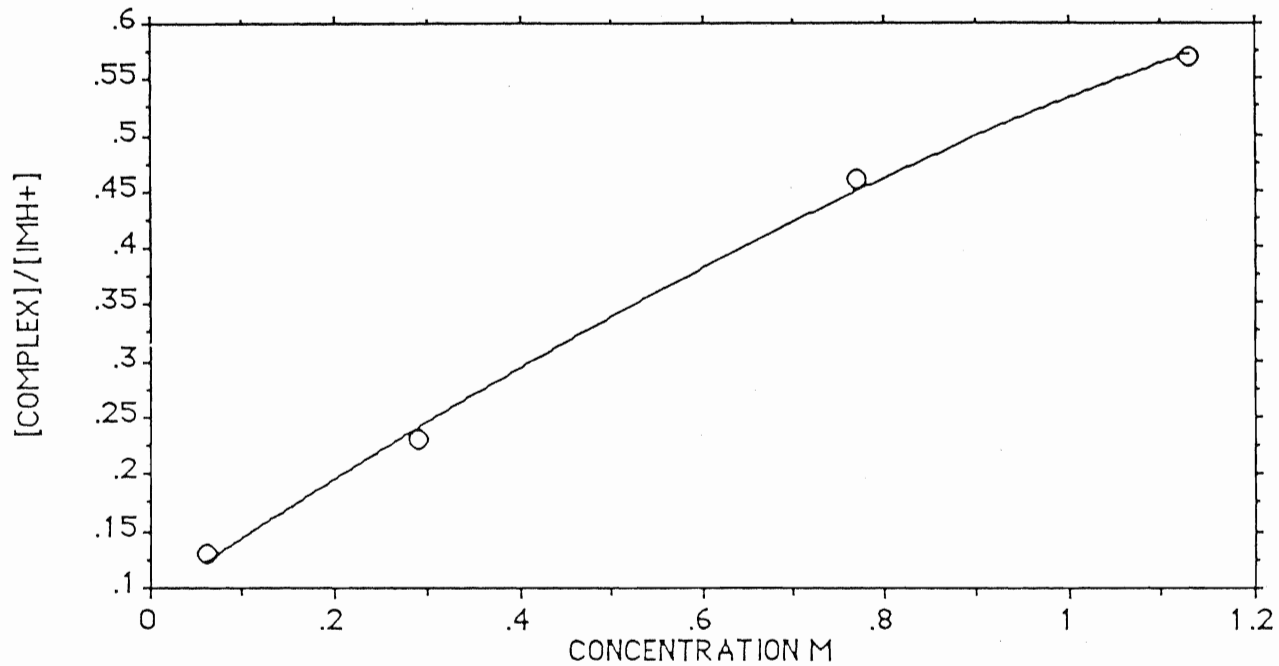

complex could stem in part from the unimolecular dissociation of the 2:1 complex in the ion source. That is to say, the 2:1 complex could be desorbed intact from the surface of the target and undergo subsequent loss of one electron donor prior to accelaration to be detected as the 1:1 complex. When the complex carried a formal charge as above, the effect on the total ion current were not significant. However, matrix spectrum seemed more suppressed.

It seems that even though the contributions from the gas and condensed phases are not clearly separated in determining the appearance of the FABMS spectra of the neutral hydrogen bonded complexes of imidazole. The trend observed in hydrogen bond strength in the imidazole-electron donor series as obtained by FABMS is in agreement with the expected electron donor capability of the compounds used. Nonetheless, confusion between hydrogen bonding of the neutral or protonated species is difficult to resolve at this point. The use of cationic complexes alleviate this ambiguity as well as enhancing the sensitivity of FABMS to those complexes. It has been shown that extensive rapid hydrogen exchange involving the hydrogen bond goes on in the liquid matrix. The effect of complex concentration on the spectra is coherent although not linear. This can be attributed to the fact that a complex equilibrium was being sampled. This study indicates that it is possible to obtain

qualitative information on the hydrogen bond strength of some complexes. The study of the hydrogen bonding of pre-formed ions (anions or cations) should be straightforward although this condition greatly limits the applicability of the technique. A further use of FABMS for H-bonding would be to obtain the relative proton affinities of compounds normally intractable by mass spectrometry using Cooks' method[80].

## C. Multiple Donor Systems

### C.1. Miscellaneous Systems

As mentioned in the previous section, it was concluded that the use of cationic H-bonded complex has the advantage of enhancing the FABMS sensitivity of the complex being studied. Brown and Miller[81] have investigated the H-bonding of trialkyl ammonium and pyridinium halides to a series of electron donors. We have undertaken a parallel study of cationic H-bonding systems with multiple donor-acceptor capability. The basic idea behind the having more than one H-bond in the complex was to increase the stability of the complex through multiple H-bonding.

The initial attempt in this direction was started with the bipyridyl ligand as electron donor and dimethyl ammonium chloride as the acceptor. It was hoped that both bipyridyl nitrogens could form hydrogen bonds with the two dimethyl ammonium N-H protons. The FABMS of the 'complex' gave the quasi-molecular ion of the bipyridyl ligand as the only significant ion. In order to reduce the distance between the nitrogen donors, 1,10-phenanthroline was used as the ligand. Reducing the distance betweeen the nitrogen donor atoms was thought to increase the posssibility of double H-bond formation. Complex synthesis was attempted but confirmation of H-bond formation by infra red could not

be obtained due to the presence of water. In fact all dialkyl ammonium salts suffered from this drawback. A trial run with high sample loading in NBA of the 1,10-phenanthroline-dimethyl ammonium chloride complex gave a weak peak corresponding to the cationic complex. The weak complex observed in the FABMS could be due to the fact that a double hydrogen bond was not formed. The rigidity of the phenanthroline ring would require a rather exact fit of the N-N and H-H distances.

## C.2. Sulfone Systems

Because of the proximity of the two oxygen donor sites to one another and the favorable six membered ring configuration that would result if double H-bond formation occured with the dialkyl ammonium cation, sulfones were investigated as 'double' donors. A complex synthesis was attempted with tetramethylene sulfone and dimethyl ammonium chloride. No complex formation was observed as the two compounds seperated after the solvent had evaporated under vacuum. However, a diphenyl sulfone-dimethyl ammonium chloride complex seemed to be formed as the FABMS spectrum of the complex in NBA (0.6 M ) showed a significant peak corresponding to the complex at m/z 264 and carrying 2.2% of

the total ion current. The base peak of the mass spectrum was the dimethyl ammonium cation at m/z 46. The quasi-molecular ion of the diphenyl sulfone appeared at m/z 219. A small peak corresponding to the dimethyl ammonium-NBA adduct (presumably H-bonded) was present. The $[(CH_3)_2NH_2^+]_2Cl^-$ ion due to electrostatic clustering of the type $[M^+]_nX^-_{n-1}$ where M is the cation and X is the counter ion. The scheme in figure 17 represents the possible equilibria. This scheme only takes into account the species observed in the FABMS spectrum of the diphenyl sulfone complex.

A concentration study was undertaken to see how the ion corresponding to the complex varied with concentration (table 12). The % total ion current carried by the complex increased with increasing concentration as expected. As with other systems, the matrix background and adduct peaks decrease with increasing concentration (figure 18). This was also true with respect to the [complex]/$[Ph_2SO_2H^+]$ ratio. The reasons behind the relatively high stability of this complex (presumably H-bonded) are possibly threefold. First, cationic H-bonds are usually stronger than neutral ones. Second, the possibility of forming two H-bonds instead of one could increase the complex stability. Third, if the 'double' H-bond forms, the resulting six membered cyclic structure should bring added stability to the complex. It is not

Table 12. Concentration study with the diphenyl sulfone dimethyl ammonium chloride complex

| Concentration (M/L) | [complex]/[$ph_2SO_2H^+$] |
|---|---|
| 0.06 | 0.16 |
| 0.16 | 0.37 |
| 0.61 | 0.72 |
| 1.07 | 0.91 |

Figure 17. Schematic equilibria between diphenyl sulfone and the amine salt in NBA

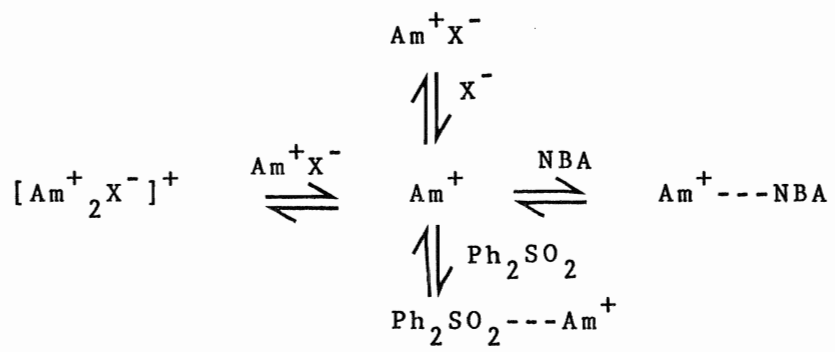

Figure 18. FAB mass spectrum of the diphenyl sulfone dimethyl ammonium chloride complex at concentrations of 0.61 M (top) and 0.16 M (bottom).

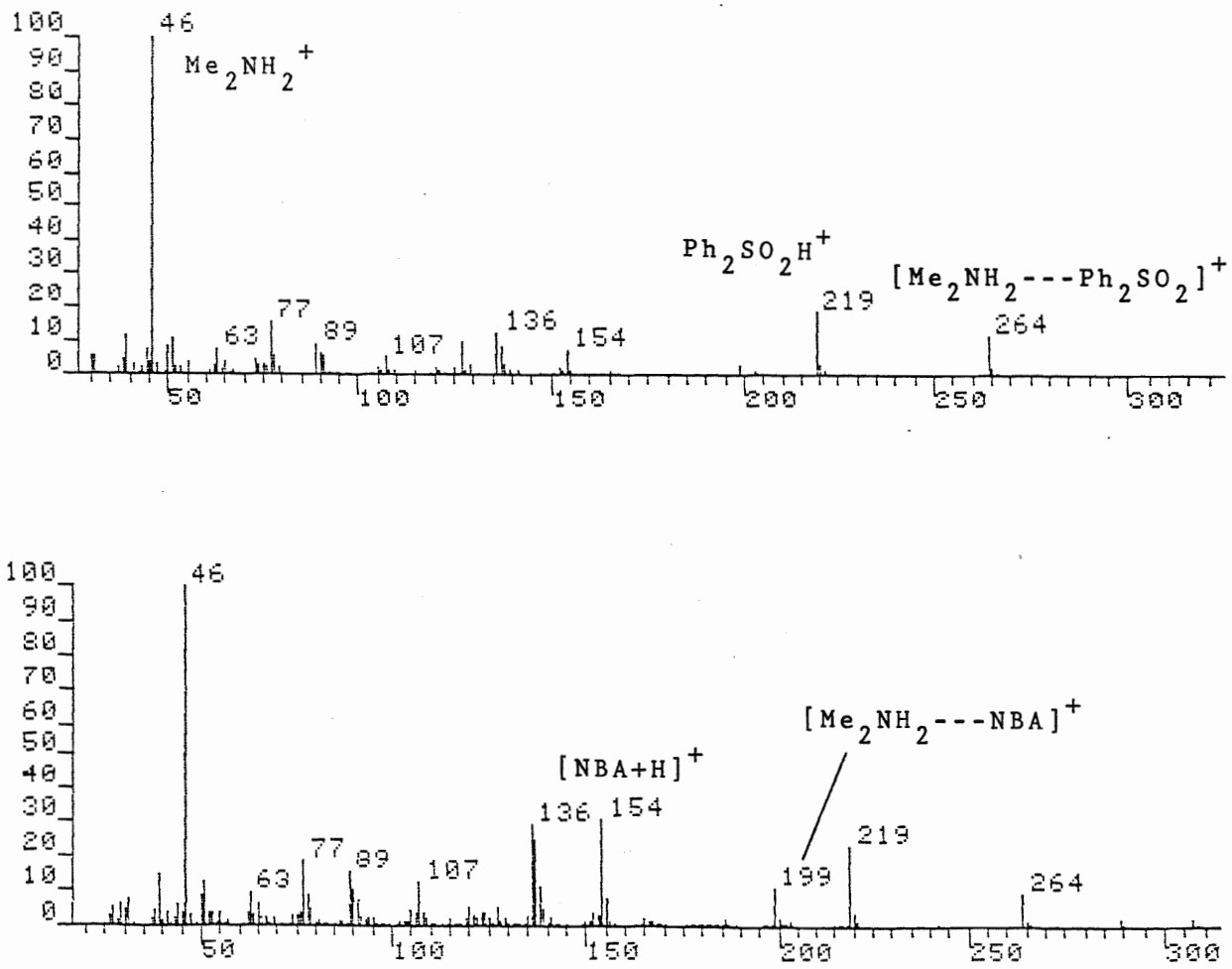

possible at this point to verify the formation of a 'double' H-bond in this system.

The stability of the complex ( i.e the fact that it is observed in FABMS) is surprising given the consistent claims in the literature concerning the weak hydrogen bonding properties of sulfones[82,83,84]. The premise that the complex is held by H-bonding was supported by the drastic reduction in the complex ion intensity (0.1% total ion current) when a stronger H-bonding matrix such as glycerol was used. The use of a stronger H-bonding matrix should interfere with the observation of a H-bonded complex.

The lesser H-bonding capability of diphenyl sulfone with respect to other electron donors was demonsrated in a competitive study with triphenyl phosphine oxide. In the first system, the diphenyl sulfone-dimethyl ammonium chloride complex was mixed in a 1:1 molar ratio with triphenyl phosphine oxide in NBA. The triphenyl phosphine oxide-dimethyl ammonium complex appeared at m/z 324 as more than 10% of the base peak. The diphenyl sulfone complex was not observed above the background noise. In an another competitive system, triphenyl phosphine oxide, diphenyl sulfone, and pyridinium iodide were mixed in a 1:1:1 molar ratio. Again, a strong triphenyl phosphine oxide-pyridinium complex was observed but no diphenyl sulfone complex.

The effect of the counter ion was investigated with the dimethyl ammonium iodide-diphenyl sulfone complex. As expected, the ion abundance of the complex was enhanced relative to that of the chloride salt. Because the cluster ion $[(Me_2NH_2^+)_2I^-]^+$ was isobaric with the diphenyl sulfone quasi-molecular ion, the m/z 219 peak was deconvoluted using the known isotopic contributions of each ion. The [complex]/[$Ph_2SO_2H$] ratio was 1.0 and 0.7 at 0.6 M for the iodide and chloride, respectively. This can easily be rationalised in terms of the H-bonding ability of the anion. With a stronger H-bonding anion, a comparatively smaller amount of the dimethyl ammonium cation will be capable of H-bonding to the diphenyl sulphone. These results correlate with those of Brown and Miller[81].

The complexes of diethyl ammonium chloride and diisopropyl ammonium iodide with diphenyl sulfone were analysed by FABMS at a concentration of 0.6 M in NBA. The results indicate a significant decrease in the ion abundance of the peak corresponding to the complex compared with the dimethyl ammonium chloride complex. As the size of the alkyl chain on the ammonium salt increased, the ion abundance of the respective complexes decreased in terms of % total ion current (table 13.). The FABMS spectrum of the di-isopropyl ammonium iodide-diphenyl sulfone complex in figure 19 illustrates this well. It can be seen that the ion due to clustering of the salt at m/z 331 is much more

Table 13. [complex$^+$]/[$Ph_2SO_2H^+$] ratio for various amine salts

| Amine salt | ratio | % TIC of complex |
|---|---|---|
| $Me_2NH_2Cl$ | 0.72 | 2.9 |
| $Me_2NH_2I$ | 1.00 | 3.1 |
| $Et_2NH_2Cl$ | 0.61 | 2.2 |
| $(i\text{-}Pr)_2NH_2I$ | 0.28 | 0.6 |
| Imidazolium iodide | 0.61 | 2.4 |
| Pyridinium bromide | 0.60 | 2.3 |

Figure 19. FAB mass spectrum of the diphenyl sulfone di-isopropyl ammonium iodide complex at a concentration of 0.6 M

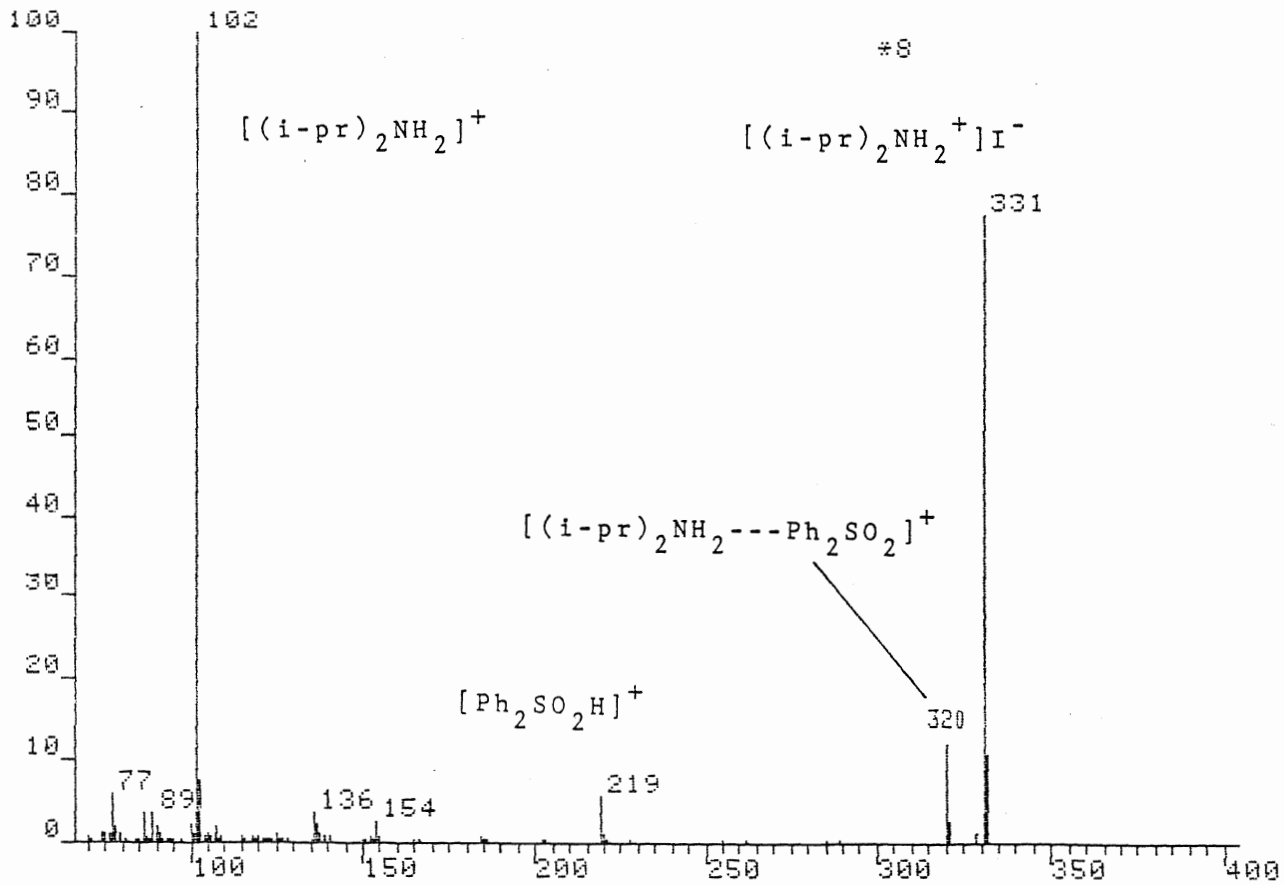

abundant than that due to the complex. This could be interpreted as a measure of the amount of uncomplexed ammonium salt. In order to see if the ability of the hydrogen bond acceptor to form more than one H-bond was a significant factor, complexes that could only be held by a single H-bond were made with pyridinium iodide and imidazolium iodide.

After failing to observe a complex ion for dimethyl sulfone and dimethyl ammonium chloride, solution infrared spectra were obtained in dry acetonitrile for dimethyl ammonium chloride, diphenyl sulfone, and the corresponding complex. No band shifts for either the N-H stretch or the S-O stretch were observed in the solution infrared spectra of the complex relative to the spectra of dimethyl ammonium chloride and diphenyl sulfone. This could be due to the use of a polar solvent which could interfere with H-bond formation. Ruostesuo[83] has studied the H-bonding properties of diphenyl sulfone in $CCl_4$ and reported that sulfones form consistently weaker H-bonds than sulfoxides, as expected. It has been reported that tetramethylene sulfone forms a weak H-bonded adduct with phenol[84]. There is no study of the H-bonding of sulfones where a 'double' H-bond is possible. Due to the ionic nature of the compound, it was not possible to use a less polar solvent to attempt to observe the H-bond.

The question then arises; is the origin of these

complexes in large part or entirely a gas-phase phenomenon? The question is central to the origin of quasi-molecular ions in FABMS and is part of ongoing efforts to elucidate more clearly the basic mechanisms in this relatively new technique. It should be stressed that to speak of 'gas' phase behavior and 'solution' behavior in FABMS is difficult since the region right above the matrix (the selvedge) where many recombination processes may take place is neither a gas nor a liquid. The positive ion ammonia chemical ionization spectra of diphenyl sulfone and sulfolane both show the $[M+NH_4]^+$] adduct as the only significant peak. Nonetheless, the gas phase origin of the complexes of this particular system seems coherent with some findings in ammonia chemical ionization. In a recent review[85], Westmore and Alauddin cited three factors that could affect the amount of $[M+NH_4]^+$ adducts (presumably H-bonded) present in positive ion $NH_3$ chemical ionization spectra. These are: the proton affinity of analyte, the site of protonation, and the presence and configuration of a bifunctional group in the analyte.

The proton affinity (PA) of the analyte (M) defines what the $[M+NH_4]^+/[M+H]^+$ ratio will be. Thus, when $PA(M)<PA(NH_3)$ the adduct to quasi-molecular ion ratio is high. When $PA(M)>PA(NH_3)$ both $[M+NH_4]^+$ and $[M+H]^+$ can be anticipated with the ratio decreasing with increasing PA(M). But if M is much less basic than $NH_3$, The $[M+NH_4]^+$ complex

is formed with little excess energy. However, the dissociation energy of the complex is also quite low so that the $[M+NH_4]^+/[M+H]^+$ will be low. In our case the site of protonation is assumed to be the sulfone oxygens and is thus constant throughout the series. The effect of the presence of a bifunctional group and its configuration on ammonia chemical ionization spectra has been shown by Stahl[86] in the case of some cyclic diols. For example, both cis and trans-1,2-cyclopentanediol exibited abundant $[M+NH_4]^+$ ions due to the fact that it is possible for both of them to attach and stabilize the ammonium ions in structures with linear H-bonds where both hydroxy moieties are involved. The $[M+H]^+$ peaks were two orders of magnitude smaller.

The present system is more complex for three reasons. First, the dialkyl ammonium cations are not 'free' as they can be solvated by the matrix or held in ion pairs by their counter ion thus preventing complex formation. Second, the steric factors are more important as the smallest cation has two methyl groups and two protons instead of just four protons for the ammonium ion. Third, in some cases the possibility of forming the 'double' hydrogen bond could be a stabilizing factor. Dialkyl and trialkyl amines have been used as chemical ionization reagents[87] for flavones but the structural complexity of the analytes and the fact that ion source conditions were not constant does not allow one to draw conclusions from the

Figure 20. Possible configuration of the $NH_4^+$ adducts of cis- and trans-1,2-cyclopentanediol

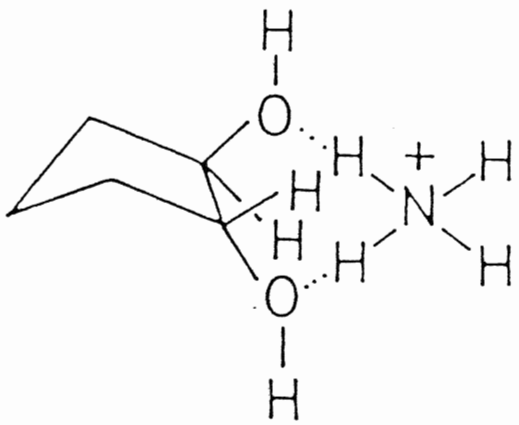

TRANS

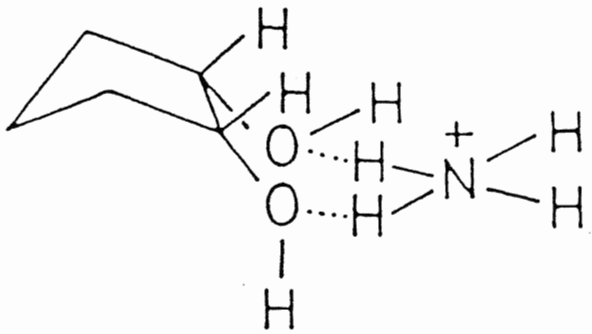

CIS

data. Table 13 gives the $[complex^+]/[Ph_2SO_2H^+]$ ratio for the various ammonium salts.

As mentioned earlier, the higher ratio for the dimethyl iodide as opposed the chloride is consistent with the greater H-bonding ability of the chloride resulting in less 'free' dimethyl ammonium cation. The difference between the dimethyl, diethyl, and di-isopropyl ammonium halides can be rationalized in terms of steric hindrance. Even though the di-isopropyl ammonium cation has the highest proton affinity and the weakest H-bonding anion, it has by far the greatest steric hindrance. Dimethyl amine and pyridine have virtually identical proton affinities and low steric hindrancce for H-bond formation. Yet dimethyl ammonium has a higher complex to diphenyl sulfone quasi-molecular ion ratio than the pyridinium despite the fact that the pyridinium has a more favorable cation-anion combination for complex formation with the sulfone. This can be explained in terms of the possibility of 'double' H-bond formation for the dimethyl ammonium ion which would increase the stability of the complex. On the other hand, the pyridinium ion does not have that capability. The fact that diphenyl sulfone forms an abundant adduct ion with $NH_4^+$ and virtually no $[M+H]^+$ in the positive ion ammonia chemical ionization spectrum is an indication that its proton affinity is significantly lower than that of ammonia. Hence, diphenyl sulfone is much less basic than the amines

used in this study so that increasing proton affinities of the amine will result in less $[Ph_2SO_2\text{--}H_2NR_2]^+$ being observed in the FABMS spectrum.

To conclude, the evidence at hand does not allow one to conclude that FABMS reflects the solution behavior of the system. The magnitude of the $[complex^+]/[Ph_2SO_2H^+]$ ratio can be rationalized qualitatively by using the following factors: strenght of cation-counter ion interaction, absence or presence of the possibility for the ammonium cations to form a 'double' H-bond, and finally steric hindrance factors. It is also difficult to interpret the effect of proton affinities given the strong influence of other factors. The competitive experiments indicate that the diphenyl sulfone-dimethyl ammonium complex is weaker than that with triphenyl phosphine oxide.

## D. Conclusion

It has been shown that FABMS has good potential for the study of condensed phase systems. The FABMS results obtained for the tdoha-alkali metal halide system correlated qualitatively with those in the literature[56] (obtained by potentiometry). The only disagreement concerned the affinity of tdoha for the lithium cation but this discrepancy was found to be consistent with the difference in solvent systems. When a more analoguous solvent system (glycerol/water) was used in FABMS, There was better relative agreement with the potentiometric values.

The FABMS spectra of the H-bonded imidazole-electron donor complexes were found to agree with the expected order of H-bond strenghts. The influence of the H-bonding ability of the matrix liquid on the complex abundance was demonstrated. The imidazolium bromide-triphenyl phosphine oxide complex was shown to be stronger in the FABMS spectra than its neutral counterpart. This result was supported by phosphorus-31 nmr.

Although it was not possible to ascertain whether FABMS truly reflected solution chemistry, the value of the $[complex^+]/[Ph_2SO_2H^+]$ ratio was consistent with certain qualitative considerations such as steric hindrance and strength of ion pairs. The FABMS results from the

competitive systems was consistent with studies showing that the sulfones form weaker H-bonds than phosphine oxides[88].

The use $^{15}N$ nmr would be interesting since all the compounds studied were nitrogen containing. However, the technique is not straightforward but would be useful in providing additional data on the systems investigated. The fact that the contribution of solution or gas phase ionization mechanisms in FABMS have not been resolved limits the conclusions one can draw from the spectra. This implies a certain amount of caution in interpreting FABMS results. The trend in the literature at this point is to rationalize FABMS processes along the lines of gas phase behavior. This is hardly surprising since fundamental research in mass spectrometry is carried out by 'gaseous ion' chemists. Nonetheless, the author prefers the approach of Fenseleau[89] and Cotter which acknowledges the existence of multiple mechanisms of ion formation in FABMS and that the contribution of those mechanisms is largely system dependent. However, this does not prevent one from obtaining a qualitative image of solution processes from FABMS provided data interpretation is cautious and preferably supported by another method.

The difference in solvent systems used in FABMS as opposed to other methods (IR and nmr, for example) for the study of solution processes is a significant limitation in terms of data comparison since both qualitative and

quantitative aspects of the FABMS spectrum are influenced by the solution chemistry of the liquid matrix. The use of continuous flow probes may alleviate this drawback by allowing the use of more volatile and more common solvents. Cook and Todd have recommended that matrices be characterized by their dielectric constants and have started to measure and tabulate these physical constants for the most popular matrices. The increased availability of physical data on liquid matrices should enhance our understanding of FABMS processes and lead the technique from an empirical to a more systematic approach. Although the initial optimism which originally greeted FABMS has been somewhat dampened by a more critical look at the limitations of the technique, there is no doubt that the potential of investigating the dynamics of the condensed phase with a technique that analyses gaseous ions broadens the field of mass spectrometry into a new and exciting area.

## References


1. M. Barber, R.S Bordoli, E.J. Elliott, R.P. Sedgewick and A.N. Tyler, Nature, 293 , 270 (1981).

2. A. Benninghoven, Surface Science, 35 , 427, (1973).

3. A. Benninghoven, Int. J. Mass Spectrom. Ion Proc., 46 , 459, (1983).

4. F.M. Devienne, J.C. Roustan, Org. Mass Spectrom., 17 , 173, (1983).

5. A.L. Burlingame, T. Baillie, P.J. Derrick, Anal. Chem., 58 , 165R, (1986).

6. J. Perel, J. Mahoney, S. Taylor, Am. Lab., March 1984, 92.

7. J. Perel, in Desorption Mass Spectrometry, Are SIMS and FAB the Same? , P.A. Lyon, ed., A.C.S. Symposium Series, No. 291, Am. Chem. Soc., Washington, 1985.

8. K. Biemann, S.A. Martin, C.E. Costello, Anal. Chem. 54 , 2362, (1982).

9. R. Stoll, V. Schade, F.W. Rollgen, U. Geissmann, D.F. Barofsky, Int. J. Mass Spectrom. Ion Proc. 43 , 227, (1982).

10. D.S. Wong, R. Stoll, F.W. Rollgen, Z. Natursforsch, 37A , 718, (1982).

11. N.A. Rudat, C.N. McEwen, Int. J. Mass Spectrom. Ion Proc. 46 , 351, (1983).

12. D.F Barofsky, in Desorption Mass Spectrometry, Are SIMS and FAB the Same? , P.A. Lyon, ed., A.C.S. Symposium Series, No. 291, Am. Chem. Soc., Washington, (1985).

13. J.F. Mahoney, J. Perel, A.T. Forrester, Appl. Phys. Lett., 38 , 320, (1983).

14. J. Frank, Int. J. Mass Spectrom. Ion Proc., 46 , 343, (1983).

15. a) C.W. Maggee, in Desorption Mass Spectrometry Are SIMS and FAB the Same? , P.A. Lyon, ed., A.C.S. Symposium series, No. 291, Am. Chem. Soc., Washington, 1985.
    b) J. Perel, IBID.

16. A. Burlingame, Anal. Chem., 56 , 2195, (1984).

17. J.L. Gower, Biomed. Mass Spectrom., 12 , 191, (1985).

18. E. DePauw, Mass Spectrom. Rev., 5 , 191, (1986).

19. M. Barber, R.S. Bordoli, G.J. Elliott, R.D. Sedgewick, A.N. Tyler, Anal. Chem., 54 , 645A, (1982).

20. B.D. Musselman, J.D. Watson, C.K. Chang, Org. Mass Spectrom., 21 , 215, (1986).

21. T. Keough, Anal. Chem., 57 , 2022, (1985).

22. B.D. Musselman, J. Allison, J. Watson, Anal. Chem., 57 , 242, (1985).

23. E. DePauw, G. Pelzer, J. Marien, J. Piette, M. Purdan, Org. Mass Spectrom., 20 , 692, (1985).

24. M.M. Ran, D.A. Kidwell, J.E. Campana, Anal. Chem., 56 , 2142, (1984).

25. E. Tolun, C.J. Porter, J.F.J. Todd, M.A. Walsh, J.A. Connor, Org. Mass Spectrom., 19 294, (1984).

26. R.M. Caprioli, T. Fan, J.S. Cottrell, Anal. chem., 58 , 2092, (1986).

27. R.M. Caprioli, T. Fan, Biochem. Biophys. Res. Comm., 141 , 1058, (1986).

28. R.M. Caprioli, Anal. Chem., 55 , 2387, (1983).

29. L.A. Smith, R.M. Caprioli, Biomed. Mass Spectrom., 10 , 98, (1983).

30. R.A.W. Johnstone, M.E. Rose, J. Chem. Soc.Chem. Comm., 1268, (1983).

31. H.T. Kalinowski, U. Haskell, G.D. Daves jr., D.F. and E. Barofsky, J. Am. Chem. Soc., 107 , 6476, (1985).

32. K. Saito, R. Kato, Biochem. Biophys. Res. Comm., 124 , 1, (1984).

33. M.E. Rose, C. Longstaff, P.D.G. Dean, Biomed. Mass Spectrom., 10 , 512, (1983).

34. L.A. Smith, R.M. Caprioli, C.F. Beckner, Int. J. Mass Spectrom. Ion Proc., 46 , 419, (1983).

35. L.A. Smith, R.M. Caprioli, Anal. Chem., 58 , 2949, (1986).

36. G. Pelzer, E. DePauw, Dao Viet Dung, J. Marien, J. Phys. Chem., 88 , 5065, (1984).

37. P.J. Gale, B.L. Bentz, D.T. Chait, F.H. Field, R.J. Cotter, Anal. Chem., 58 , 1070, (1986).

38. Mass Spectrometry: a Specialist Periodical Report , M.E. Rose, Senior Reporter, The Royal Society of Chemistry, 1985.

39. K.D. Cook, Mass Spectrom. Rev. 5 , 467, (1986).

40. K.W.S. Chan, K.D. Cook, Anal. Chem., 55 1422, (1982)

41. V.F. Man, J.D. Lin, K.D. Cook, J. Am. Chem. Soc., 107 , 4635, (1985).

42. M.D. Joestan, J.L. Schaad, Hydrogen bonding , Marcel Dekker inc., New York, 1974.

43. P. Kebarle, Ann. Rev. in Phys. Chem. 28 , (1977).

44. M.M. Bursey, T.A. Lehman, Ion Cyclotron Resonance Spectrometry , Wiley, New York, 1976.

45. J.H. Clark, M. Green, R. Madder, C.D. Reynolds, Z. Dauter, J.M. Miller, T. Jones, J. Am. Chem. Soc., 106 , 4056, (1984).

46. T.R. Sharp, M.R. White, J.F. Davis, P.J. Strong, 31st Conf. Am. Soc. Mass Spectrom., Boston, 1983.

47. G. Soula, J. Org. Chem., 50 3717, (1985).

48. F. Voegtle, E. Weber, Angew. Chem. Int. Ed. Engl., 18 , 753, (1979).

49. F. Voegtle, W.M. Muller, W. Wehner, E. Bucheier, Angew. Chem. Int. Ed. Engl., 16 , 548, (1977).

50. F. Voegtle, K. Frensch, Tet. Lett., 1977 , 2573.

51. C.L. Liota, H.P. Harris, J. Am. Chem. Soc. 96 , 2250, (1974).

52. J.H.Clark, J.M. Miller, J. Chem. Soc. Chem. Comm., 1982 , 1318.

53. M. Witanowski, L. Stefaniak, G.A. Webb, Ann. Rep. NMR Spectros., 18 (1986).

54. R.A.W. Johnstone, M.E. Rose, I.A.S. Lewis, Tetrahedron, 39 , 1597, (1983).

55. J.D. Lamb, R.M. Izatt, J.J. Christensen, D.J. Eatough, in, Coordination Chemistry of Macrocyclic Compounds , G.A. Melson, ed., Plenum press, New York, 1979.

56. F. Voegtle, U. Heimann, M.H. Erzhoff, Chem. Ber., 112 , 1392, (1979).

57. F. Voegtle, E. Weber, The Chemistry of Functional Groups, Supplement E: The Chemistry of Ethers, Crown Ethers, OH Groups, and their Sulphur Analogues, Part 1, p142 J. Wiley and Sons, New York, 1983.

58. G. Weber, G.M. Sheldrick, Inorg. Chim. Acta., 45 , L35, (1979).

59. W Saenger, Host-Guest Chemistry: Macrocycles , Springer Verlag, New York, 1985.

60. J.M. Lehn, Structure and Bonding, 16 , 1, (1973)

61. J.M. Lehn, J.P. Sauvage, J. Am. Chem. Soc., 97 , 6700, (1975).

62. J.H. Clark, M. Green, R.G. Madden, J. Chem. Soc. Chem. Comm., 1983 , 136.

63. S.J. Brown, J.M. Miller, R.Theberge, J.H.Clark, Can. J. Chem., 64 , 1277, (1986).

64. J. Emsley, J. Chem. Soc. Chem. Rev., 10 , 91, (1980)

65. R.L. Cochran, Appl. Spectros. Rev., 22 , 137 (1986).

66. B. Riley, J.L. Gerlock, T.J. Prater, D. Schuetzle, Anal. Chem., 56 , 2145, (1984).

67. E. Clayton, A. Wakefield, J. Chem. Soc. Chem. Comm., 969, (1984).

68. R.G. Cooks,K.Busch, Int. J. Mass Spectrom. Ion Proc., 53 , 111, (1983).

69. H. Budziekiewicz, E. Schroder, H. Munster, Org. Mass Spectrom., 21 , 707, (1986).

70. J.A. Sunner, S. Kulatunga, P. Kebarle., Anal. Chem., 58 , 1312, (1986).

71. J.A. Sunner, A. Morales, P.Kebarle, Anal. Chem., 59 , 1378, (1987).

72. Barber M., R.S. Bordoli, G.J. Elliott, R.D. Sedgewick, A.N. Tyler, J. Chem. Soc. Faraday Trans. 1, 79 , 1249, (1983).

73. W.V. Ligon, S.B. Dorn, Int. J. Mass Spectrom. Ion Proc., 57 , 75, (1984).

74. S.S. Wong, F.W. Rollgen, Nucl. Inst. and Meth., B14 , 436, (1986).

75. S.S. Wong, F.W. Rollgen, I. Manz, M. Przybylski, Biomed. Mass Spectrom., 12 43, (1985).

76. W.V. Ligon, Int. J. Mass Spectrom. Ion Proc., 52 , 183, (1983)

77. J.A. McCloskey, S.K. Sehti, S.C. Pomerantz, Anal. Chem., 58 , 2890, (1986).

78. S.K. Sehti, C.C. Nelson, J.A. McCloskey, Anl. Chem., 56 , 1975, (1984).

79. O.W. Kolling, Trans. of the Kansas Acad. of Science, 87 , 115, (1984).

80. R.G. Cooks, J. Am. Chem. Soc., 103 , 1313, (1981).

81. S.J. Brown, J.M. Miller, J. Chem. Soc. Perkin Trans 1, In press.

82. T. Durst, in Comprehensive Organic Chemistry , D. Barton, ed, Pergammon Press, 1979.

83. P. Ruostesuo, J. Karjalainen, Spectrochim. Acta, 37A , 535, (1981).

84. R.S. Drago, B. Wayland, R.L. Carson, J. Am. Chem. Soc., 85 , 3125, (1963).

85. J.B. Westmore, M.M. Alauddin, Mass Spectrom. Rev., 5 , 381, (1986).

86. D.J. Stahl, F.D. Winkler, Adv. Mass Spectrom., 8A , 887, (1980).

87. V.S. Bantova, N.N. Mallova, S.S. Popov, Org. Mass Spectrom., 21 , 109, (1986).

88. A.A Maskowsky, A. Niabullin, S.E. Odinokov, Spectrochim. acta, 39A , 1065, (1983).

89. C. Fenseleau, R.J. Cotter, Chem. Rev., 87 , 501, (1987).

# Appendix I

Part 1. The FAB mass spectra of the tdoha-alkali metal halide saturated solutions

## FAB of LiCl/tdoha saturated solution

5i5LCL.1 [TIC=397360, 100%=110804] EI

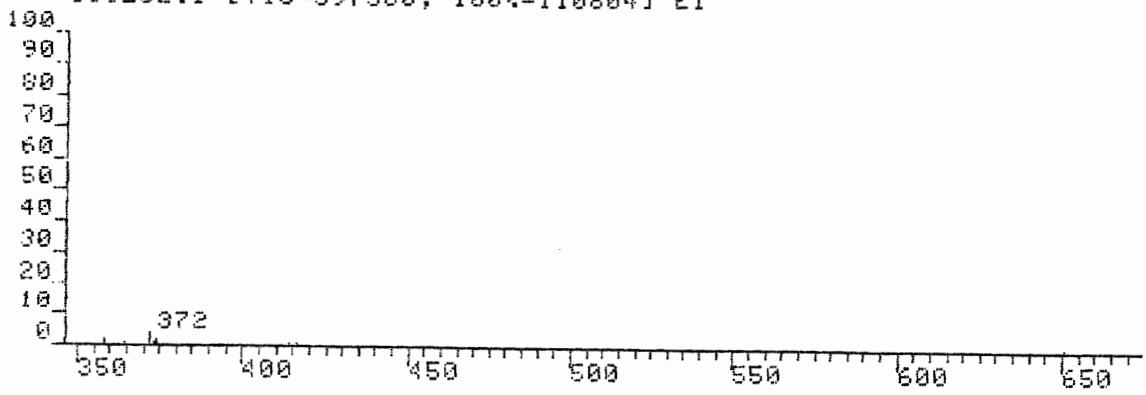


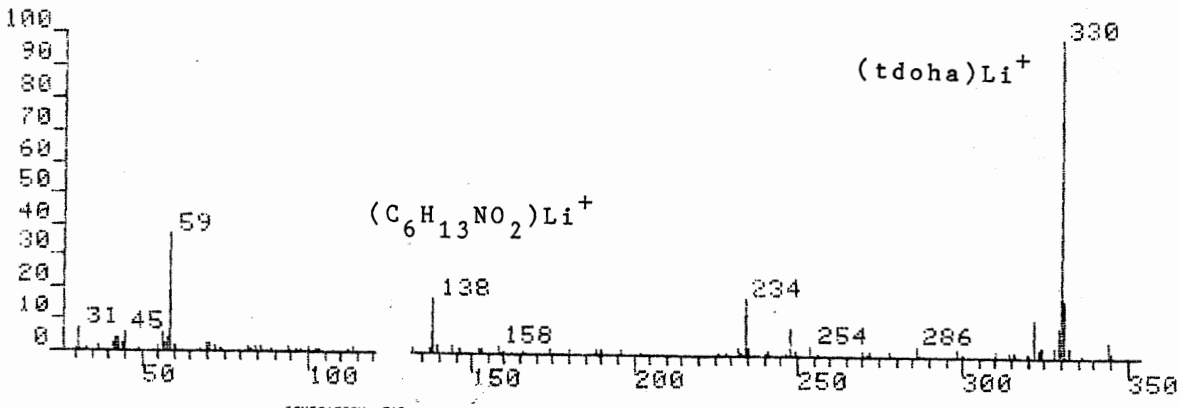


IONISATION: FAB
NO. PEAKS: 95
BASE/NREF INT: 110804./ 110804.
TIC: 397360.
MASS RANGE: 30 - 651

| PEAK NO. | MEASURED MASS | NO. POINTS | ABSOLUTE INTENSITY | % INT. BASE | % INT. NREF | % TOT. ION |
|---|---|---|---|---|---|---|
| 4 | 374 | 21 | 1329. | 1.2 | 1.2 | 0.3 |
| 5 | 373 | 21 | 1278. | 1.2 | 1.2 | 0.3 |
| 6 | 372 | 35 | 3842. | 3.5 | 3.5 | 1.0 |
| 8 | 358 | 29 | 1432. | 1.3 | 1.3 | 0.4 |
| 9 | 345 | 21 | 1151. | 1.0 | 1.0 | 0.3 |
| 10 | 344 | 35 | 5037. | 4.5 | 4.5 | 1.3 |
| 12 | 332 | 35 | 2946. | 2.7 | 2.7 | 0.7 |
| 13 | 331 | 43 | 19413. | 17.5 | 17.5 | 4.9 |
| 14 | 330 | 51 | 110804. | 100.0 | 100.0 | 27.9* |
| 15 | 329 | 43 | 10128. | 9.1 | 9.1 | 2.5 |
| 16 | 328 | 35 | 3352. | 3.0 | 3.0 | 0.8* |
| 17 | 324 | 35 | 3455. | 3.1 | 3.1 | 0.9 |
| 18 | 323 | 25 | 2088. | 1.9 | 1.9 | 0.5 |
| 19 | 322 | 43 | 12562. | 11.3 | 11.3 | 3.2 |
| 20 | 316 | 25 | 1179. | 1.1 | 1.1 | 0.3 |
| 21 | 314 | 25 | 1424. | 1.3 | 1.3 | 0.4 |
| 23 | 298 | 29 | 2115. | 1.9 | 1.9 | 0.5 |
| 25 | 286 | 29 | 3224. | 2.9 | 2.9 | 0.8 |
| 26 | 278 | 25 | 1530. | 1.4 | 1.4 | 0.4 |
| 27 | 272 | 21 | 1198. | 1.1 | 1.1 | 0.3 |
| 29 | 270 | 29 | 1924. | 1.7 | 1.7 | 0.5 |
| 31 | 254 | 35 | 2737. | 2.5 | 2.5 | 0.7 |
| 32 | 249 | 25 | 1270. | 1.1 | 1.1 | 0.3 |
| 33 | 248 | 43 | 9178. | 8.3 | 8.3 | 2.3 |
| 35 | 241 | 25 | 1460. | 1.3 | 1.3 | 0.4 |
| 37 | 235 | 29 | 2448. | 2.2 | 2.2 | 0.6 |
| 38 | 234 | 43 | 20363. | 18.4 | 18.4 | 5.1 |
| 40 | 232 | 29 | 2336. | 2.1 | 2.1 | 0.6 |
| 42 | 226 | 21 | 1116. | 1.0 | 1.0 | 0.3 |
| 44 | 196 | 25 | 1662. | 1.5 | 1.5 | 0.4 |
| 45 | 190 | 25 | 1225. | 1.1 | 1.1 | 0.3 |
| 46 | 188 | 29 | 1547. | 1.4 | 1.4 | 0.4 |
| 47 | 180 | 25 | 1192. | 1.1 | 1.1 | 0.3 |
| 48 | 174 | 25 | 1243. | 1.1 | 1.1 | 0.3 |
| 52 | 158 | 29 | 2458. | 2.2 | 2.2 | 0.6 |
| 53 | 153 | 25 | 1162. | 1.0 | 1.0 | 0.3 |
| 54 | 152 | 21 | 1159. | 1.0 | 1.0 | 0.3 |
| 55 | 146 | 25 | 1430. | 1.3 | 1.3 | 0.4 |
| 56 | 144 | 29 | 2403. | 2.2 | 2.2 | 0.6 |
| 57 | 139 | 29 | 2009. | 1.8 | 1.8 | 0.5 |
| 58 | 138 | 43 | 18802. | 17.0 | 17.0 | 4.7 |
| 59 | 137 | 25 | 1782. | 1.6 | 1.6 | 0.4 |
| 60 | 132 | 25 | 1536. | 1.4 | 1.4 | 0.4 |
| 62 | 114 | 25 | 1608. | 1.5 | 1.5 | 0.4 |
| 66 | 100 | 25 | 1797. | 1.6 | 1.6 | 0.5 |
| 67 | 98 | 21 | 1110. | 1.0 | 1.0 | 0.3 |
| 69 | 94 | 25 | 1248. | 1.1 | 1.1 | 0.3 |
| 71 | 86 | 35 | 1579. | 1.4 | 1.4 | 0.4 |
| 72 | 84 | 25 | 1207. | 1.1 | 1.1 | 0.3 |
| 74 | 82 | 25 | 1634. | 1.5 | 1.5 | 0.4 |
| 76 | 72 | 29 | 1929. | 1.7 | 1.7 | 0.5 |
| 77 | 71 | 29 | 2208. | 2.0 | 2.0 | 0.6 |
| 78 | 70 | 29 | 2102. | 1.9 | 1.9 | 0.5 |
| 80 | 60 | 21 | 1398. | 1.3 | 1.3 | 0.4 |
| 81 | 59 | 51 | 40592. | 36.6 | 36.6 | 10.2* |

# FAB of LiCl/tdoha saturated solution

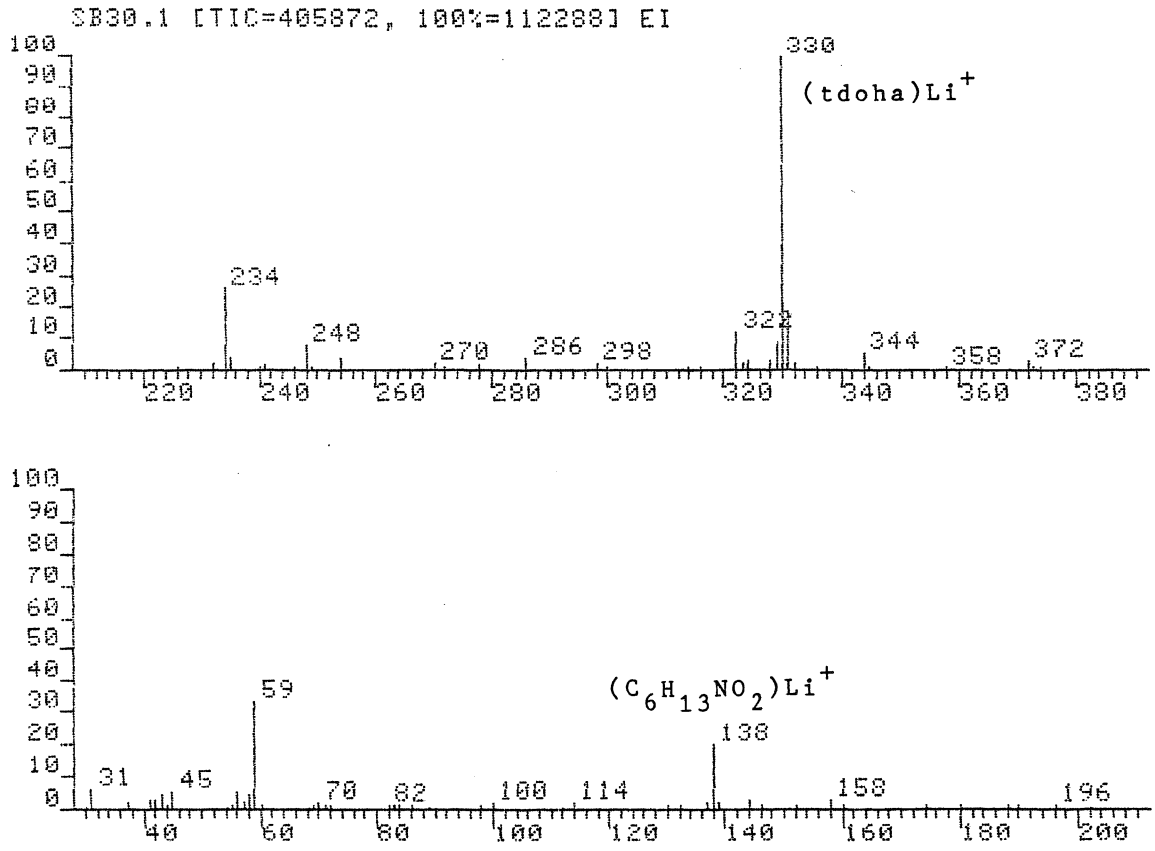


IONISATION: FAB LICL IN TDA-1 SAT
NO. PEAKS: 78
BASE/NREF INT: 112288./ 112288.
TIC: 405872.
MASS RANGE: 30 - 374
RETN TIME/MISC: 0: 0/ 0/ 0/ 0
PAGE 1

| PEAK NO. | MEASURED MASS | NO. POINTS | ABSOLUTE INTENSITY | % INT. BASE | % INT. NREF | % TOT ION |
|---|---|---|---|---|---|---|
| 6 | 344 | 29 | 5823. | 5.2 | 5.2 | 1.4 |
| 9 | 331 | 35 | 19524. | 17.4 | 17.4 | 4.8 |
| 10 | 330 | 43 | 112288. | 100.0 | 100.0 | 27.7 |
| 11 | 329 | 35 | 10150. | 9.0 | 9.0 | 2.5 |
| 15 | 322 | 35 | 13144. | 11.7 | 11.7 | 3.2 |
| 26 | 248 | 35 | 8510. | 7.6 | 7.6 | 2.1 |
| 31 | 234 | 35 | 28755. | 25.6 | 25.6 | 7.1 |
| 46 | 138 | 35 | 22620. | 20.1 | 20.1 | 5.6 |
| 65 | 59 | 43 | 37951. | 33.8 | 33.8 | 9.4 |
| 68 | 56 | 29 | 5996. | 5.3 | 5.3 | 1.5 |
| 71 | 45 | 35 | 6320. | 5.6 | 5.6 | 1.6 |
| 77 | 31 | 35 | 6842. | 6.1 | 6.1 | 1.7 |

FAB of LiBr/tdoha saturated solution

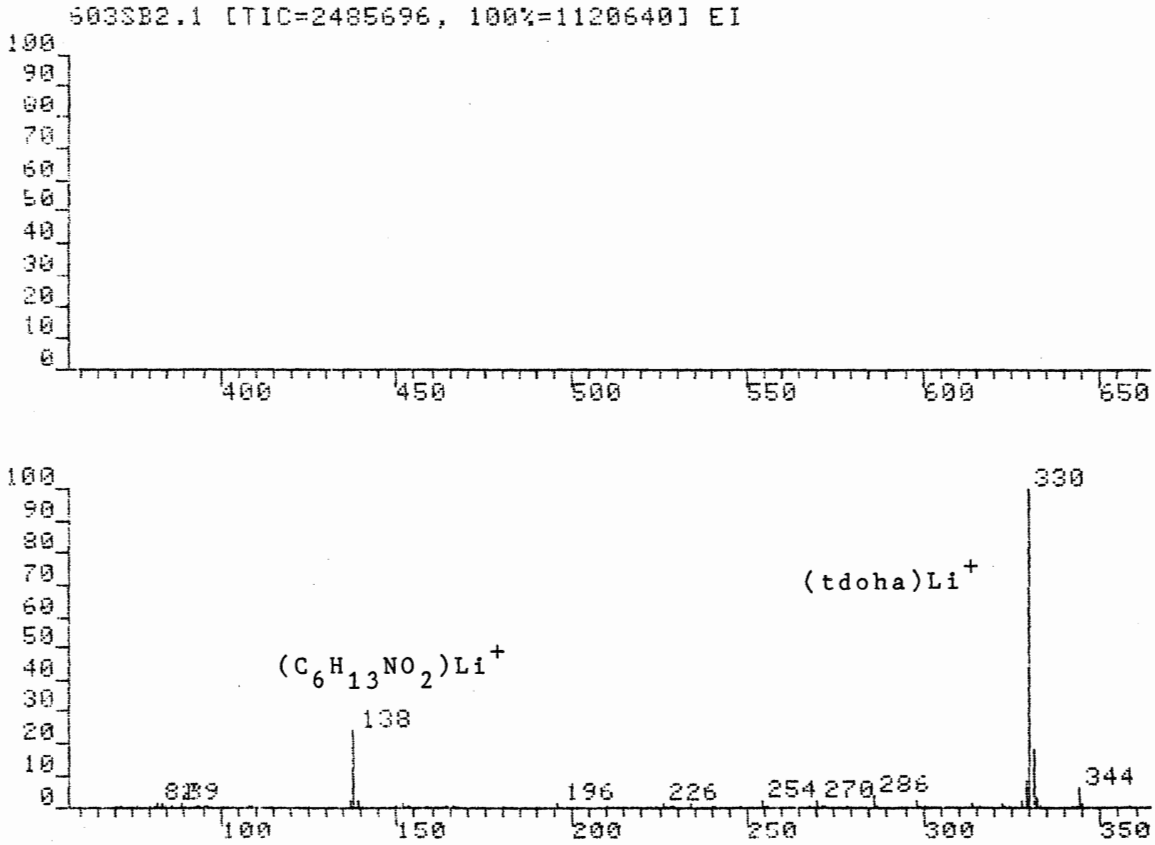

# FAB of NaCl/tdoha saturated solution

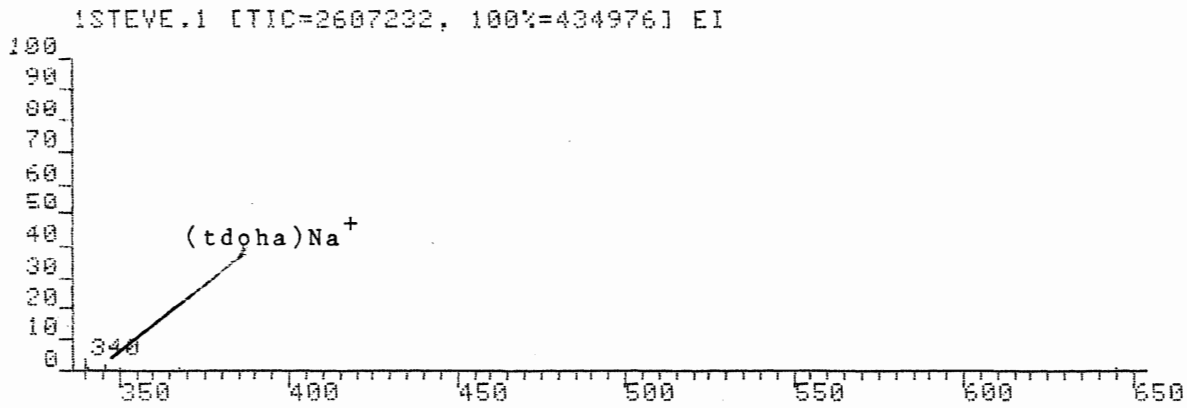


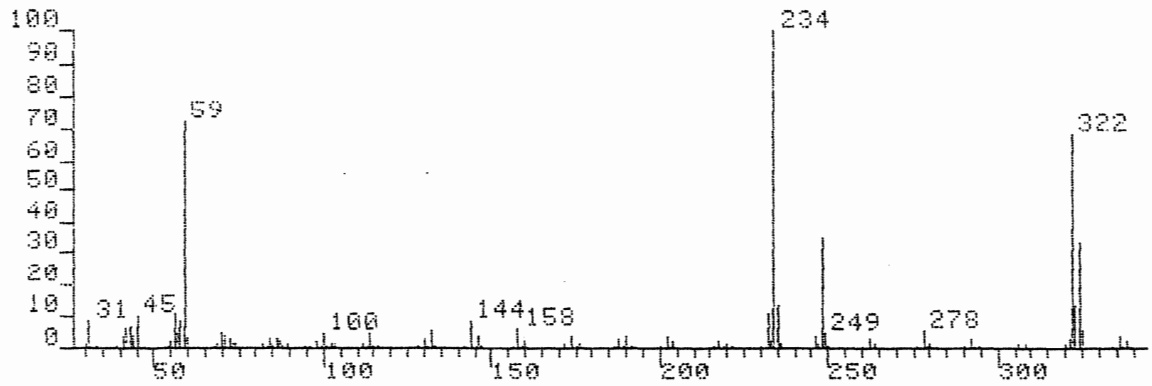


DP0:1STEVE.MS
SCAN: 1, 2/ 3/86 17:30

IONISATION: FAB TDA-1/HACL SAT.
NO. PEAKS: 197
BASE/NREF INT: 434976./ 434976.
TIC: 2607232.
MASS RANGE: 30 - 646
RETN TIME/MISC: 0: 0/ 0/ 0/ 0
PAGE 1

| PEAK NO. | MEASURED MASS | NO. POINTS | ABSOLUTE INTENSITY | % INT. BASE | % INT. NREF | % TOT. ION |
|---|---|---|---|---|---|---|
| 14 | 424 | 21 | 577. | 0.1 | 0.1 | 0.0 |
| 15 | 423 | 21 | 570. | 0.1 | 0.1 | 0.0 |
| 16 | 412 | 25 | 1332. | 0.3 | 0.3 | 0.1 |
| 17 | 382 | 25 | 786. | 0.2 | 0.2 | 0.0 |
| 18 | 380 | 21 | 602. | 0.1 | 0.1 | 0.0 |
| 19 | 369 | 21 | 492. | 0.1 | 0.1 | 0.0 |
| 20 | 368 | 29 | 2238. | 0.5 | 0.5 | 0.1 |
| 21 | 366 | 21 | 644. | 0.1 | 0.1 | 0.0 |
| 22 | 354 | 25 | 879. | 0.2 | 0.2 | 0.0 |
| 23 | 352 | 29 | 1302. | 0.3 | 0.3 | 0.0 |
| 24 | 351 | 21 | 697. | 0.2 | 0.2 | 0.0 |
| 25 | 350 | 35 | 2644. | 0.6 | 0.6 | 0.1 |
| 26 | 348 | 21 | 691. | 0.2 | 0.2 | 0.0 |
| 27 | 347 | 25 | 913. | 0.2 | 0.2 | 0.0 |
| 28 | 346 | 35 | 5755. | 1.3 | 1.3 | 0.2 |
| 29 | 341 | 29 | 2709. | 0.6 | 0.6 | 0.1 |
| 30 | 340 | 35 | 15877. | 3.7 | 3.7 | 0.6 |
| 31 | 339 | 29 | 1635. | 0.4 | 0.4 | 0.1 |
| 32 | 338 | 35 | 8706. | 2.0 | 2.0 | 0.3 |
| 33 | 337 | 35 | 3327. | 0.8 | 0.8 | 0.1 |
| 34 | 336 | 35 | 15893. | 3.7 | 3.7 | 0.6 |
| 35 | 335 | 25 | 959. | 0.2 | 0.2 | 0.0 |
| 36 | 334 | 29 | 1769. | 0.4 | 0.4 | 0.1 |
| 38 | 325 | 43 | 24436. | 5.6 | 5.6 | 0.9 |
| 39 | 324 | 71 | 146192. | 33.6 | 33.6 | 5.6 |
| 40 | 323 | 59 | 58138. | 13.4 | 13.4 | 2.2* |
| 41 | 322 | 103 | 295648. | 68.0 | 68.0 | 11.3* |
| 62 | 278 | 43 | 22417. | 5.2 | 5.2 | 0.9 |
| 77 | 248 | 71 | 153832. | 35.4 | 35.4 | 5.9* |
| 84 | 235 | 51 | 55714. | 12.8 | 12.8 | 2.1 |
| 85 | 234 | 103 | 434976. | 100.0 | 100.0 | 16.7* |
| 87 | 232 | 43 | 46562. | 10.7 | 10.7 | 1.8 |
| 123 | 158 | 43 | 24919. | 5.7 | 5.7 | 1.0 |
| 130 | 144 | 43 | 36501. | 8.4 | 8.4 | 1.4 |
| 134 | 132 | 43 | 23073. | 5.3 | 5.3 | 0.9 |
| 181 | 59 | 87 | 311696. | 71.7 | 71.7 | 12.0* |

# FAB of NaI/tdoha saturated solution

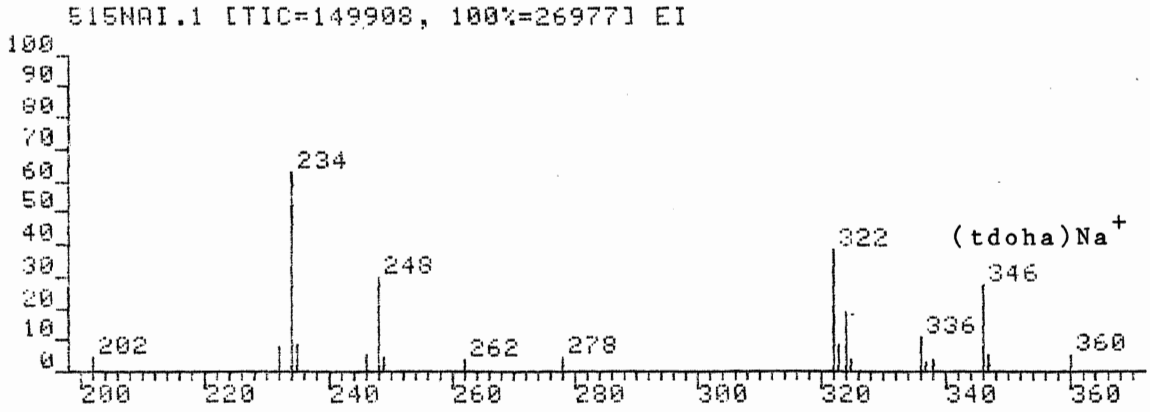


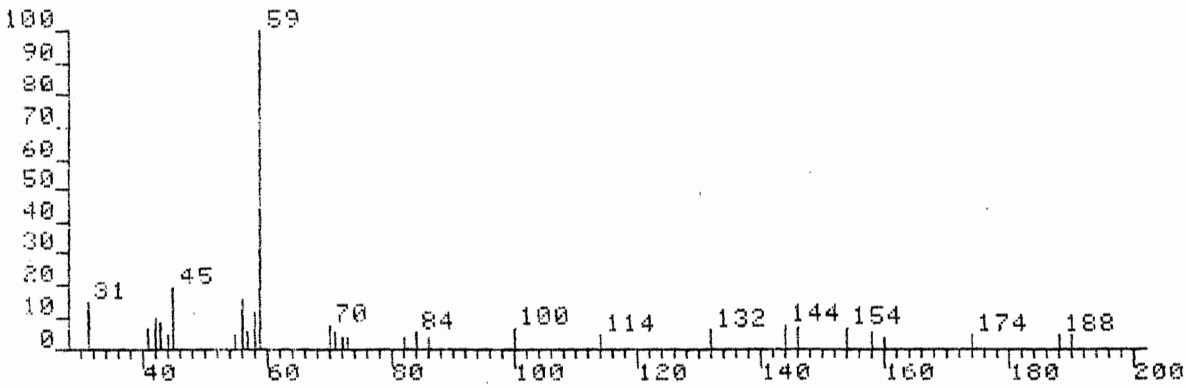


IONISATION: FAB
NO. PEAKS: 48
BASE/NREF INT: 26977./ 26977.
TIC: 149908.
MASS RANGE: 31 - 360

| PEAK NO. | MEASURED MASS | NO POINTS | ABSOLUTE INTENSITY | % INT. BASE | % INT. NREF | % TOT. ION | |
|---|---|---|---|---|---|---|---|
| 1 | 360 | 21 | 1448. | 5.4 | 5.4 | 1.0 | |
| 2 | 347 | 25 | 1477. | 5.5 | 5.5 | 1.0 | |
| 3 | 346 | 35 | 7386. | 27.4 | 27.4 | 4.9 | — |
| 4 | 338 | 21 | 1078. | 4.0 | 4.0 | 0.7 | |
| 5 | 337 | 17 | 829. | 3.1 | 3.1 | 0.6 | |
| 6 | 336 | 35 | 3027. | 11.2 | 11.2 | 2.0 | |
| 7 | 325 | 17 | 1045. | 3.9 | 3.9 | 0.7 | |
| 8 | 324 | 35 | 5032. | 18.7 | 18.7 | 3.4 | — |
| 9 | 323 | 29 | 2198. | 8.1 | 8.1 | 1.5 | |
| 10 | 322 | 43 | 10339. | 38.3 | 38.3 | 6.9 | |
| 11 | 278 | 25 | 1359. | 5.0 | 5.0 | 0.9 | |
| 12 | 262 | 21 | 1079. | 4.0 | 4.0 | 0.7 | |
| 13 | 249 | 21 | 1292. | 4.8 | 4.8 | 0.9 | |
| 14 | 248 | 35 | 8082. | 30.0 | 30.0 | 5.4 | |
| 15 | 246 | 21 | 1426. | 5.3 | 5.3 | 1.0 | ← |
| 16 | 235 | 15 | 2401. | 8.9 | 8.9 | 1.6 | |
| 17 | 234 | 43 | 16845. | 62.4 | 62.4 | 11.2 | — |
| 18 | 232 | 29 | 2165. | 8.0 | 8.0 | 1.4 | |
| 19 | 202 | 25 | 1356. | 5.0 | 5.0 | 0.9 | |
| 20 | 190 | 21 | 1290. | 4.8 | 4.8 | 0.9 | |
| 21 | 188 | 17 | 1306. | 4.8 | 4.8 | 0.9 | |
| 22 | 174 | 25 | 1295. | 4.8 | 4.8 | 0.9 | |
| 23 | 160 | 25 | 1125. | 4.2 | 4.2 | 0.8 | |
| 24 | 158 | 25 | 1522. | 5.6 | 5.6 | 1.0 | |
| 25 | 154 | 25 | 1833. | 6.8 | 6.8 | 1.2 | |
| 26 | 146 | 29 | 1866. | 6.9 | 6.9 | 1.2 | |
| 27 | 144 | 29 | 1977. | 7.3 | 7.3 | 1.3 | |
| 28 | 132 | 25 | 1712. | 6.3 | 6.3 | 1.1 | |
| 29 | 114 | 21 | 1276. | 4.7 | 4.7 | 0.9 | |
| 30 | 100 | 29 | 1906. | 7.1 | 7.1 | 1.3 | |
| 31 | 86 | 21 | 957. | 3.5 | 3.5 | 0.6 | |
| 32 | 84 | 29 | 1383. | 5.1 | 5.1 | 0.9 | |
| 33 | 82 | 21 | 877. | 3.3 | 3.3 | 0.6 | |
| 34 | 73 | 21 | 1097. | 4.1 | 4.1 | 0.7 | |
| 35 | 72 | 21 | 888. | 3.3 | 3.3 | 0.6 | |
| 36 | 71 | 29 | 1409. | 5.2 | 5.2 | 0.9* | |
| 37 | 70 | 35 | 2072. | 7.7 | 7.7 | 1.4 | |
| 38 | 59 | 43 | 26977. | 100.0 | 100.0 | 18.0 | |
| 39 | 58 | 43 | 3083. | 11.4 | 11.4 | 2.1* | |
| 40 | 57 | 25 | 1497. | 5.5 | 5.5 | 1.0 | |
| 41 | 56 | 35 | 4115. | 15.3 | 15.3 | 2.7 | |
| 42 | 55 | 25 | 1265. | 4.7 | 4.7 | 0.8 | |
| 43 | 45 | 43 | 5233. | 19.4 | 19.4 | 3.5 | |
| 44 | 44 | 25 | 1216. | 4.5 | 4.5 | 0.8 | |
| 45 | 43 | 35 | 2398. | 8.9 | 8.9 | 1.6* | |
| 46 | 42 | 29 | 2651. | 9.8 | 9.8 | 1.8 | |
| 47 | 41 | 29 | 1828. | 6.8 | 6.8 | 1.2 | |
| 48 | 31 | 35 | 3992. | 14.8 | 14.8 | 2.7 | |

# FAB of KF/tdoha saturated solution

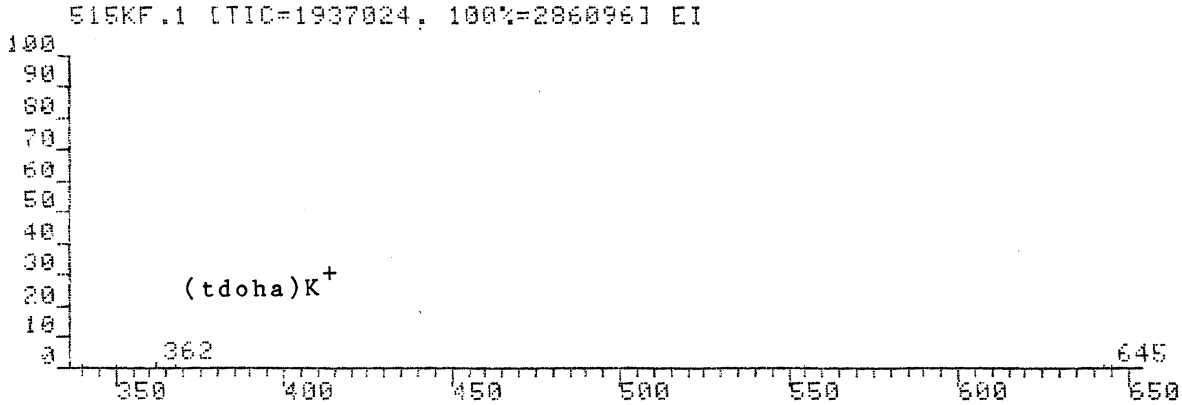


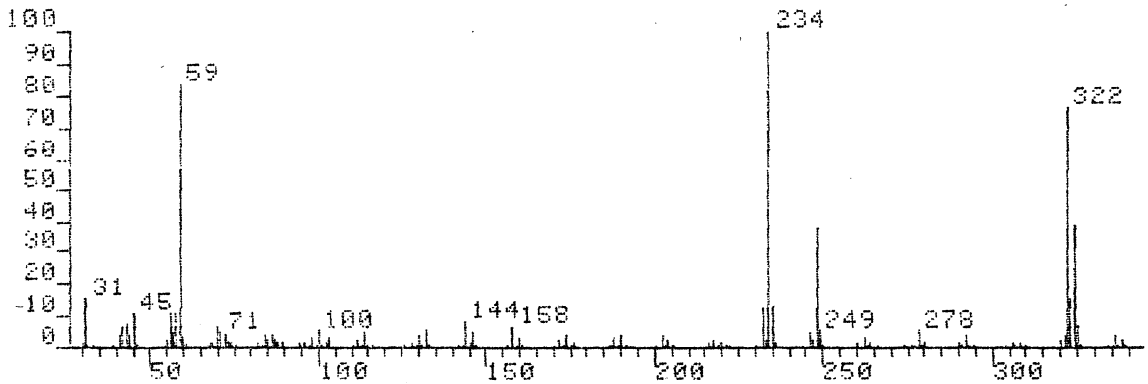


IONISATION: FAB
NO. PEAKS: 168
BASE/NREF INT: 286096./ 286096.
TIC: 1937024.
MASS RANGE: 30 - 646

| PEAK NO. | MEASURED MASS | NO. POINTS | ABSOLUTE INTENSITY | % INT. BASE | % INT. NREF | % TOT. ION |
|---|---|---|---|---|---|---|
| 2 | 645 | 29 | 3371. | 1.2 | 1.2 | 0.2 |
| 22 | 362 | 35 | 4389. | 1.5 | 1.5 | 0.2 |
| 28 | 338 | 35 | 6275. | 2.2 | 2.2 | 0.3 |
| 30 | 336 | 35 | 12090. | 4.2 | 4.2 | 0.6 |
| 33 | 326 | 29 | 2784. | 1.0 | 1.0 | 0.1 |
| 34 | 325 | 43 | 18563. | 6.5 | 6.5 | 1.0 |
| 35 | 324 | 59 | 112356. | 39.3 | 39.3 | 5.8* |
| 36 | 323 | 59 | 43442. | 15.2 | 15.2 | 2.2* |
| 37 | 322 | 87 | 219980. | 76.9 | 76.9 | 11.4* |
| 38 | 321 | 43 | 11314. | 4.0 | 4.0 | 0.6* |
| 39 | 320 | 35 | 6153. | 2.2 | 2.2 | 0.3 |
| 41 | 308 | 35 | 3926. | 1.4 | 1.4 | 0.2 |
| 43 | 306 | 35 | 3317. | 1.2 | 1.2 | 0.2 |
| 48 | 292 | 35 | 9968. | 3.5 | 3.5 | 0.5 |
| 50 | 290 | 35 | 3721. | 1.3 | 1.3 | 0.2 |
| 51 | 280 | 35 | 3304. | 1.2 | 1.2 | 0.2 |
| 53 | 278 | 43 | 15674. | 5.5 | 5.5 | 0.8 |
| 58 | 264 | 35 | 4801. | 1.7 | 1.7 | 0.2 |
| 60 | 262 | 43 | 8425. | 2.9 | 2.9 | 0.4 |
| 62 | 260 | 35 | 3669. | 1.3 | 1.3 | 0.2 |
| 64 | 249 | 43 | 15589. | 5.4 | 5.4 | 0.8 |
| 65 | 248 | 59 | 109388. | 38.2 | 38.2 | 5.6* |
| 66 | 247 | 35 | 5845. | 2.0 | 2.0 | 0.3 |
| 67 | 246 | 43 | 12392. | 4.3 | 4.3 | 0.6 |
| 69 | 236 | 35 | 4690. | 1.6 | 1.6 | 0.2 |
| 70 | 235 | 51 | 36960. | 12.9 | 12.9 | 1.9 |
| 71 | 234 | 87 | 286096. | 100.0 | 100.0 | 14.8* |
| 72 | 233 | 43 | 5943. | 2.1 | 2.1 | 0.3 |
| 73 | 232 | 51 | 34219. | 12.0 | 12.0 | 1.8 |
| 77 | 220 | 35 | 4951. | 1.7 | 1.7 | 0.3 |
| 79 | 218 | 35 | 5387. | 1.9 | 1.9 | 0.3 |
| 81 | 216 | 35 | 3188. | 1.1 | 1.1 | 0.2 |
| 83 | 204 | 35 | 5283. | 1.8 | 1.8 | 0.3 |
| 85 | 202 | 43 | 10375. | 3.6 | 3.6 | 0.5 |
| 87 | 200 | 29 | 2620. | 0.9 | 0.9 | 0.1 |
| 89 | 190 | 43 | 10524. | 3.7 | 3.7 | 0.5 |
| 91 | 188 | 43 | 9073. | 3.2 | 3.2 | 0.5 |
| 94 | 176 | 35 | 4619. | 1.6 | 1.6 | 0.2 |
| 96 | 174 | 43 | 11741. | 4.1 | 4.1 | 0.6 |
| 98 | 172 | 35 | 5022. | 1.8 | 1.8 | 0.3 |
| 102 | 160 | 43 | 8888. | 3.1 | 3.1 | 0.5 |
| 104 | 158 | 43 | 18694. | 6.5 | 6.5 | 1.0 |
| 107 | 146 | 43 | 12757. | 4.5 | 4.5 | 0.7 |
| 108 | 145 | 35 | 3071. | 1.1 | 1.1 | 0.2 |
| 109 | 144 | 43 | 24457. | 8.5 | 8.5 | 1.3 |
| 113 | 132 | 43 | 15989. | 5.6 | 5.6 | 0.8 |
| 115 | 130 | 43 | 10387. | 3.6 | 3.6 | 0.5 |
| 117 | 128 | 35 | 3379. | 1.2 | 1.2 | 0.2 |
| 121 | 114 | 43 | 12636. | 4.4 | 4.4 | 0.7 |
| 123 | 112 | 35 | 6437. | 2.2 | 2.2 | 0.3 |
| 125 | 103 | 43 | 7946. | 2.8 | 2.8 | 0.4 |
| 126 | 102 | 35 | 4813. | 1.7 | 1.7 | 0.2 |
| 128 | 100 | 43 | 15188. | 5.3 | 5.3 | 0.8 |
| 130 | 98 | 43 | 8450. | 3.0 | 3.0 | 0.4 |
| 132 | 96 | 35 | 2953. | 1.0 | 1.0 | 0.2 |
| 133 | 94 | 35 | 4186. | 1.5 | 1.5 | 0.2 |
| 134 | 89 | 35 | 4414. | 1.5 | 1.5 | 0.2 |
| 135 | 88 | 35 | 3123. | 1.1 | 1.1 | 0.2 |
| 136 | 87 | 43 | 5912. | 2.1 | 2.1 | 0.3 |
| 137 | 86 | 43 | 10480. | 3.7 | 3.7 | 0.5 |
| 138 | 85 | 51 | 5051. | 1.8 | 1.8 | 0.3 |
| 139 | 84 | 51 | 9797. | 3.4 | 3.4 | 0.5 |
| 141 | 82 | 35 | 4952. | 1.7 | 1.7 | 0.3 |
| 143 | 74 | 43 | 4328. | 1.5 | 1.5 | 0.2 |
| 144 | 73 | 43 | 3915. | 1.4 | 1.4 | 0.2* |
| 145 | 72 | 59 | 10280. | 3.6 | 3.6 | 0.5 |
| 146 | 71 | 59 | 14230. | 5.0 | 5.0 | 0.7 |
| 147 | 70 | 51 | 16682. | 5.8 | 5.8 | 0.9 |
| 148 | 69 | 43 | 4220. | 1.5 | 1.5 | 0.2 |
| 149 | 68 | 35 | 3026. | 1.1 | 1.1 | 0.2 |
| 152 | 60 | 43 | 8447. | 3.0 | 3.0 | 0.4 |
| 153 | 59 | 71 | 240252. | 84.0 | 84.0 | 12.4* |
| 154 | 58 | 59 | 31640. | 11.1 | 11.1 | 1.6 |

# FAB of KCl/tdoha saturated solution

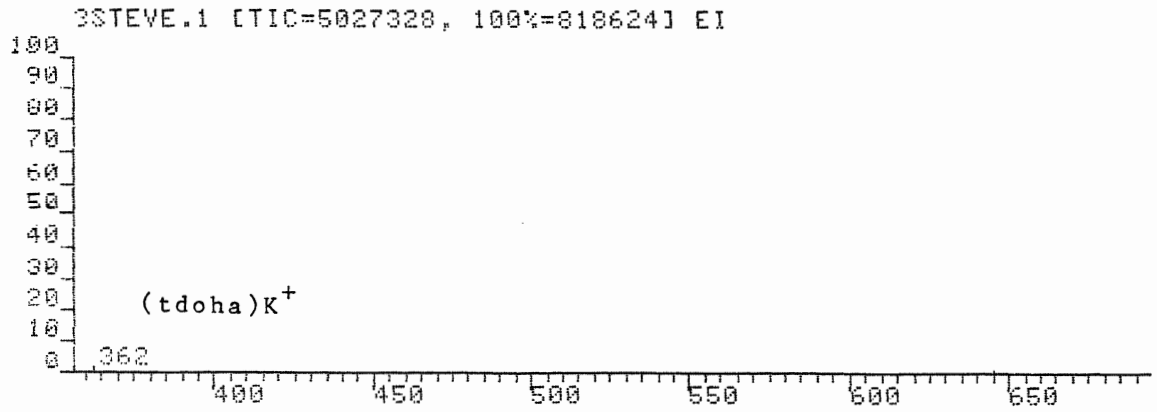


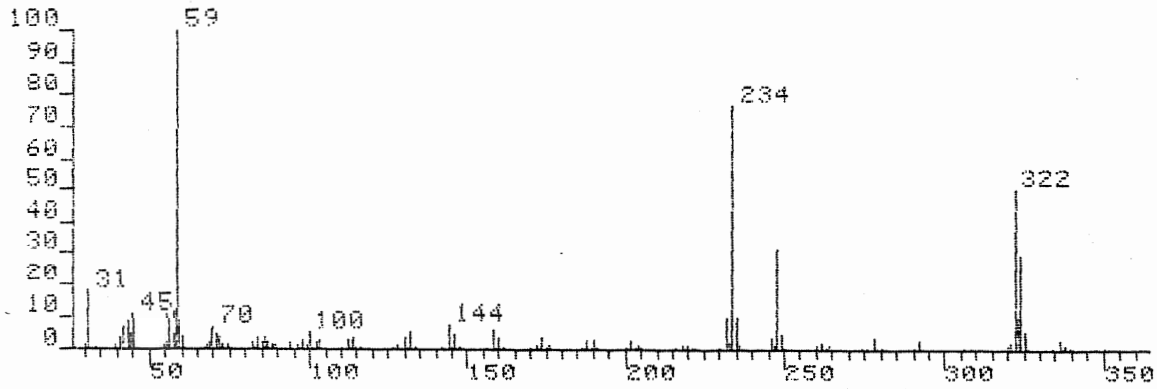


IONISATION: FAB TDA/KCL SATURATED
NO. PEAKS: 234
BASE/NREF INT: 818624./ 818624.
TIC: 5027328.
MASS RANGE: 30 - 687
RETN TIME/MISC: 0: 0/ 0/ 0/ 0
PAGE 1

| PEAK NO. | MEASURED MASS | NO. POINTS | ABSOLUTE INTENSITY | % INT. BASE | % INT. NREF | % TOT. ION |
|---|---|---|---|---|---|---|
| 1 | 687 | 25 | 1108. | 0.1 | 0.1 | 0.0 |
| 2 | 647 | 21 | 678. | 0.1 | 0.1 | 0.0 |
| 3 | 646 | 29 | 1746. | 0.2 | 0.2 | 0.0 |
| 4 | 645 | 35 | 5088. | 0.6 | 0.6 | 0.1 |
| 5 | 644 | 29 | 1358. | 0.2 | 0.2 | 0.0* |
| 6 | 643 | 29 | 2256. | 0.3 | 0.3 | 0.0 |
| 7 | 615 | 17 | 589. | 0.1 | 0.1 | 0.0 |
| 8 | 585 | 25 | 976. | 0.1 | 0.1 | 0.0 |
| 9 | 583 | 21 | 739. | 0.1 | 0.1 | 0.0 |
| 10 | 569 | 25 | 1527. | 0.2 | 0.2 | 0.0 |
| 11 | 568 | 21 | 787. | 0.1 | 0.1 | 0.0 |
| 12 | 557 | 21 | 841. | 0.1 | 0.1 | 0.0 |
| 13 | 556 | 21 | 896. | 0.1 | 0.1 | 0.0 |
| 14 | 555 | 35 | 2416. | 0.3 | 0.3 | 0.0 |
| 15 | 525 | 17 | 631. | 0.1 | 0.1 | 0.0 |
| 16 | 495 | 21 | 1081. | 0.1 | 0.1 | 0.0 |
| 17 | 493 | 17 | 869. | 0.1 | 0.1 | 0.0 |
| 18 | 481 | 25 | 1101. | 0.1 | 0.1 | 0.0 |
| 19 | 480 | 21 | 924. | 0.1 | 0.1 | 0.0 |
| 20 | 479 | 25 | 1058. | 0.1 | 0.1 | 0.0 |
| 21 | 467 | 25 | 1479. | 0.2 | 0.2 | 0.0 |
| 22 | 453 | 25 | 1303. | 0.2 | 0.2 | 0.0 |
| 23 | 451 | 21 | 811. | 0.1 | 0.1 | 0.0 |
| 24 | 426 | 25 | 980. | 0.1 | 0.1 | 0.0 |
| 25 | 424 | 25 | 1220. | 0.1 | 0.1 | 0.0 |
| 26 | 423 | 21 | 1017. | 0.1 | 0.1 | 0.0 |
| 27 | 412 | 35 | 2219. | 0.3 | 0.3 | 0.0 |
| 28 | 382 | 25 | 1394. | 0.2 | 0.2 | 0.0 |
| 30 | 378 | 21 | 729. | 0.1 | 0.1 | 0.0 |
| 31 | 376 | 21 | 973. | 0.1 | 0.1 | 0.0 |
| 32 | 368 | 35 | 3587. | 0.4 | 0.4 | 0.1 |
| 33 | 366 | 21 | 762. | 0.1 | 0.1 | 0.0 |
| 34 | 364 | 35 | 2275. | 0.3 | 0.3 | 0.0 |
| 35 | 363 | 35 | 3110. | 0.4 | 0.4 | 0.1 |
| 36 | 362 | 43 | 15568. | 1.9 | 1.9 | 0.3 |
| 37 | 360 | 21 | 906. | 0.1 | 0.1 | 0.0 |
| 38 | 354 | 21 | 1031. | 0.1 | 0.1 | 0.0 |
| 39 | 352 | 35 | 2346. | 0.3 | 0.3 | 0.0 |
| 40 | 351 | 29 | 1645. | 0.2 | 0.2 | 0.0 |
| 55 | 324 | 71 | 241836. | 29.5 | 29.5 | 4.8* |
| 56 | 323 | 71 | 83604. | 10.2 | 10.2 | 1.7* |
| 57 | 322 | 103 | 419680. | 51.3 | 51.3 | 8.3* |
| 98 | 248 | 71 | 263248. | 32.2 | 32.2 | 5.2 |
| 106 | 234 | 103 | 625264. | 76.4 | 76.4 | 12.4* |
| 108 | 232 | 51 | 83432. | 10.2 | 10.2 | 1.7 |
| 217 | 59 | 103 | 818624. | 100.0 | 100.0 | 16.3* |

FAB of KBr/tdoha Satturated Solution

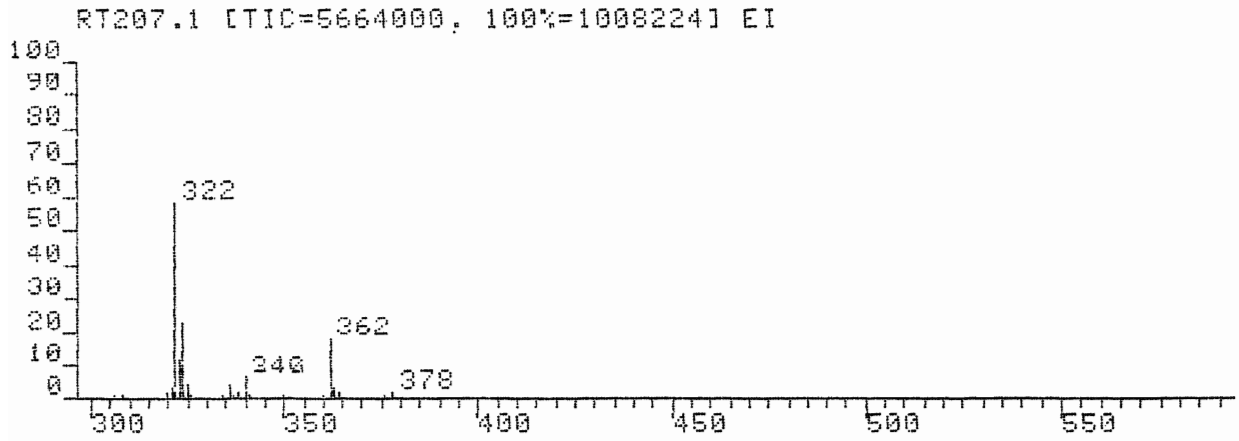


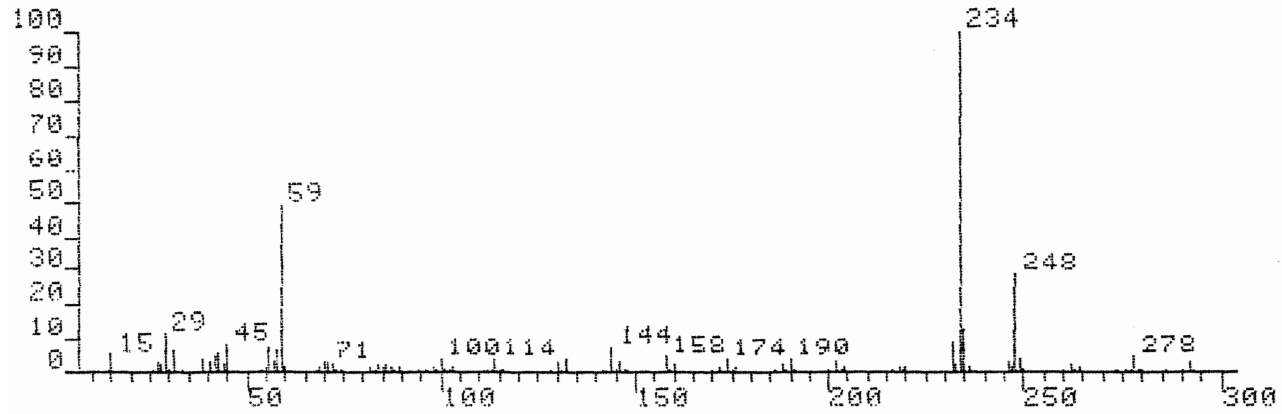


SCAN: 1, 6/22/87 17:34
IONISATION: FAB KBR/TDOHA 1:1
NO. PEAKS: 216
BASE/NREF INT: 1008224./ 1008224.
TIC: 5664000.
MASS RANGE: 13 - 570
RETN TIME/MISC: 0: 0/ 0/ 0/ 0
PAGE 1

| PEAK NO. | MEASURED MASS | NO. POINTS | ABSOLUTE INTENSITY | % INT. BASE | % INT. NREF | % TOT. ION |
|---|---|---|---|---|---|---|
| 30 | 362 | 71 | 178716. | 17.7 | 17.7 | 3.2 |
| 53 | 324 | 87 | 231776. | 23.0 | 23.0 | 4.1* |
| 54 | 323 | 71 | 117568. | 11.7 | 11.7 | 2.1* |
| 55 | 322 | 119 | 588752. | 58.4 | 58.4 | 10.4* |
| 98 | 248 | 103 | 288992. | 28.7 | 28.7 | 5.1 |
| 105 | 235 | 59 | 129380. | 12.8 | 12.8 | 2.3* |
| 106 | 234 | 175 | 1008224. | 100.0 | 100.0 | 17.8* |
| 194 | 59 | 87 | 495952. | 49.2 | 49.2 | 8.8 |
| 210 | 29 | 71 | 113540. | 11.3 | 11.3 | 2.0* |

**FAB of KI/tdoha Satturated Solution**

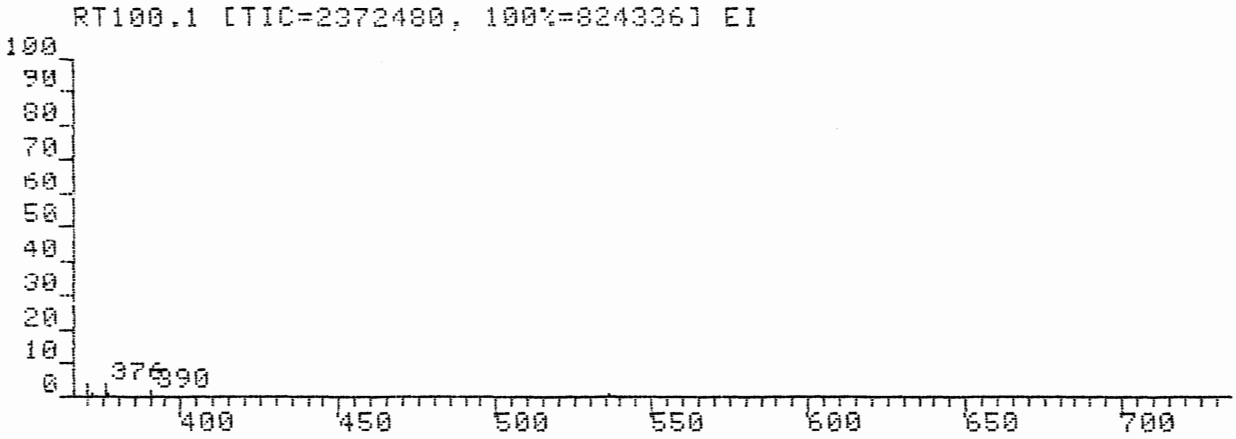


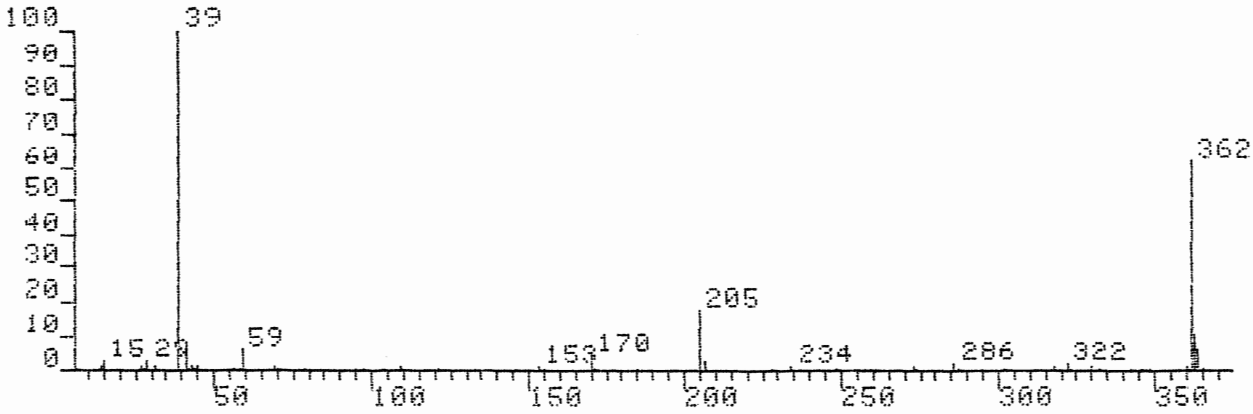


Drv:R1100.MS
SCAN: 1, 6/11/87 18:15
IONISATION: FAB KI/TDOHA (1:1)
NO. PEAKS: 118
BASE/NREF INT: 824336./ 824336.
TIC: 2372480.
MASS RANGE: 12 - 725
RETN TIME/MISC: 0: 0/ 0/ 0/ 0
PAGE 1

| PEAK NO. | MEASURED MASS | NO. POINTS | ABSOLUTE INTENSITY | % INT. BASE | % INT. NREF | % TOT. ION |
|---|---|---|---|---|---|---|
| 25 | 363 | 51 | 87560. | 10.6 | 10.6 | 3.7% |
| 26 | 362 | 87 | 511440. | 62.0 | 62.0 | 21.6% |
| 68 | 205 | 43 | 151328. | 18.4 | 18.4 | 6.4 |
| 109 | 39 | 87 | 824336. | 100.0 | 100.0 | 34.7% |

# FAB of RbF/tdoha saturated solution

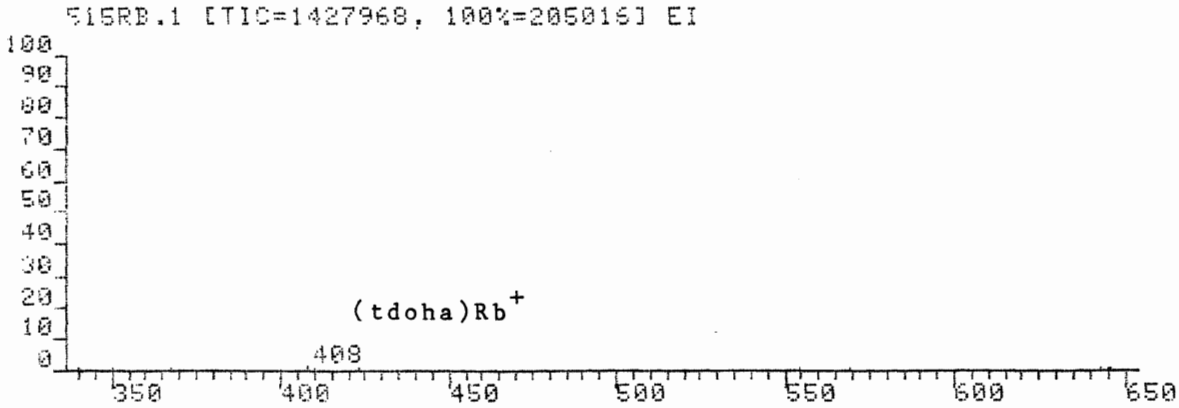


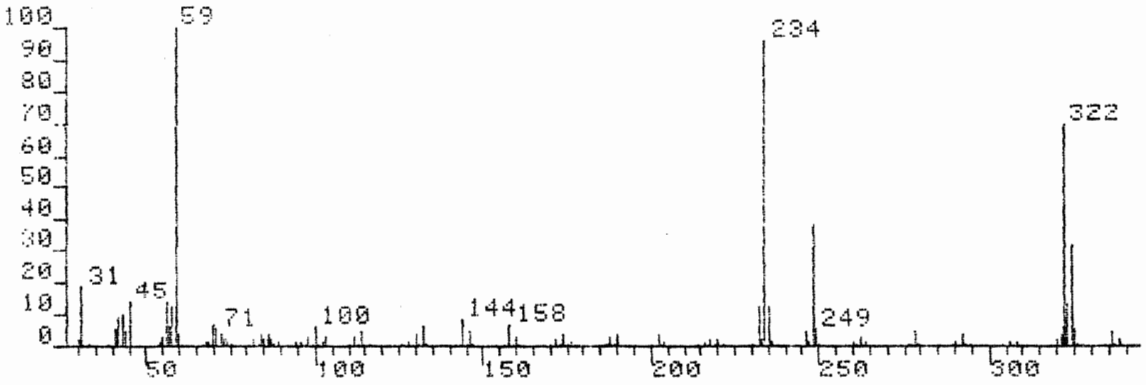


IONISATION: FAB
NO. PEAKS: 149
BASE/NREF INT: 205016./ 205016.
TIC: 1427968.
MASS RANGE: 30 - 646

| PEAK NO. | MEASURED MASS | NO. POINTS | ABSOLUTE INTENSITY | % INT. BASE | % INT. NREF | % TOT. ION |
|---|---|---|---|---|---|---|
| 14 | 408 | 29 | 2861. | 1.4 | 1.4 | 0.2 |
| 21 | 338 | 29 | 3663. | 1.8 | 1.8 | 0.3 |
| 23 | 336 | 35 | 8991. | 4.4 | 4.4 | 0.6 |
| 27 | 325 | 35 | 11074. | 5.4 | 5.4 | 0.8 |
| 28 | 324 | 51 | 65708. | 32.1 | 32.1 | 4.6 |
| 29 | 323 | 43 | 27750. | 13.5 | 13.5 | 1.9 |
| 30 | 322 | 71 | 142692. | 69.6 | 69.6 | 10.0% |
| 31 | 321 | 35 | 8039. | 3.9 | 3.9 | 0.6 |
| 53 | 249 | 35 | 10498. | 5.1 | 5.1 | 0.7 |
| 54 | 248 | 51 | 78396. | 38.2 | 38.2 | 5.5% |
| 55 | 247 | 35 | 3402. | 1.7 | 1.7 | 0.2 |
| 56 | 246 | 35 | 9394. | 4.6 | 4.6 | 0.7 |
| 57 | 236 | 29 | 2970. | 1.4 | 1.4 | 0.2 |
| 58 | 235 | 43 | 24962. | 12.2 | 12.2 | 1.7 |
| 59 | 234 | 71 | 198388. | 96.8 | 96.8 | 13.9% |
| 60 | 233 | 35 | 4219. | 2.1 | 2.1 | 0.3 |
| 61 | 232 | 43 | 24399. | 11.9 | 11.9 | 1.7 |
| 92 | 144 | 43 | 18270. | 8.9 | 8.9 | 1.3 |
| 96 | 132 | 43 | 12135. | 5.9 | 5.9 | 0.8 |
| 98 | 130 | 35 | 8254. | 4.0 | 4.0 | 0.6 |
| 99 | 129 | 35 | 3293. | 1.1 | 1.1 | 0.2 |
| 103 | 114 | 43 | 10166. | 5.0 | 5.0 | 0.7 |
| 105 | 112 | 35 | 5279. | 2.6 | 2.6 | 0.4 |
| 107 | 103 | 35 | 5609. | 2.7 | 2.7 | 0.4 |
| 108 | 102 | 35 | 3307. | 1.6 | 1.6 | 0.2 |
| 110 | 100 | 43 | 12854. | 6.3 | 6.3 | 0.9 |
| 112 | 98 | 35 | 6376. | 3.1 | 3.1 | 0.4 |
| 114 | 96 | 35 | 2676. | 1.3 | 1.3 | 0.2 |
| 115 | 94 | 35 | 3060. | 1.5 | 1.5 | 0.2 |
| 116 | 89 | 35 | 3133. | 1.5 | 1.5 | 0.2 |
| 118 | 87 | 35 | 4688. | 2.3 | 2.3 | 0.3 |
| 119 | 86 | 43 | 8463. | 4.1 | 4.1 | 0.6 |
| 120 | 85 | 59 | 4881. | 2.4 | 2.4 | 0.3% |
| 121 | 84 | 43 | 7576. | 3.7 | 3.7 | 0.5 |
| 123 | 82 | 35 | 4645. | 2.3 | 2.3 | 0.3 |
| 125 | 74 | 35 | 3791. | 1.8 | 1.8 | 0.3 |
| 126 | 73 | 43 | 3626. | 1.8 | 1.8 | 0.3% |
| 127 | 72 | 51 | 8268. | 4.0 | 4.0 | 0.6 |
| 128 | 71 | 51 | 11452. | 5.6 | 5.6 | 0.8 |
| 129 | 70 | 51 | 13712. | 6.7 | 6.7 | 1.0 |
| 130 | 69 | 35 | 3432. | 1.7 | 1.7 | 0.2 |
| 131 | 68 | 35 | 2821. | 1.4 | 1.4 | 0.2 |
| 133 | 60 | 43 | 6694. | 3.3 | 3.3 | 0.5 |
| 134 | 59 | 71 | 205016. | 100.0 | 100.0 | 14.4 |

# FAB of CsF/tdoha saturated solution

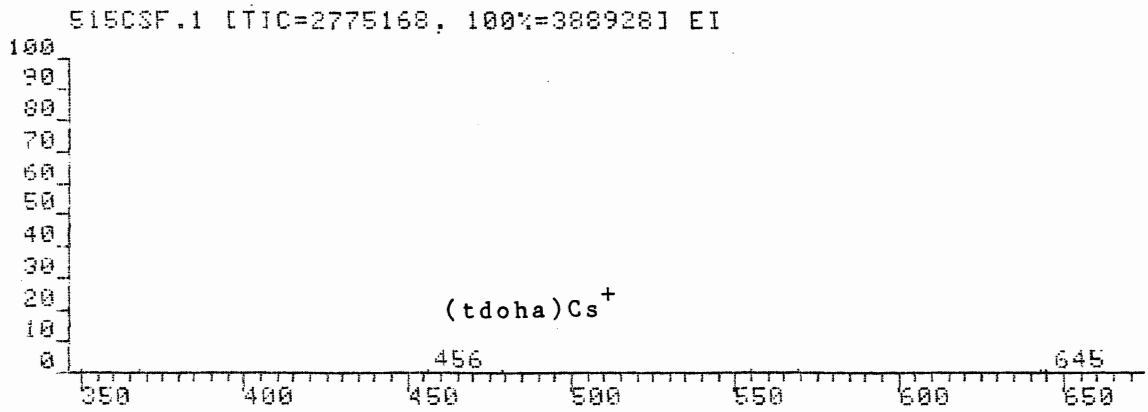


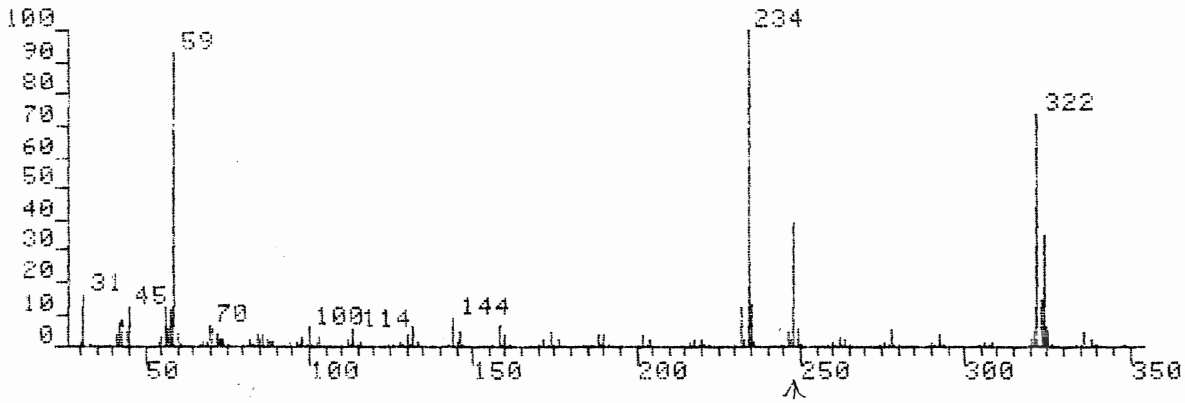


SCAN: 1. 5/15/85 13:17

IONISATION: FAB
NO. PEAKS: 316
BASE/NREF INT: 388928./ 388928.
TIC: 2775168.
MASS RANGE: 30 - 659

| | | | | | | |
|---|---|---|---|---|---|---|
| 4 | 645 | 35 | 4613. | 1.2 | 1.2 | 0.2 |
| 32 | 456 | 35 | 4062. | 1.0 | 1.0 | 0.1 |
| 50 | 338 | 43 | 7822. | 2.0 | 2.0 | 0.3 |
| 52 | 336 | 43 | 17639. | 4.5 | 4.5 | 0.5 |
| 56 | 325 | 51 | 33203. | 8.5 | 8.5 | 0.8* |
| 57 | 324 | 71 | 136129. | 35.0 | 35.0 | 4.9* |
| 58 | 323 | 71 | 56472. | 14.5 | 14.5 | 2.0* |
| 59 | 322 | 103 | 286960. | 73.8 | 73.8 | 10.3* |
| 60 | 321 | 51 | 16731. | 4.3 | 4.3 | 0.6* |
| 61 | 320 | 43 | 9016. | 2.3 | 2.3 | 0.3 |
| 66 | 308 | 35 | 5607. | 1.4 | 1.4 | 0.2 |
| 68 | 306 | 43 | 5313. | 1.4 | 1.4 | 0.2 |
| 73 | 292 | 43 | 14640. | 3.8 | 3.8 | 0.5 |
| 75 | 290 | 35 | 5789. | 1.5 | 1.5 | 0.2 |
| 80 | 278 | 43 | 19782. | 5.1 | 5.1 | 0.7 |
| 82 | 276 | 35 | 4216. | 1.1 | 1.1 | 0.2 |
| 87 | 264 | 43 | 7198. | 1.9 | 1.9 | 0.3 |
| 89 | 262 | 43 | 11800. | 3.0 | 3.0 | 0.4 |
| 91 | 260 | 43 | 6097. | 1.6 | 1.6 | 0.2 |
| 94 | 249 | 43 | 20670. | 5.3 | 5.3 | 0.7 |
| 95 | 248 | 71 | 150560. | 38.7 | 38.7 | 5.4* |
| 102 | 334 | 103 | 388928. | 100.0 | 100.0 | 14.0* |
| 111 | 218 | 43 | 7888. | 2.0 | 2.0 | 0.3 |
| 113 | 216 | 35 | 4805. | 1.2 | 1.2 | 0.2 |
| 116 | 204 | 43 | 7568. | 1.9 | 1.9 | 0.3 |
| 118 | 202 | 43 | 15357. | 3.9 | 3.9 | 0.6 |
| 122 | 190 | 43 | 13687. | 3.5 | 3.5 | 0.5 |
| 124 | 188 | 51 | 13109. | 3.4 | 3.4 | 0.5* |
| 130 | 176 | 43 | 6987. | 1.8 | 1.8 | 0.3 |
| 132 | 174 | 51 | 17271. | 4.4 | 4.4 | 0.6 |
| 134 | 172 | 43 | 7604. | 2.0 | 2.0 | 0.3 |
| 140 | 160 | 51 | 13179. | 3.4 | 3.4 | 0.5 |
| 142 | 158 | 51 | 27487. | 7.1 | 7.1 | 1.0 |
| 145 | 146 | 51 | 18407. | 4.7 | 4.7 | 0.7 |
| 146 | 145 | 35 | 4676. | 1.2 | 1.2 | 0.2 |
| 147 | 144 | 51 | 36448. | 9.4 | 9.4 | 1.3 |
| 150 | 133 | 59 | 5181. | 1.3 | 1.3 | 0.2* |
| 151 | 132 | 51 | 23172. | 6.0 | 6.0 | 0.8 |
| 153 | 130 | 51 | 15869. | 4.1 | 4.1 | 0.6 |
| 155 | 128 | 43 | 4817. | 1.2 | 1.2 | 0.2 |
| 160 | 116 | 35 | 4021. | 1.0 | 1.0 | 0.1 |
| 162 | 114 | 51 | 20080. | 5.2 | 5.2 | 0.7 |
| 164 | 112 | 43 | 9442. | 2.4 | 2.4 | 0.3 |
| 168 | 103 | 43 | 11352. | 2.9 | 2.9 | 0.4 |
| 169 | 102 | 51 | 6723. | 1.7 | 1.7 | 0.2 |
| 171 | 100 | 51 | 23413. | 6.0 | 6.0 | 0.8 |
| 173 | 98 | 51 | 12050. | 3.1 | 3.1 | 0.4 |
| 175 | 96 | 43 | 4557. | 1.2 | 1.2 | 0.2 |
| 177 | 94 | 43 | 6361. | 1.6 | 1.6 | 0.2 |
| 178 | 89 | 43 | 6316. | 1.6 | 1.6 | 0.2* |
| 179 | 88 | 43 | 4573. | 1.2 | 1.2 | 0.2 |
| 180 | 87 | 51 | 9246. | 2.4 | 2.4 | 0.3 |
| 181 | 86 | 51 | 15869. | 4.1 | 4.1 | 0.6 |
| 182 | 85 | 51 | 7323. | 1.9 | 1.9 | 0.3 |
| 183 | 84 | 59 | 14651. | 3.8 | 3.8 | 0.5 |
| 185 | 82 | 43 | 8469. | 2.2 | 2.2 | 0.3 |
| 189 | 74 | 43 | 6908. | 1.8 | 1.8 | 0.2 |
| 190 | 73 | 59 | 7165. | 1.8 | 1.8 | 0.3 |
| 191 | 72 | 71 | 15546. | 4.0 | 4.0 | 0.6 |
| 192 | 71 | 59 | 21069. | 5.4 | 5.4 | 0.8 |
| 193 | 70 | 71 | 25248. | 6.5 | 6.5 | 0.9 |
| 194 | 69 | 51 | 6724. | 1.7 | 1.7 | 0.2 |
| 195 | 68 | 43 | 5212. | 1.3 | 1.3 | 0.2 |
| 199 | 60 | 51 | 12629. | 3.2 | 3.2 | 0.5 |
| 199 | 59 | 87 | 362112. | 93.1 | 93.1 | 13.0* |
| 200 | 58 | 71 | 46105. | 11.9 | 11.9 | 1.7 |
| 201 | 57 | 59 | 20791. | 5.3 | 5.3 | 0.7 |
| 202 | 56 | 59 | 48212. | 12.4 | 12.4 | 1.7 |

FAB of CsCl(bottom) and NaF(top) tdoha saturated solution

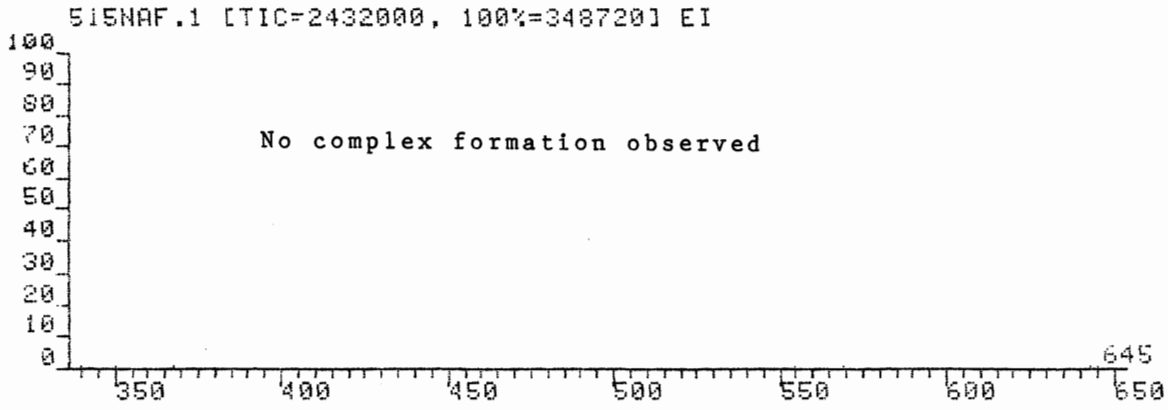


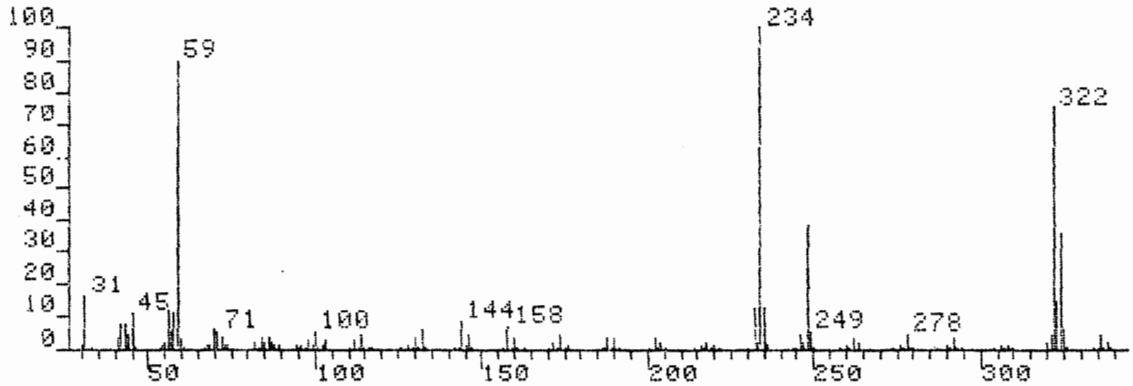


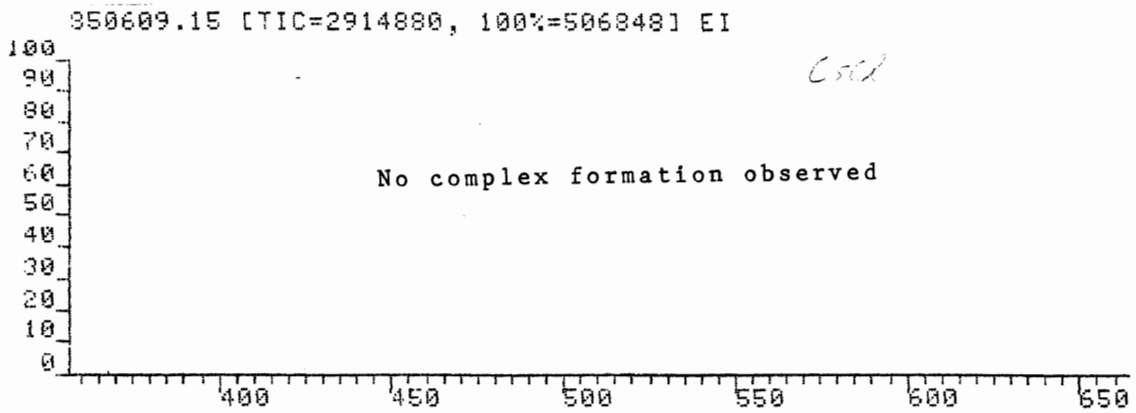


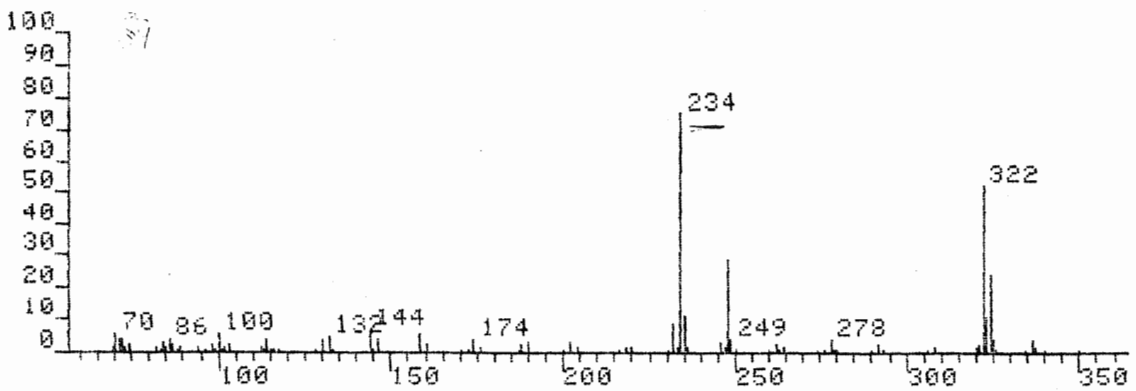

## Appendix I

Part 2 Crown ether-tdoha competitive systems.

Data for the crown ether-tdoha systems

| System | complex | % of base peak | %total ion current |
|---|---|---|---|
| tdoha/LiCl/18C6 | (tdoha)$Li^+$ | 48.8 | 8.1 |
| | (18C6)$Li^+$ | 14.2 | 2.4 |
| tdoha/LiCl/15C5 | (tdoha)$Li^+$ | 27.1 | 4.7 |
| | (15C5)$Li^+$ | 14.4 | 2.5 |
| tdoha/LiCl/12C4 | (tdoha)$Li^+$ | 12.3 | 1.8 |
| | (12C4)$Li^+$ | 0.3 | 0.0 |
| tdoha/NaCl/18C6 | (tdoha)$Na^+$ | --- | --- |
| | (18C6)$Na^+$ | 1.0 | 0.2 |
| tdoha/NaCl/15C5 | (tdoha)$Na^+$ | 5.4 | 0.9 |
| | (15C5)$Na^+$ | 3.6 | 0.6 |
| tdoha/NaCl/12C4 | (tdoha)$Na^+$ | 4.3 | 0.7 |
| | (12C4)$Na^+$ | --- | --- |
| tdoha/KCl/18C6 | (tdoha)$K^+$ | 2.8 | 0.5 |
| | (18C6)$K^+$ | 19.7 | 3.8 |
| tdoha/KCl/15C5 | (tdoha)$K^+$ | 7.0 | 1.4 |
| | (15C5)$K^+$ | 8.5 | 1.7 |
| tdoha/KCL/12C4 | (tdoha)$K^+$ | 2.0 | 0.3 |
| | (12C4)$K^+$ | --- | --- |

FAB mass spectrum of the tdoha/18C6/LiCl system

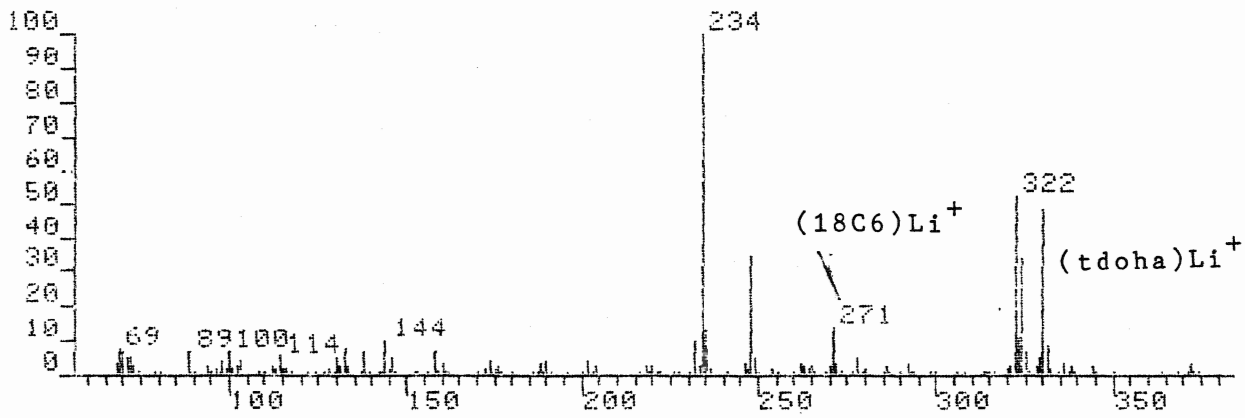


FAB mass spectrum of the tdoha/15C5/LiCl system

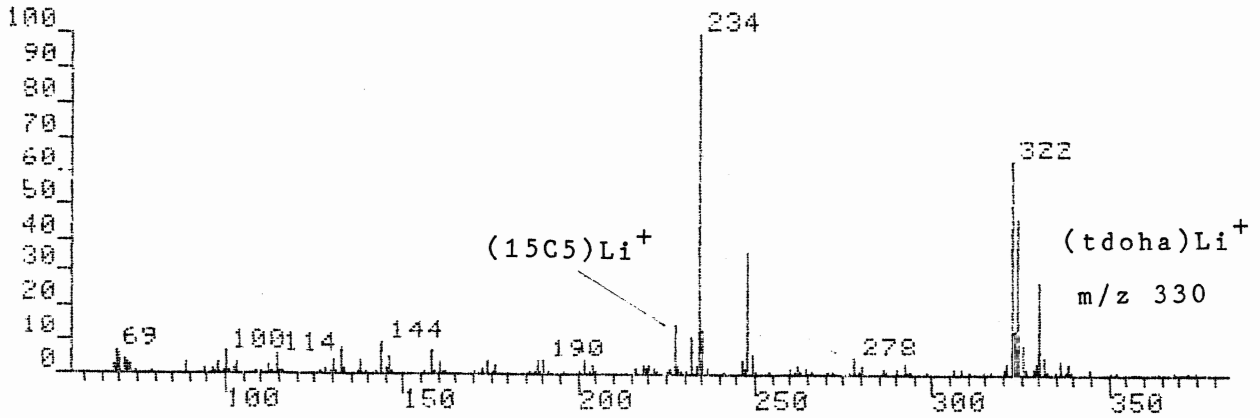


FAB mass spectrum of the tdoha/12C4/LiCl system

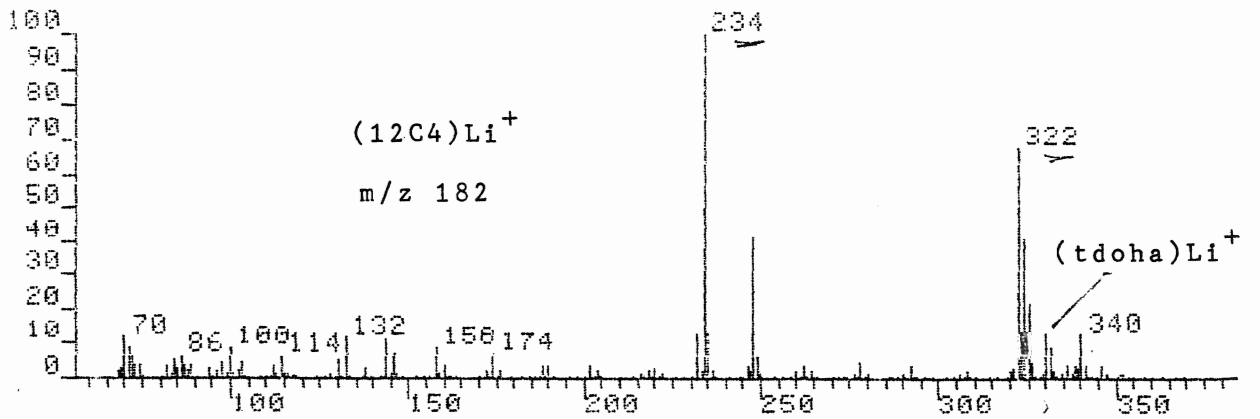

FAB mass spectrum of the tdoha/18C6/NaCl system

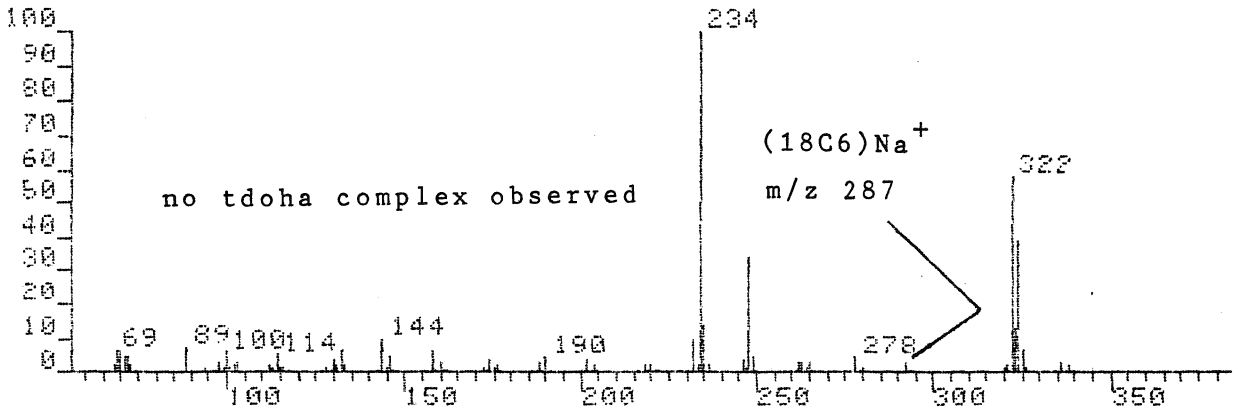


FAB mass spectrum of the tdoha/15C5/NaCl system

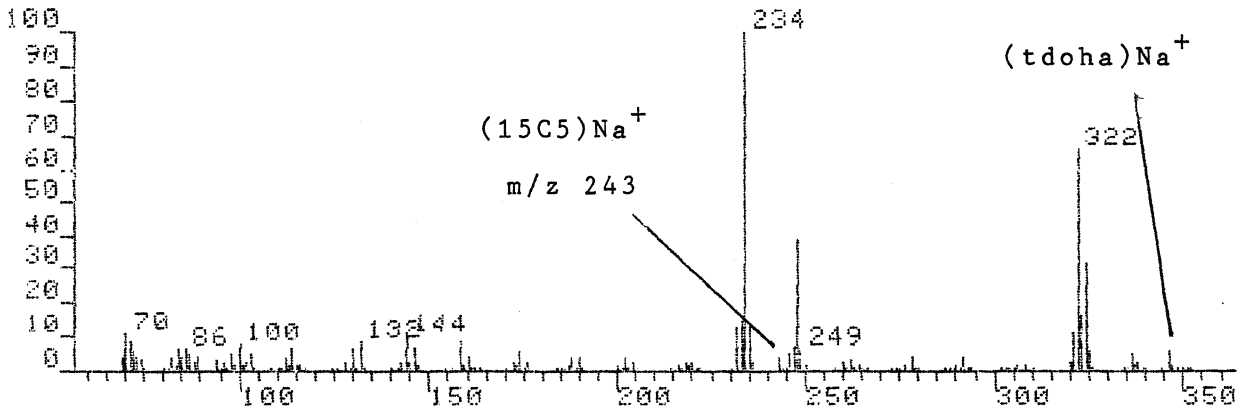


FAB mass spectrum of the tdoha/12C4/NaCl system

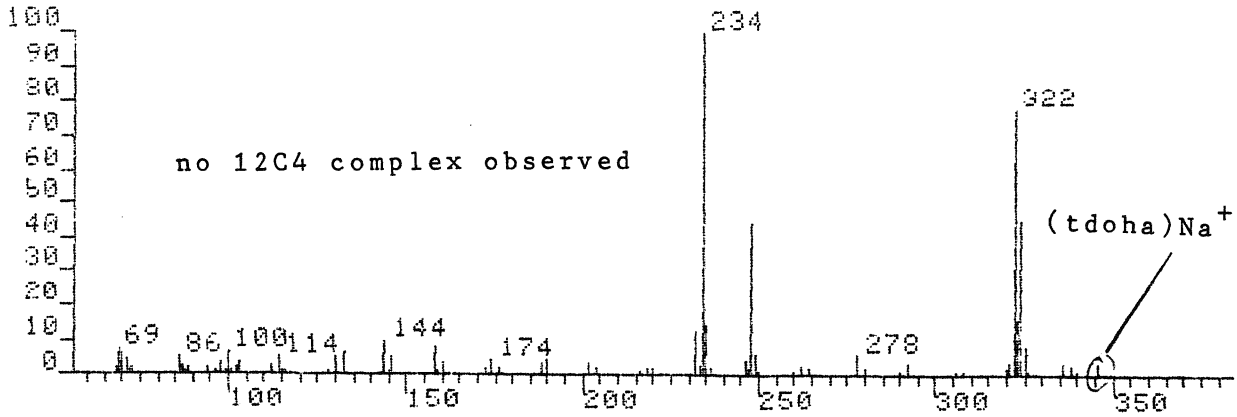

FAB mass spectrum of the tdoha/18C6/KCl system

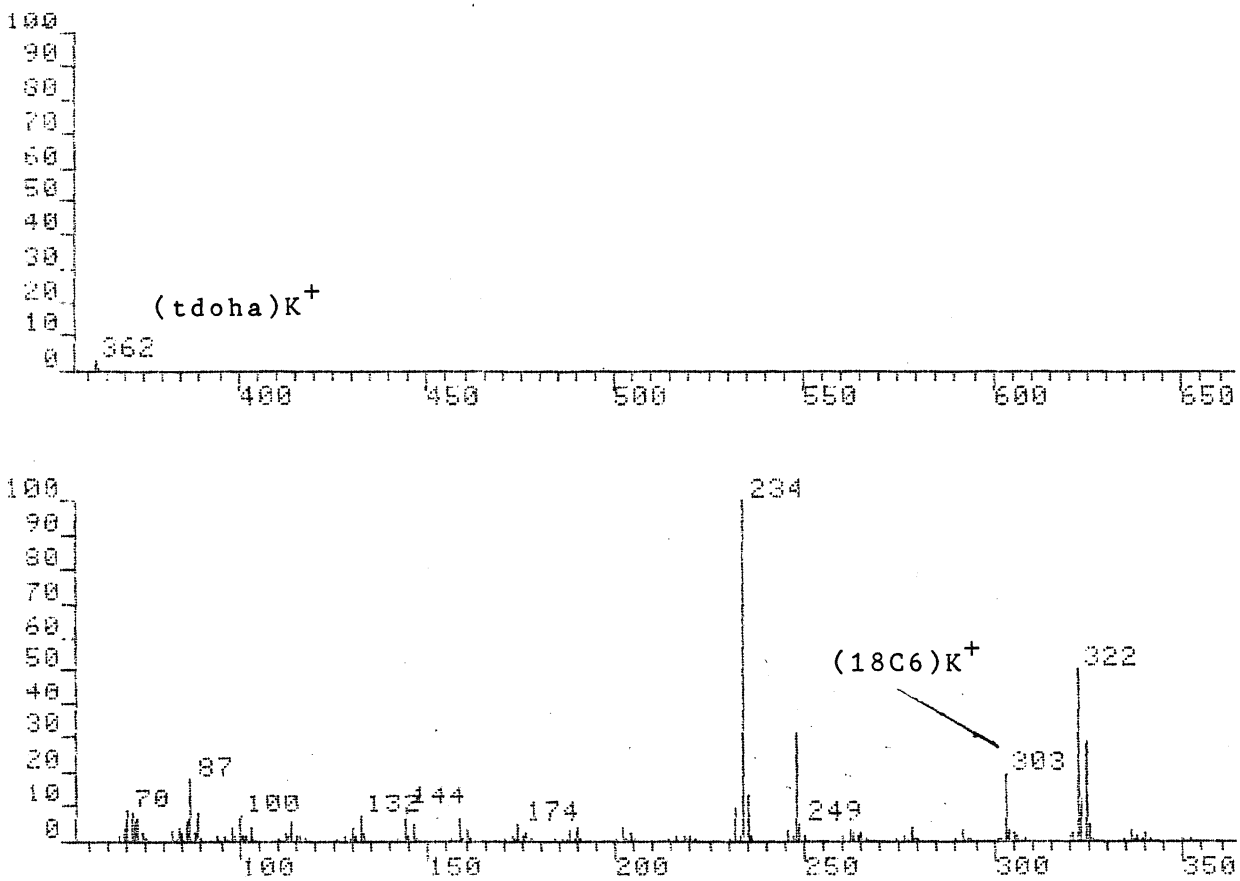

FAB mass spectrum of the tdoha/12C4/KCl system

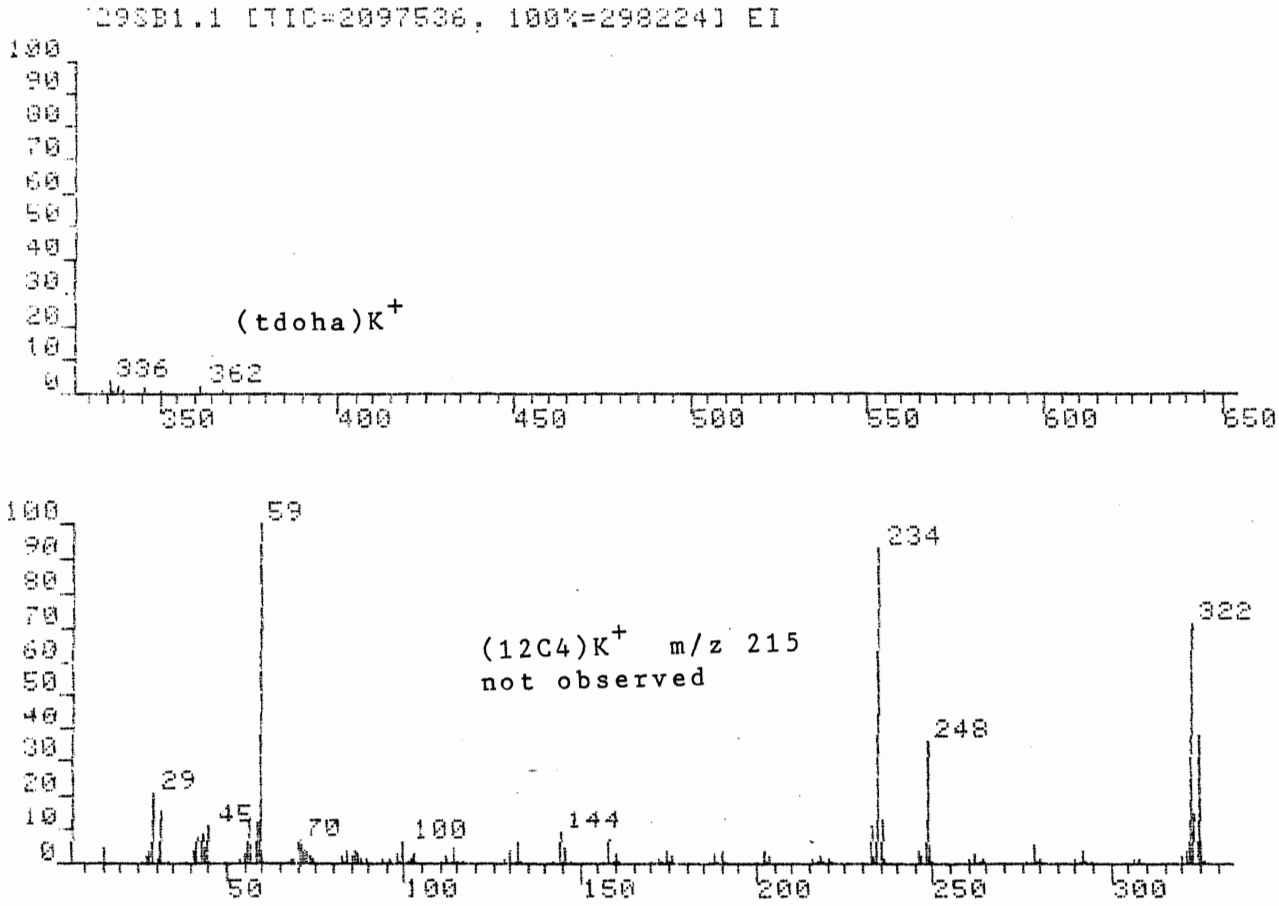


FAB mass spectrum of the tdoha/15C5/KCl system

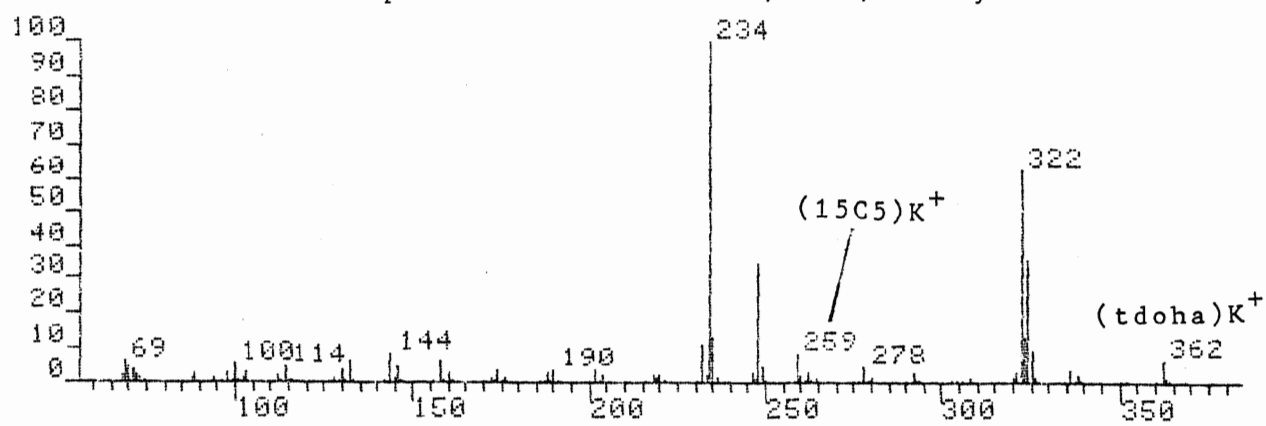

## Appendix II

The positive FAB mass spectra of the imidazole complexes with various electron donors

A21

**FAB of imidazole , 1.3 M in NBA**

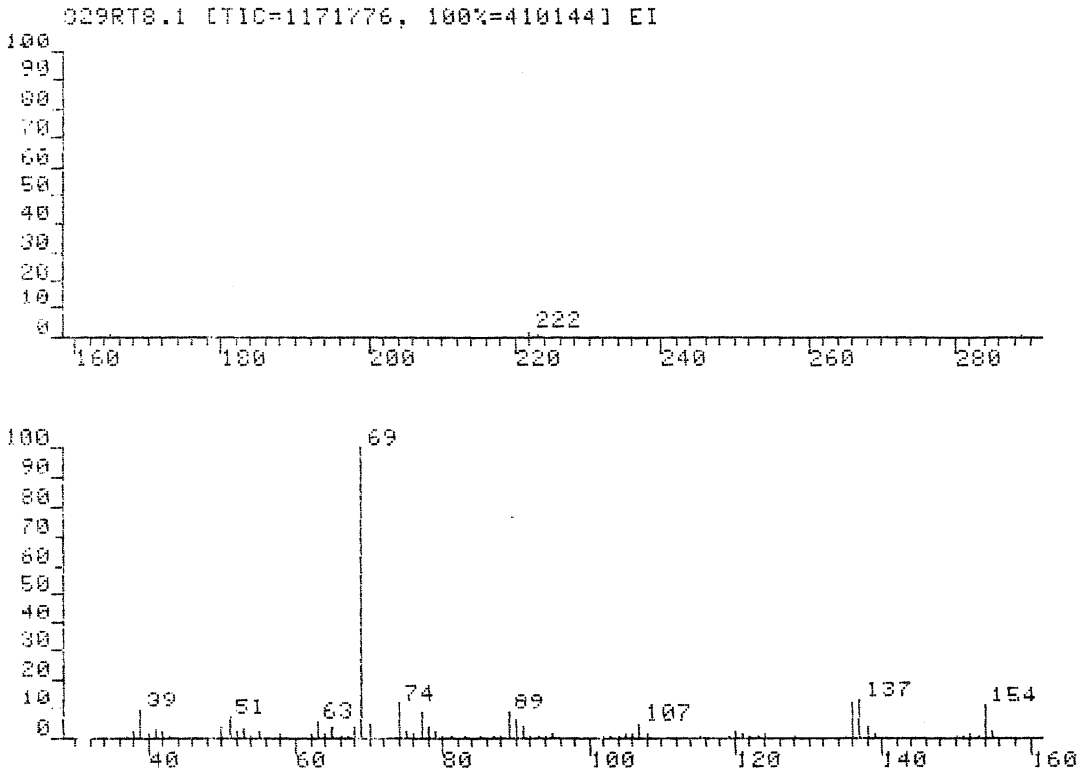


DB0.829RT8.MS
SCAN: 1. 8/29/85 16: 6
IONISATION: FAB 1M/NBA 6MG/100MG
NO. PEAKS: 74
BASE/NREF INT: 410144./ 410144.
TIC: 1171778.
MASS RANGE: 37 - 289

| PEAK NO. | MEASURED MASS | NO. POINTS | ABSOLUTE INTENSITY | % INT. BASE | % INT. NREF | % TOT. ION |
|---|---|---|---|---|---|---|
| 3 | 222 | 35 | 9519. | 2.3 | 2.3 | 0.8 |
| 7 | 155 | 35 | 9381. | 2.3 | 2.3 | 0.8 |
| 8 | 154 | 43 | 44164. | 10.8 | 10.8 | 3.8 |
| 10 | 152 | 35 | 4669. | 1.1 | 1.1 | 0.4 |
| 11 | 151 | 35 | 4144. | 1.0 | 1.0 | 0.4 |
| 13 | 139 | 35 | 5494. | 1.3 | 1.3 | 0.5 |
| 14 | 138 | 35 | 16313. | 4.0 | 4.0 | 1.4 |
| 15 | 137 | 51 | 53090. | 12.9 | 12.9 | 4.5 |
| 16 | 136 | 43 | 46941. | 11.4 | 11.4 | 4.0 |
| 19 | 124 | 35 | 4866. | 1.2 | 1.2 | 0.4 |
| 22 | 121 | 35 | 4433. | 1.1 | 1.1 | 0.4 |
| 23 | 120 | 35 | 8635. | 2.1 | 2.1 | 0.7 |
| 26 | 108 | 35 | 5690. | 1.4 | 1.4 | 0.5 |
| 27 | 107 | 35 | 19986. | 4.9 | 4.9 | 1.7 |
| 28 | 106 | 35 | 6648. | 1.6 | 1.6 | 0.6 |
| 29 | 105 | 35 | 7135. | 1.7 | 1.7 | 0.6 |
| 33 | 95 | 35 | 4426. | 1.1 | 1.1 | 0.4 |
| 37 | 91 | 43 | 13363. | 3.3 | 3.3 | 1.1 |
| 38 | 90 | 43 | 23511. | 5.7 | 5.7 | 2.0 |
| 39 | 89 | 43 | 32744. | 8.0 | 8.0 | 2.8 |
| 46 | 79 | 43 | 8405. | 2.0 | 2.0 | 0.7 |
| 47 | 78 | 35 | 15454. | 3.8 | 3.8 | 1.3 |
| 48 | 77 | 43 | 33661. | 8.2 | 8.2 | 2.9 |
| 49 | 76 | 35 | 6427. | 1.6 | 1.6 | 0.5 |
| 50 | 75 | 59 | 8191. | 2.0 | 2.0 | 0.7* |
| 51 | 74 | 71 | 46427. | 11.3 | 11.3 | 4.0* |
| 52 | 70 | 43 | 19162. | 4.7 | 4.7 | 1.6 |
| 53 | 69 | 21 | 410144. | 100.0 | 100.0 | 35.0* |
| 54 | 68 | 35 | 14539. | 3.5 | 3.5 | 1.2 |

# FAB of $ph_2SO$ complex, 1.26 M in NBA

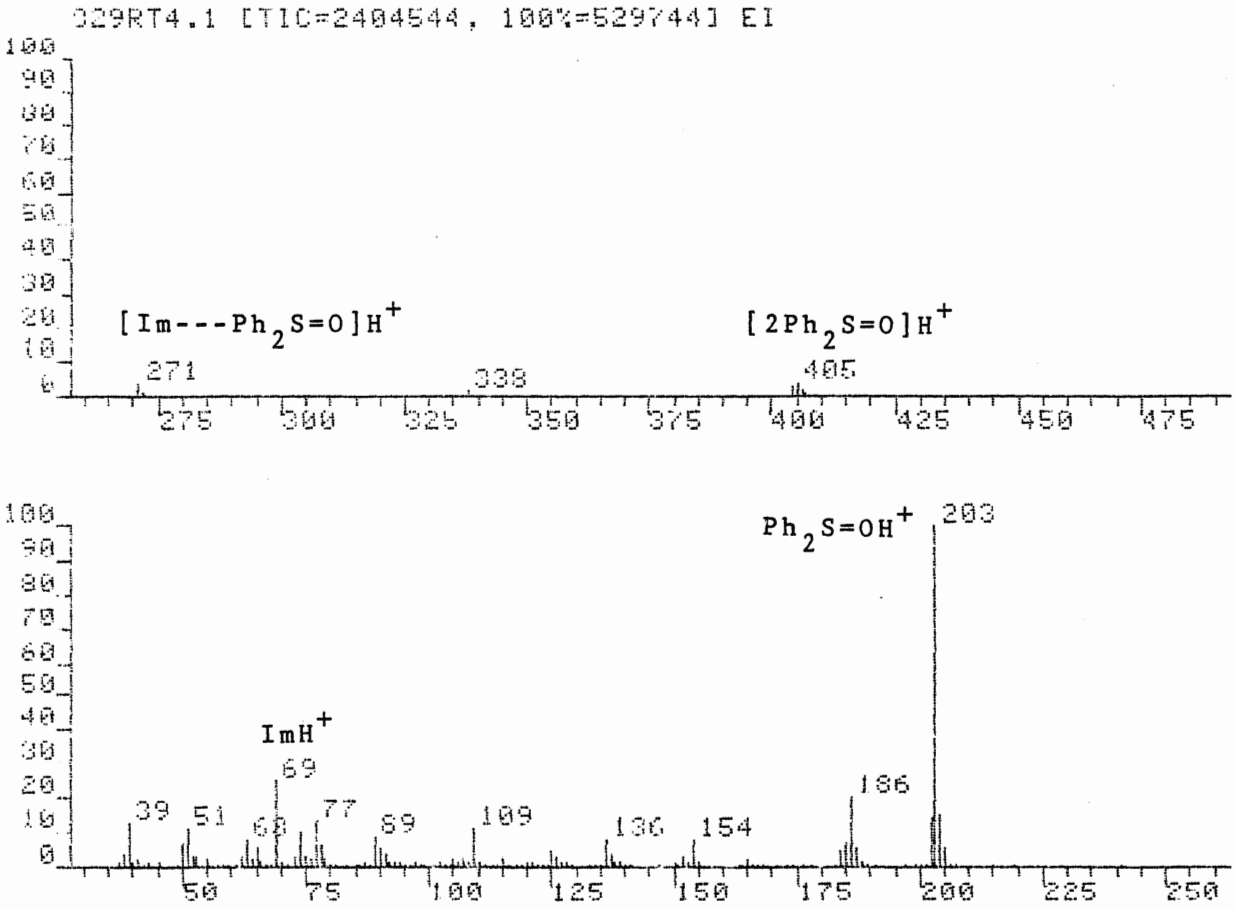


SP0:329RT4.MS
SCAN: 1, 8/29/85 14:46
IONISATION: FAB PH2SO-IM/NBA 23MG/100MG
NO. PEAKS: 168
BASE/NREF INT: 529744./ 529744.
TIC: 2404541.
MASS RANGE: 37 - 472

| PEAK NO. | MEASURED MASS | NO. POINTS | ABSOLUTE INTENSITY | % INT. BASE | % INT. NREF | % TOT. ION |
|---|---|---|---|---|---|---|
| 1 | 472 | 21 | 1645. | 0.3 | 0.3 | 0.1 |
| 2 | 407 | 29 | 3536. | 0.7 | 0.7 | 0.1 |
| 3 | 406 | 35 | 7427. | 1.4 | 1.4 | 0.3 |
| 4 | 405 | 35 | 22048. | 4.2 | 4.2 | 0.9 |
| 5 | 404 | 35 | 15460. | 2.9 | 2.9 | 0.6 |
| 6 | 403 | 21 | 1426. | 0.3 | 0.3 | 0.1 |
| 7 | 339 | 29 | 1673. | 0.3 | 0.3 | 0.1 |
| 8 | 338 | 35 | 6791. | 1.3 | 1.3 | 0.3 |
| 9 | 337 | 21 | 1261. | 0.2 | 0.2 | 0.1 |
| 10 | 279 | 25 | 1985. | 0.4 | 0.4 | 0.1 |
| 11 | 273 | 21 | 1501. | 0.3 | 0.3 | 0.1 |
| 12 | 272 | 29 | 4027. | 0.8 | 0.8 | 0.2 |
| 13 | 271 | 35 | 19347. | 3.7 | 3.7 | 0.8 |
| 25 | 204 | 51 | 78400. | 14.8 | 14.8 | 3.3* |
| 26 | 203 | 119 | 529744. | 100.0 | 100.0 | 22.0* |
| 27 | 202 | 71 | 74396. | 14.0 | 14.0 | 3.1* |
| 38 | 186 | 51 | 108324. | 20.4 | 20.4 | 4.5* |
| 103 | 109 | 43 | 58128. | 11.0 | 11.0 | 2.4 |
| 121 | 90 | 43 | 27477. | 5.2 | 5.2 | 1.1 |
| 122 | 89 | 43 | 46196. | 8.7 | 8.7 | 1.9 |
| 132 | 78 | 43 | 33458. | 6.3 | 6.3 | 1.4 |
| 133 | 77 | 51 | 69408. | 13.1 | 13.1 | 2.9 |
| 136 | 74 | 71 | 52852. | 10.0 | 10.0 | 2.2 |
| 140 | 69 | 87 | 132620. | 25.0 | 25.0 | 5.5 |
| 144 | 65 | 43 | 27910. | 5.3 | 5.3 | 1.2 |
| 146 | 63 | 43 | 40817. | 7.7 | 7.7 | 1.7 |
| 156 | 51 | 43 | 57687. | 10.9 | 10.9 | 2.4 |
| 157 | 50 | 43 | 35556. | 6.7 | 6.7 | 1.5 |
| 164 | 39 | 51 | 64836. | 12.2 | 12.2 | 2.7* |

# FAB of $ph_2SO$ complex, 2.14 M in NBA

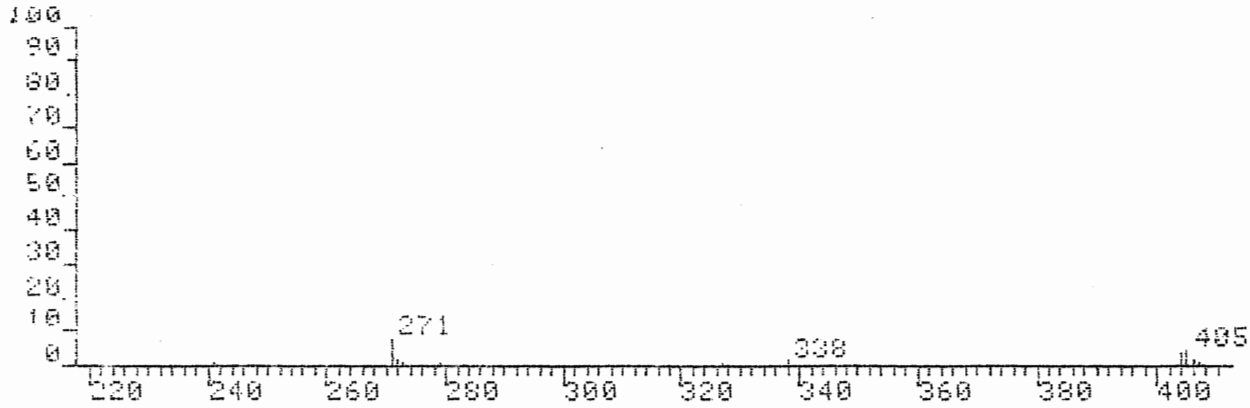


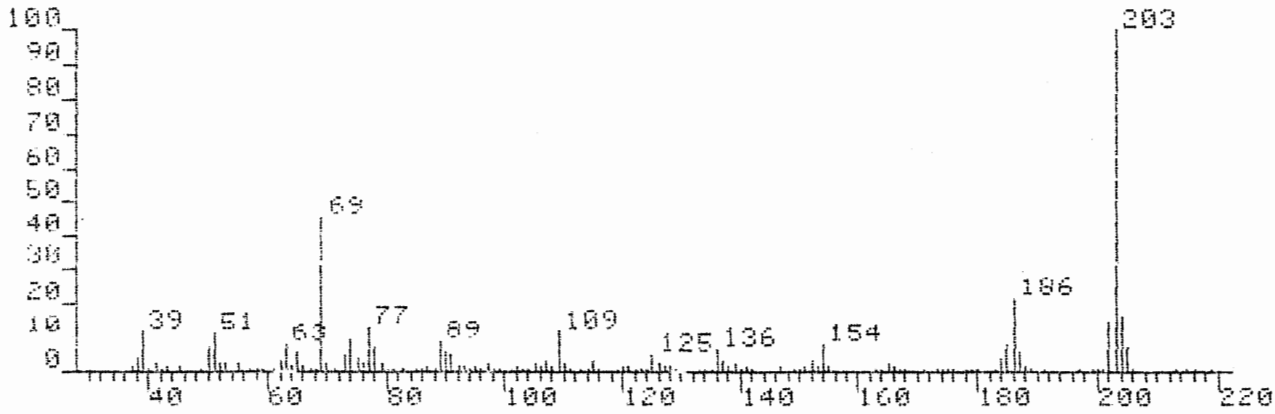


IONISATION: FAB PH2SO-IN/NBA 39MG/100MC
NO. PEAKS: 144
BASE/NREF INT: 372624./ 372624.
TIC: 1821376.
MASS RANGE: 37 - 407

| PEAK NO. | MEASURED MASS | NO. POINTS | ABSOLUTE INTENSITY | % INT. BASE | % INT. NREF | % TOT. ION |
|---|---|---|---|---|---|---|
| 1 | 407 | 29 | 3483. | 0.9 | 0.9 | 0.2 |
| 2 | 406 | 29 | 4801. | 1.3 | 1.3 | 0.3 |
| 3 | 405 | 43 | 17855. | 4.8 | 4.8 | 1.0 |
| 4 | 404 | 35 | 12640. | 3.4 | 3.4 | 0.7 |
| 5 | 338 | 29 | 4536. | 1.2 | 1.2 | 0.2 |
| 6 | 327 | 29 | 1902. | 0.5 | 0.5 | 0.1 |
| 7 | 279 | 29 | 2672. | 0.7 | 0.7 | 0.1 |
| 8 | 273 | 29 | 2410. | 0.6 | 0.6 | 0.1 |
| 9 | 272 | 35 | 5069. | 1.4 | 1.4 | 0.3 |
| 10 | 271 | 43 | 28730. | 7.7 | 7.7 | 1.6 |
| 19 | 204 | 51 | 59388. | 15.9 | 15.9 | 3.3 |
| 20 | 203 | 87 | 372624. | 100.0 | 100.0 | 20.5* |
| 21 | 202 | 59 | 54632. | 14.7 | 14.7 | 3.0* |
| 30 | 186 | 51 | 80568. | 21.6 | 21.6 | 4.4* |
| 63 | 109 | 43 | 42564. | 11.4 | 11.4 | 2.3 |
| 101 | 90 | 43 | 21070. | 5.7 | 5.7 | 1.2 |
| 102 | 89 | 43 | 30805. | 8.3 | 8.3 | 1.7 |
| 111 | 78 | 43 | 24332. | 6.5 | 6.5 | 1.3 |
| 112 | 77 | 51 | 50501. | 13.6 | 13.6 | 2.8* |
| 115 | 74 | 71 | 34398. | 9.2 | 9.2 | 1.9* |
| 119 | 69 | 87 | 170076. | 45.6 | 45.6 | 9.3 |
| 123 | 65 | 43 | 20471. | 5.5 | 5.5 | 1.1 |
| 125 | 63 | 43 | 28497. | 7.6 | 7.6 | 1.6 |
| 134 | 51 | 43 | 40821. | 11.0 | 11.0 | 2.2 |
| 135 | 50 | 43 | 25044. | 6.7 | 6.7 | 1.4 |
| 142 | 39 | 59 | 42053. | 11.3 | 11.3 | 2.3* |

# FAB of $ph_3PO$ complex, 0.08 M in NBA

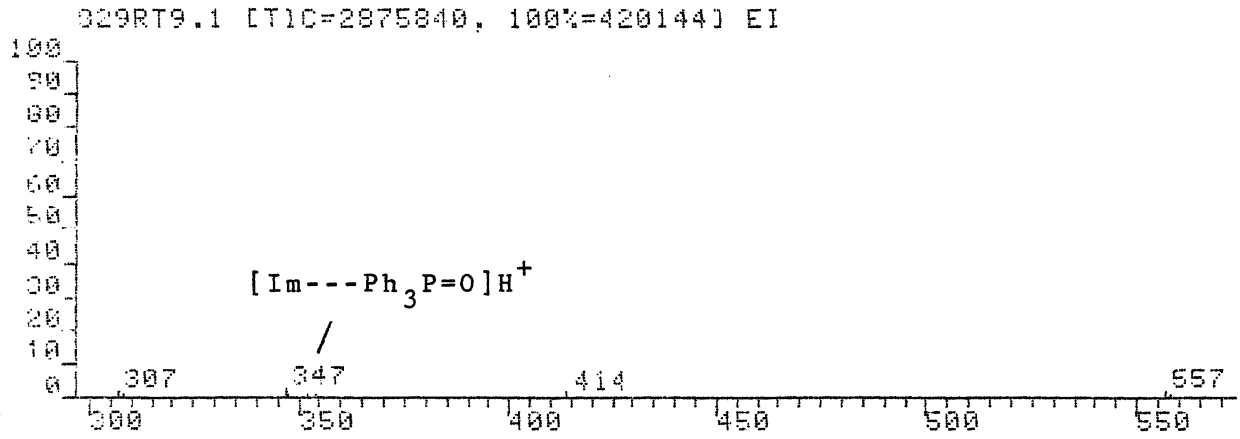


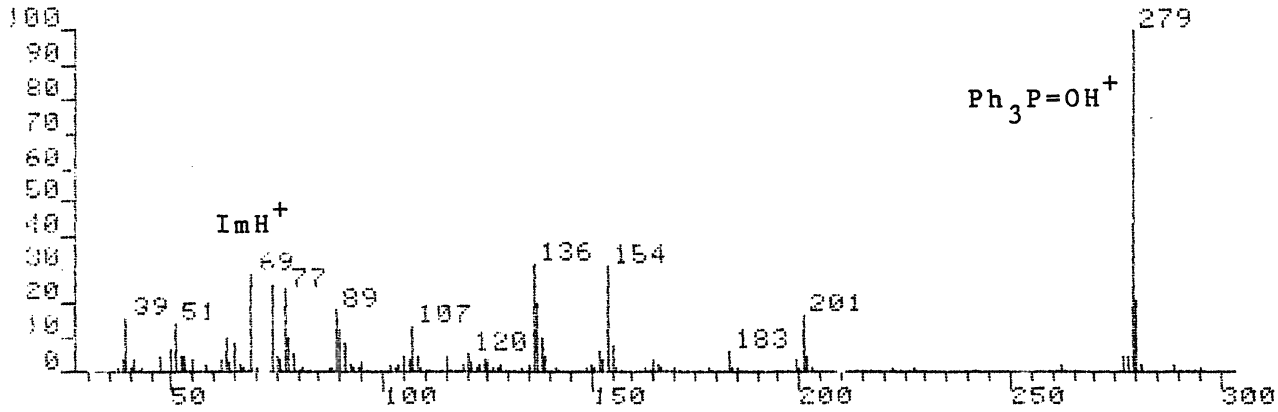


DP0:329RT9.MS
SCAN: 1, 8/29/85 17:42

IONISATION: FAB PH3PO/IM/NBA 2MG/100MG
NO. PEAKS: 185
BASE/NREF INT: 420144./ 420144.
TIC: 2875840.
MASS RANGE: 37 - 558
RETN TIME/MISC: 0: 0/ 0/ 0/ 0
PAGE 1

| PEAK NO. | MEASURED MASS | NO. POINTS | ABSOLUTE INTENSITY | % INT. BASE | % INT. NREF | % TOT. ION |
|---|---|---|---|---|---|---|
| 1 | 558 | 29 | 4184. | 1.0 | 1.0 | 0.1 |
| 2 | 557 | 35 | 9689. | 2.3 | 2.3 | 0.3 |
| 3 | 414 | 35 | 5243. | 1.2 | 1.2 | 0.2 |
| 4 | 354 | 25 | 2056. | 0.5 | 0.5 | 0.1 |
| 5 | 352 | 29 | 2635. | 0.6 | 0.6 | 0.1 |
| 6 | 348 | 29 | 3499. | 0.8 | 0.8 | 0.1 |
| 7 | 347 | 35 | 14011. | 3.3 | 3.3 | 0.5 |
| 8 | 308 | 29 | 2938. | 0.7 | 0.7 | 0.1 |
| 9 | 307 | 35 | 9968. | 2.4 | 2.4 | 0.3 |
| 10 | 303 | 25 | 1519. | 0.4 | 0.4 | 0.1 |
| 20 | 280 | 87 | 88104. | 21.0 | 21.0 | 3.1% |
| 21 | 279 | 119 | 420144. | 100.0 | 100.0 | 14.6% |
| 53 | 201 | 51 | 66952. | 15.9 | 15.9 | 2.3% |
| 85 | 154 | 59 | 131676. | 31.3 | 31.3 | 4.6% |
| 98 | 137 | 51 | 84936. | 20.2 | 20.2 | 3.0% |
| 99 | 136 | 59 | 134568. | 32.0 | 32.0 | 4.7% |
| 126 | 107 | 59 | 55717. | 13.3 | 13.3 | 1.9 |
| 141 | 90 | 51 | 52820. | 12.6 | 12.6 | 1.8 |
| 142 | 89 | 51 | 77268. | 18.4 | 18.4 | 2.7 |
| 152 | 78 | 51 | 43103. | 10.3 | 10.3 | 1.5 |
| 153 | 77 | 71 | 103092. | 24.5 | 24.5 | 3.6% |
| 156 | 74 | 87 | 107416. | 25.6 | 25.6 | 3.7 |
| 159 | 69 | 71 | 120620. | 28.7 | 28.7 | 4.2% |
| 165 | 63 | 43 | 43325. | 10.3 | 10.3 | 1.5 |
| 175 | 51 | 51 | 58944. | 14.0 | 14.0 | 2.0 |
| 183 | 39 | 51 | 65644. | 15.6 | 15.6 | 2.3 |

# FAB of $ph_3PO$ complex, 0.42 M in NBA

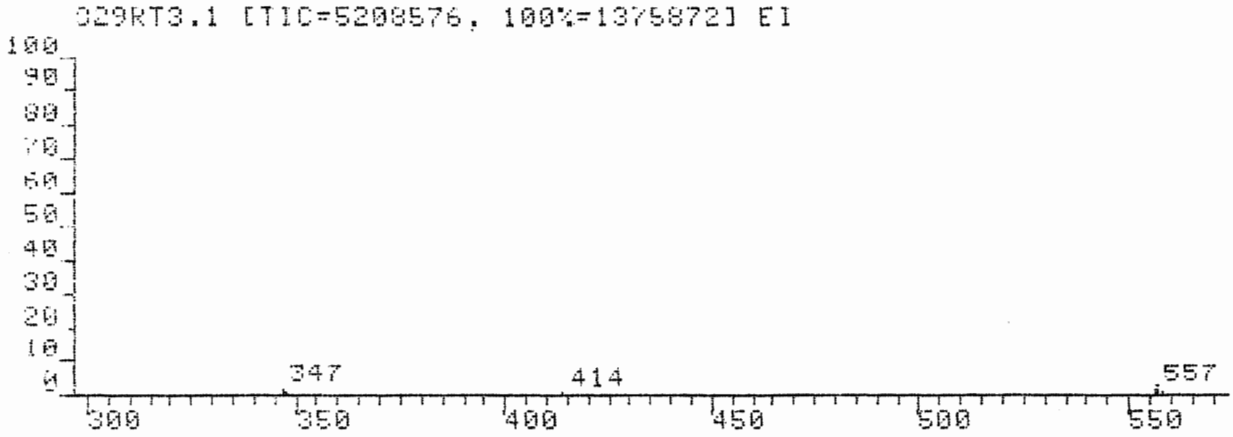


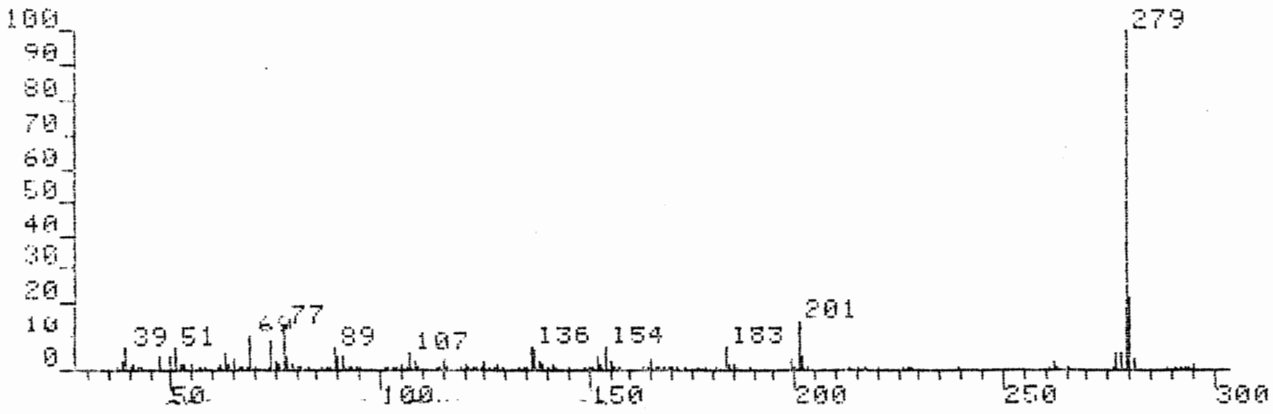


BC0:329RT3.MS
CLEAN: Y 9/29/85 11:19
IONISATION: FAB PH3PO-IM/NBA 10MG/100MG
NO. PEAKS: 202
BASE/NREF INT: 1375872./ 1375872.
TIC: 5208576.
MASS RANGE: 37 - 558

| PEAK NO. | MEASURED MASS | NO. POINTS | ABSOLUTE INTENSITY | % INT. BASE | % INT. NREF | % TOT. ION |
|---|---|---|---|---|---|---|
| 1 | 558 | 35 | 13967. | 1.0 | 1.0 | 0.3 |
| 2 | 557 | 43 | 36318. | 2.6 | 2.6 | 0.7 |
| 3 | 556 | 43 | 33340. | 2.4 | 2.4 | 0.6 |
| 6 | 414 | 35 | 15340. | 1.1 | 1.1 | 0.3 |
| 14 | 347 | 43 | 28150. | 2.0 | 2.0 | 0.5 - |
| 20 | 295 | 43 | 16674. | 1.2 | 1.2 | 0.3 |
| 28 | 281 | 51 | 35451. | 2.6 | 2.6 | 0.7 |
| 29 | 280 | 103 | 294528. | 21.4 | 21.4 | 5.7% |
| 30 | 279 | 175 | - 1375872. | 100.0 | 100.0 | 26.4%^- |
| 31 | 278 | 87 | 68021. | 4.9 | 4.9 | 1.3% |
| 32 | 277 | 103 | 65043. | 4.7 | 4.7 | 1.2% |
| 105 | 154 | 51 | 88848. | 6.5 | 6.5 | 1.7 |
| 169 | 79 | 51 | 23249. | 1.7 | 1.7 | 0.4 |
| 170 | 78 | 43 | 57357. | 4.2 | 4.2 | 1.1 |
| 171 | 77 | 59 | 177584. | 12.9 | 12.9 | 3.4 |
| 172 | 76 | 43 | 20045. | 1.5 | 1.5 | 0.4 |
| 173 | 75 | 71 | 25018. | 1.8 | 1.8 | 0.5% |
| 174 | 74 | 87 | -109680. | 8.0 | 8.0 | 2.1% |
| 177 | 69 | 71 | -140192. | 10.2 | 10.2 | 2.7 |
| 181 | 65 | 43 | 42486. | 3.1 | 3.1 | 0.8 |
| 182 | 64 | 43 | 15568. | 1.1 | 1.1 | 0.3 |
| 183 | 63 | 43 | 60194. | 4.4 | 4.4 | 1.2 |

# FAB of $ph_3PO$ complex, 0.84 M in NBA

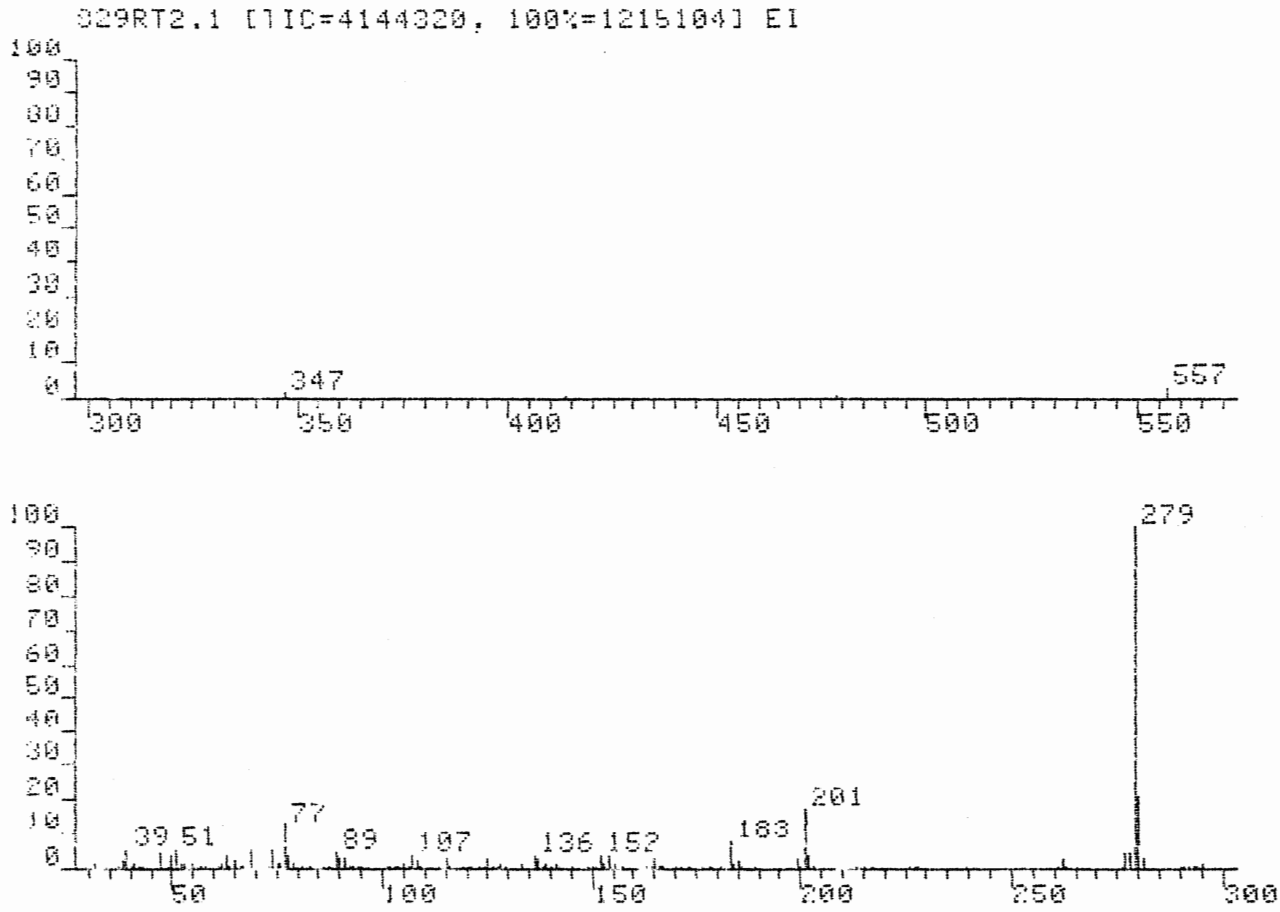


DP0:029RT2.MS
SCAN: 1. 8/29/95 11: 2
IONISATION: FAB PH3PO-IM/NBA 20MG/100MG
NO. PEAKS: 187
BASE/NREF INT: 1215104./ 1215104.
TIC: 4144320.
MASS RANGE: 31 - 557

| PEAK NO. | MEASURED MASS | NO POINTS | ABSOLUTE INTENSITY | % INT. BASE | % INT. NREF | % TOT. ION |
|---|---|---|---|---|---|---|
| 1 | 557 | 51 | 35607. | 2.9 | 2.9 | 0.9% |
| 2 | 479 | 35 | 6979. | 0.6 | 0.6 | 0.2% |
| 3 | 415 | 29 | 3249. | 0.3 | 0.3 | 0.1 |
| 4 | 414 | 35 | 10215. | 0.8 | 0.8 | 0.2 |
| 5 | 385 | 29 | 3009. | 0.2 | 0.2 | 0.1 |
| 6 | 355 | 25 | 2236. | 0.2 | 0.2 | 0.1 |
| 7 | 354 | 29 | 3350. | 0.3 | 0.3 | 0.1 |
| 8 | 352 | 29 | 2664. | 0.2 | 0.2 | 0.1 |
| 9 | 348 | 35 | 4542. | 0.4 | 0.4 | 0.1 |
| 10 | 347 | 35 | 17442. | 1.4 | 1.4 | 0.4 |
| 25 | 280 | 87 | 255748. | 21.0 | 21.0 | 6.2% |
| 26 | 279 | 175 | 1215104. | 100.0 | 100.0 | 29.3% |
| 61 | 201 | 71 | 201860. | 16.6 | 16.6 | 4.9 |
| 146 | 91 | 43 | 31925. | 2.6 | 2.6 | 0.8 |
| 147 | 90 | 43 | 31802. | 2.6 | 2.6 | 0.8 |
| 148 | 89 | 43 | 56774. | 4.7 | 4.7 | 1.4 |
| 156 | 78 | 43 | 40906. | 3.4 | 3.4 | 1.0 |
| 157 | 77 | 51 | 149812. | 12.3 | 12.3 | 3.6 |
| 160 | 74 | 87 | 68936. | 5.7 | 5.7 | 1.7% |
| 163 | 69 | 71 | 67472. | 5.6 | 5.6 | 1.6 |
| 166 | 65 | 43 | 28187. | 2.3 | 2.3 | 0.7 |
| 168 | 63 | 43 | 45294. | 3.7 | 3.7 | 1.1 |
| 176 | 51 | 43 | 67628. | 5.6 | 5.6 | 1.6 |
| 177 | 50 | 43 | 39322. | 3.2 | 3.2 | 0.9 |
| 179 | 47 | 51 | 58116. | 4.8 | 4.8 | 1.4 |
| 184 | 39 | 43 | 65096. | 5.4 | 5.4 | 1.6 |

# FAB of $ph_3PO$ complex, 1.26 M in NBA

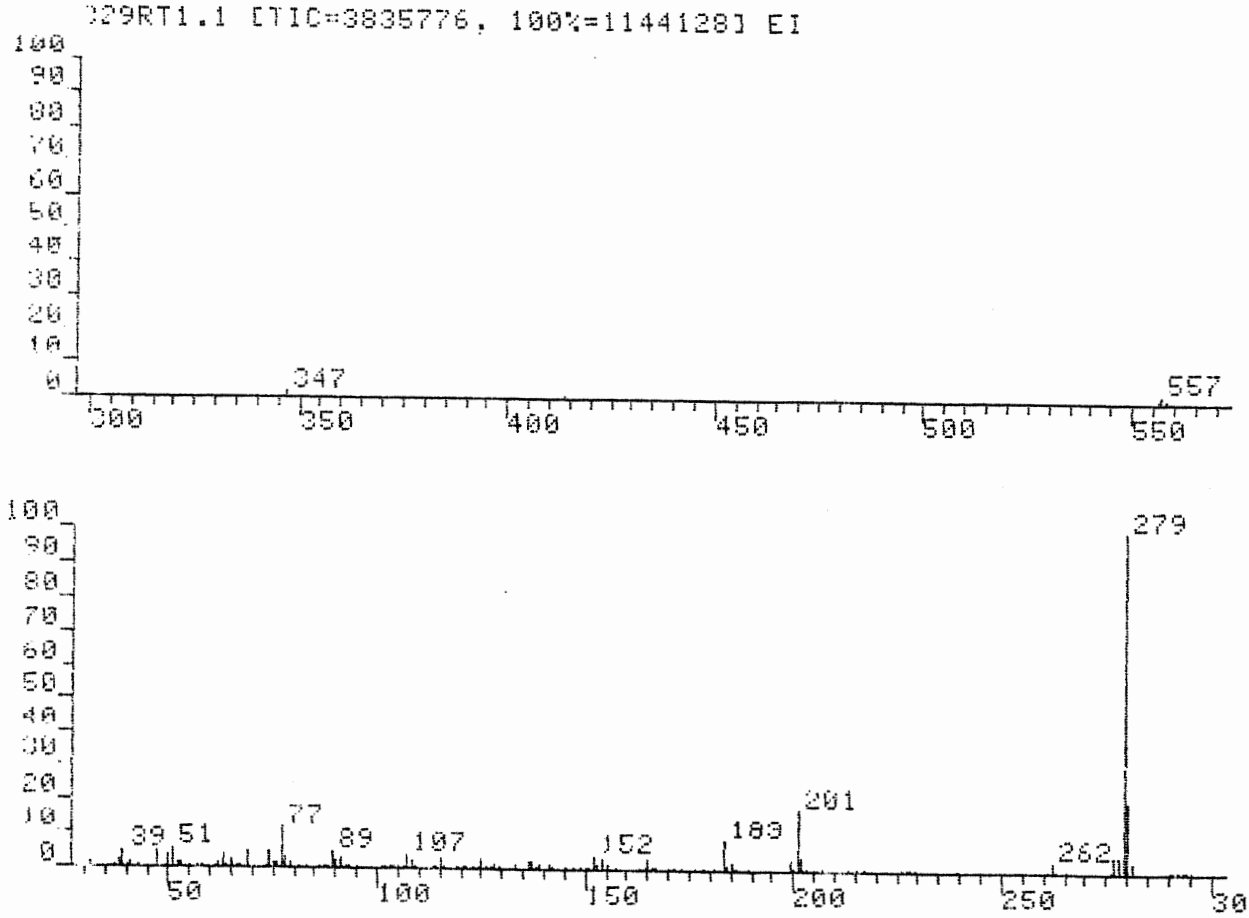


DB0:829RT1.MS
SCAN: 1, 8/29/85 10:46
IONISATION: FAB PH3PO-IM/NBA 30MG/100MG
NO. PEAKS: 186
BASE/NREF INT: 1144128./ 1144128.
TIC: 3835776.
MASS RANGE: 31 - 558

| PEAK NO. | MEASURED MASS | NO. POINTS | ABSOLUTE INTENSITY | % INT. BASE | % INT. NREF | % TOT. ION |
|---|---|---|---|---|---|---|
| 1 | 558 | 35 | 12071. | 1.1 | 1.1 | 0.3 |
| 2 | 557 | 43 | 29923. | 2.6 | 2.6 | 0.8 |
| 3 | 556 | 35 | 13393. | 1.2 | 1.2 | 0.3 |
| 4 | 480 | 35 | 3593. | 0.3 | 0.3 | 0.1 |
| 5 | 479 | 35 | 9855. | 0.9 | 0.9 | 0.3 |
| 6 | 415 | 29 | 2800. | 0.2 | 0.2 | 0.1 |
| 7 | 414 | 35 | 8059. | 0.7 | 0.7 | 0.2 |
| 8 | 385 | 29 | 2412. | 0.2 | 0.2 | 0.1 |
| 9 | 355 | 29 | 2194. | 0.2 | 0.2 | 0.1 |
| 10 | 354 | 29 | 2445. | 0.2 | 0.2 | 0.1 |
| 11 | 348 | 35 | 4269. | 0.4 | 0.4 | 0.1 |
| 12 | 347 | 35 | 16068. | 1.4 | 1.4 | 0.4 |
| 26 | 280 | 103 | 238780. | 20.9 | 20.9 | 6.2* |
| 27 | 279 | 175 | 1144128. | 100.0 | 100.0 | 29.8* |
| 63 | 201 | 71 | 201944. | 17.7 | 17.7 | 5.3* |
| 146 | 91 | 43 | 28311. | 2.5 | 2.5 | 0.7 |
| 147 | 90 | 43 | 26579. | 2.3 | 2.3 | 0.7 |
| 148 | 89 | 43 | 49494. | 4.3 | 4.3 | 1.3 |
| 156 | 78 | 43 | 36287. | 3.2 | 3.2 | 0.9 |
| 157 | 77 | 59 | 132952. | 11.6 | 11.6 | 3.5 |
| 160 | 74 | 87 | 56392. | 4.9 | 4.9 | 1.5* |
| 162 | 69 | 71 | 55904. | 4.9 | 4.9 | 1.5 |
| 166 | 65 | 43 | 25043. | 2.2 | 2.2 | 0.7 |
| 168 | 63 | 43 | 39562. | 3.5 | 3.5 | 1.0 |
| 176 | 51 | 43 | 62532. | 5.5 | 5.5 | 1.6 |
| 177 | 50 | 43 | 39301. | 3.4 | 3.4 | 1.0 |
| 179 | 47 | 51 | 55153. | 4.8 | 4.8 | 1.4 |
| 183 | 39 | 51 | 56094. | 4.9 | 4.9 | 1.5 |
| 184 | 38 | 43 | 23297. | 2.0 | 2.0 | 0.6 |

FAB of $ph_3PO(ImH^+)Br^-$ complex, 0.06 M in NBA

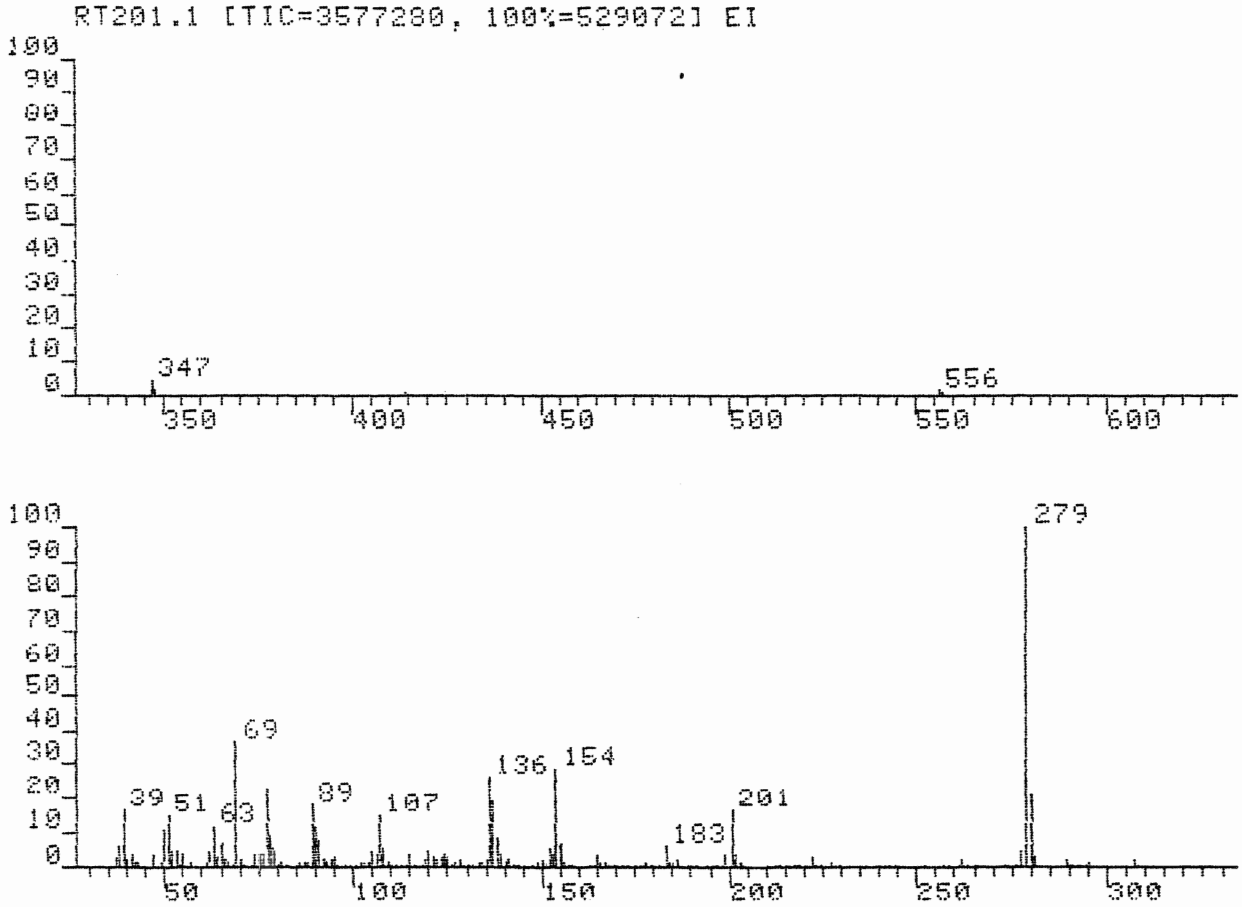


IONISATION: FAB Ph3P=O*IMH+Br- (0.062M)
NO. PEAKS: 237
BASE/NREF INT: 529072./ 529072.
TIC: 3577280.
MASS RANGE: 36 - 624
RETN TIME/MISC: 0: 0/ 0/ 0/ 0
PAGE 1

| PEAK NO. | MEASURED MASS | NO. POINTS | ABSOLUTE INTENSITY | % INT. BASE | % INT. NREF | % TOT. ION |
|---|---|---|---|---|---|---|
| 2 | 557 | 35 | 3785. | 0.7 | 0.7 | 0.1* |
| 3 | 556 | 35 | 6677. | 1.3 | 1.3 | 0.2 |
| 5 | 414 | 35 | 4317. | 0.8 | 0.8 | 0.1 |
| 12 | 348 | 35 | 6601. | 1.2 | 1.2 | 0.2 |
| 13 | 347 | 43 | 25754. | 4.9 | 4.9 | 0.7 |
| 15 | 308 | 35 | 3713. | 0.7 | 0.7 | 0.1 |
| 16 | 307 | 35 | 12299. | 2.3 | 2.3 | 0.3 |
| 28 | 280 | 71 | 109088. | 20.6 | 20.6 | 3.0* |
| 29 | 279 | 143 | 529072. | 100.0 | 100.0 | 14.8* |
| 87 | 201 | 59 | 87704. | 16.6 | 16.6 | 2.5 |
| 130 | 154 | 59 | 151460. | 28.6 | 28.6 | 4.2* |
| 147 | 137 | 51 | 100196. | 18.9 | 18.9 | 2.8 |
| 148 | 136 | 51 | 138620. | 26.2 | 26.2 | 3.9 |
| 176 | 107 | 59 | 77880. | 14.7 | 14.7 | 2.2 |
| 192 | 90 | 51 | 59972. | 11.3 | 11.3 | 1.7 |
| 193 | 89 | 51 | 97356. | 18.4 | 18.4 | 2.7 |
| 205 | 77 | 51 | 120196. | 22.7 | 22.7 | 3.4 |
| 212 | 69 | 71 | 194604. | 36.8 | 36.8 | 5.4 |
| 218 | 63 | 51 | 60632. | 11.5 | 11.5 | 1.7 |
| 226 | 51 | 51 | 78456. | 14.8 | 14.8 | 2.2 |
| 227 | 50 | 43 | 57071. | 10.8 | 10.8 | 1.6 |
| 234 | 39 | 43 | 86768. | 16.4 | 16.4 | 2.4 |

FAB of $ph_3PO(ImH^+)Br^-$ complex, 0.29 M in NBA

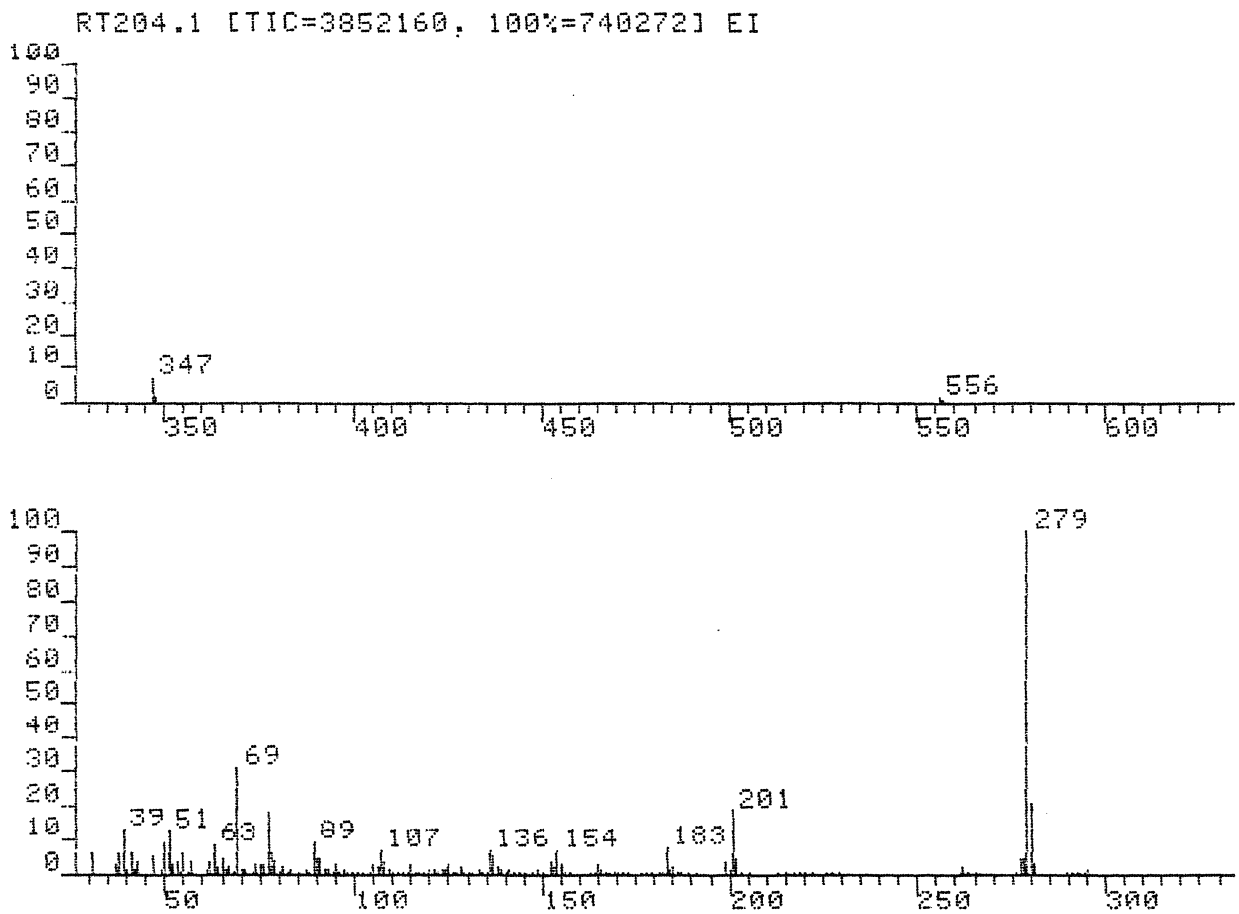


DP0:RT204.MS
SCAN: 1. 6/16/87 18:16
IONISATION: FAB Ph3P=O+IMH+Br- (0.290M)
NO. PEAKS: 206
BASE/NREF INT: 740272./ 740272.
TIC: 3852160.
MASS RANGE: 31 - 625
RETN TIME/MISC: 0: 0/ 0/ 0/ 0
PAGE 1

| PEAK NO. | MEASURED MASS | NO. POINTS | ABSOLUTE INTENSITY | % INT. BASE | % INT. NREF | % TOT. ION |
|---|---|---|---|---|---|---|
| 4 | 556 | 35 | 10972. | 1.5 | 1.5 | 0.3 |
| 9 | 348 | 35 | 13613. | 1.8 | 1.8 | 0.4 |
| 10 | 347 | 43 | 52525. | 7.1 | 7.1 | 1.4 |
| 23 | 280 | 103 | 152920. | 20.7 | 20.7 | 4.0* |
| 24 | 279 | 143 | 740272. | 100.0 | 100.0 | 19.2* |
| 62 | 201 | 87 | 138672. | 18.7 | 18.7 | 3.6* |
| 172 | 77 | 59 | 135996. | 18.4 | 18.4 | 3.5 |
| 179 | 69 | 71 | 228352. | 30.8 | 30.8 | 5.9 |

R

FAB of $ph_3PO(ImH^+)Br^-$ complex, 0.77 M in NBA

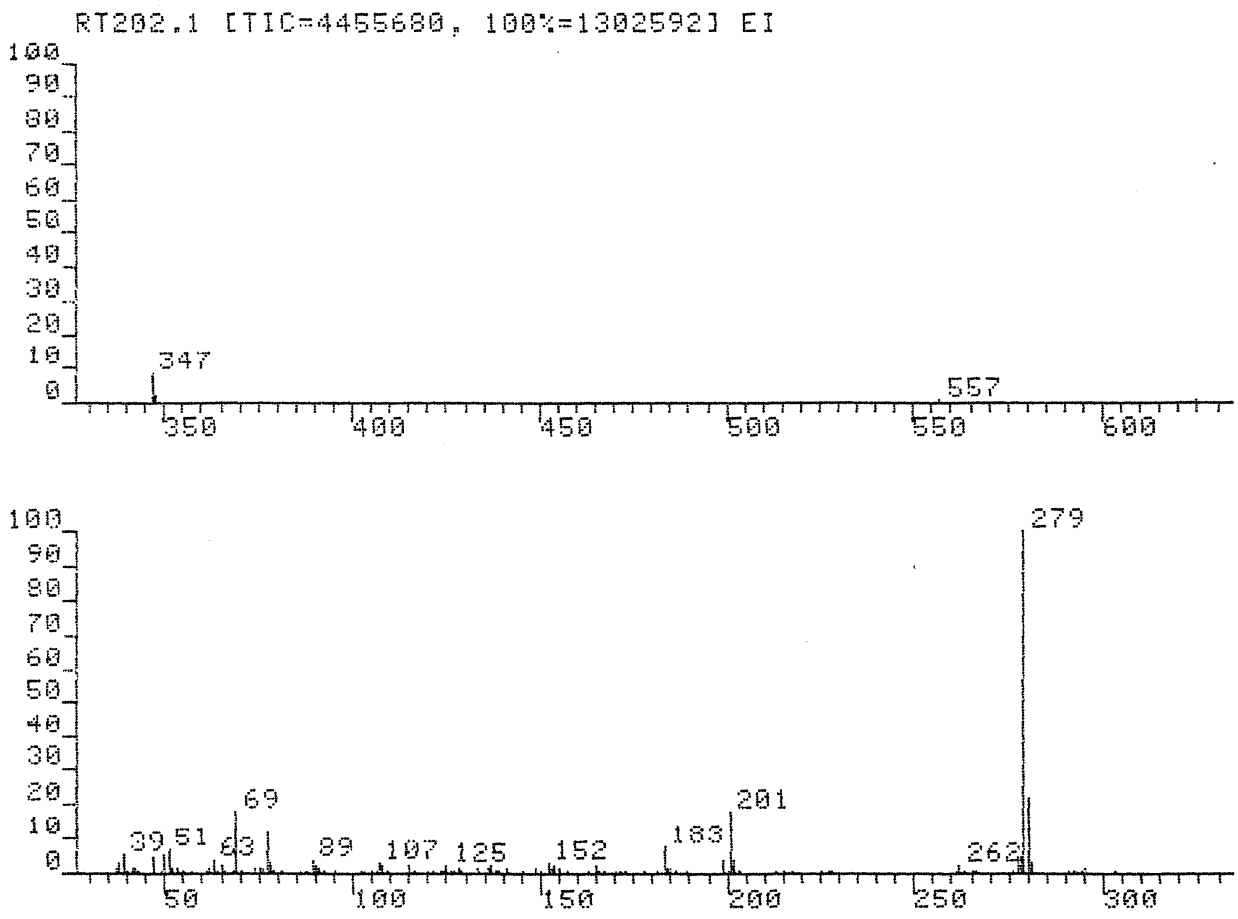


DP0:RT202.MS
SCAN: 1, 6/16/87 17: 5
IONISATION: FAB Ph3P=O*IMH+Br- (0.768M)
NO. PEAKS: 200
BASE/NREF INT: 1302592./ 1302592.
TIC: 4455680.
MASS RANGE: 37 - 626
RETN TIME/MISC: 0: 0/ 0/ 0/ 0
PAGE 1

| PEAK NO. | MEASURED MASS | NO. POINTS | ABSOLUTE INTENSITY | % INT. BASE | % INT. NREF | % TOT. ION |
|---|---|---|---|---|---|---|
| 10 | 348 | 43 | 28174. | 2.2 | 2.2 | 0.6 |
| 11 | 347 | 71 | 108576. | 8.3 | 8.3 | 2.4 |
| 28 | 280 | 103 | 282880. | 21.7 | 21.7 | 6.3* |
| 29 | 279 | 143 | 1302592. | 100.0 | 100.0 | 29.2*^ |
| 69 | 201 | 103 | 235620. | 18.1 | 18.1 | 5.3 |
| 169 | 77 | 51 | 146052. | 11.2 | 11.2 | 3.3 |
| 175 | 69 | 71 | 234116. | 18.0 | 18.0 | 5.3 |

FAB of $ph_3PO(ImH^+)Br^-$ complex, 1.13 M in NBA

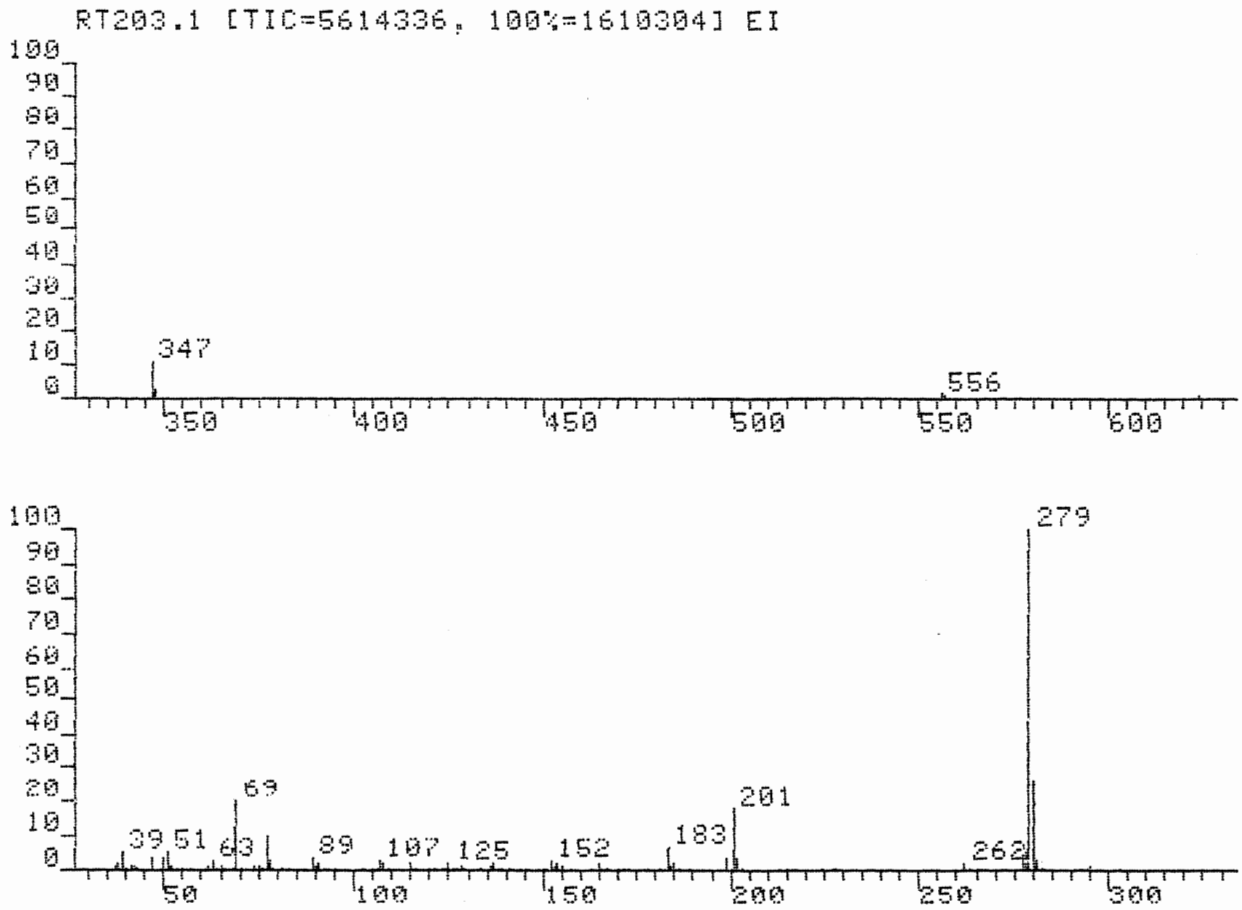


SCAN: 1, 6/16/87 17:22
IONISATION: FAB Ph3P=O+IMH+Br- (1.130M)
NO. PEAKS: 209
BASE/NREF INT: 1610304./ 1610304.
TIC: 5614336.
MASS RANGE: 37 - 625
RETN TIME/MISC: 0: 0/ 0/ 0/ 0

| PEAK NO. | MEASURED MASS | NO. POINTS | ABSOLUTE INTENSITY | % INT. BASE | % INT. NREF | % TOT. ION |
|---|---|---|---|---|---|---|
| 5 | 556 | 43 | 20443. | 1.3 | 1.3 | 0.4 |
| 14 | 348 | 51 | 47508. | 3.0 | 3.0 | 0.8 |
| 15 | 347 | 87 | 180460. | 11.2 | 11.2 | 3.2 |
| 34 | 280 | 103 | 419600. | 26.1 | 26.1 | 7.5* |
| 35 | 279 | 143 | 1610304. | 100.0 | 100.0 | 28.7*^ |
| 75 | 201 | 103 | 294096. | 18.3 | 18.3 | 5.2 |
| 177 | 77 | 51 | 163348. | 10.1 | 10.1 | 2.9 |
| 184 | 69 | 87 | 319792. | 19.9 | 19.9 | 5.7 |

FAB of $ph_3PO(ImH^+)Br^-$ complex, 2:1 in NBA

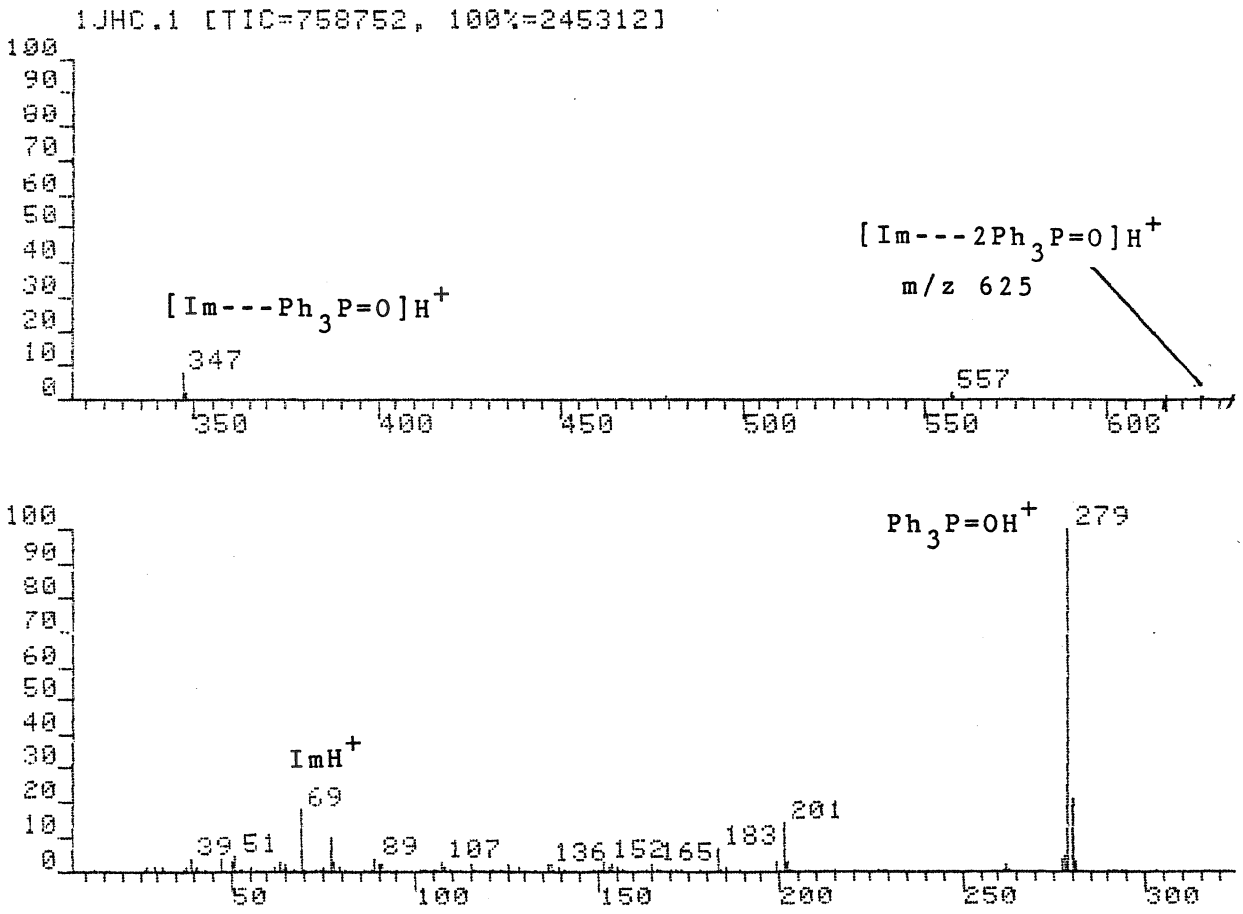


IONISATION: FAB IMH+ 2PH3PO BR- NBA
NO. PEAKS: 120
BASE/NREF INT: 245312./ 245312.
TIC: 758752.
MASS RANGE: 12 - 626
RETN TIME/MISC: 0: 0/ 0/ 0/ 0
PAGE 1

| PEAK NO. | MEASURED MASS | NO. POINTS | ABSOLUTE INTENSITY | % INT. BASE | % INT. NREF | % TOT. ION |
|---|---|---|---|---|---|---|
| 1 | 626 | 21 | 1261. | 0.5 | 0.5 | 0.2 |
| 2 | 625 | 25 | 2292. | 0.9 | 0.9 | 0.3 |
| 3 | 558 | 25 | 2007. | 0.8 | 0.8 | 0.3 |
| 4 | 557 | 29 | 4741. | 1.9 | 1.9 | 0.6 |
| 5 | 479 | 21 | 1251. | 0.5 | 0.5 | 0.2 |
| 6 | 414 | 21 | 971. | 0.4 | 0.4 | 0.1 |
| 7 | 349 | 17 | 753. | 0.3 | 0.3 | 0.1 |
| 8 | 348 | 25 | 4998. | 2.0 | 2.0 | 0.7 |
| 9 | 347 | 35 | 18413. | 7.5 | 7.5 | 2.4 |
| 10 | 303 | 25 | 1170. | 0.5 | 0.5 | 0.2 |
| 18 | 280 | 43 | 50780. | 20.7 | 20.7 | 6.7 |
| 19 | 279 | 59 | 245312. | 100.0 | 100.0 | 32.3* |
| 32 | 201 | 35 | 33989. | 13.9 | 13.9 | 4.5 |
| 38 | 183 | 35 | 16921. | 6.9 | 6.9 | 2.2 |
| 90 | 77 | 35 | 24101. | 9.8 | 9.8 | 3.2 |
| 96 | 69 | 59 | 42630. | 17.4 | 17.4 | 5.6* |

# FAB of $ph_2SO(ImH^+)Br^-$ 2:1 complex in NBA

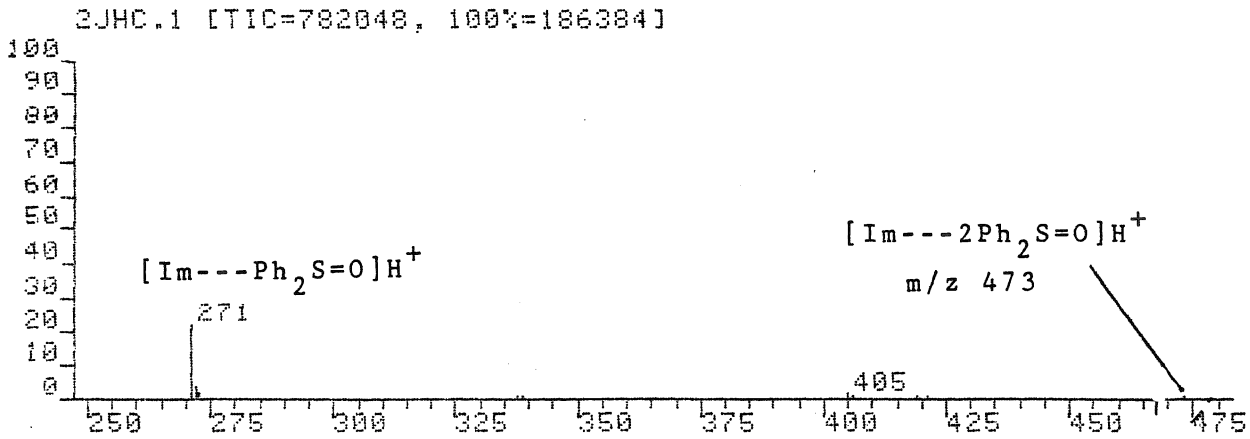


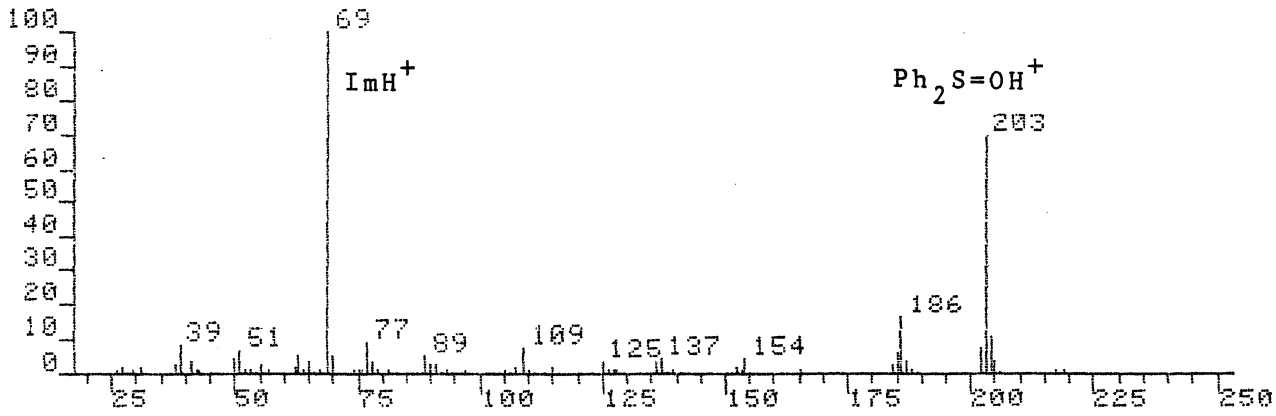


IONISATION: FAB IMH+ 2PH2SO BR- NBA
NO. PEAKS: 109
BASE/NREF INT: 186384./ 186384.
TIC: 782048.
MASS RANGE: 26 - 473
RETN TIME/MISC: 0: 0/ 0/ 0/ 0
PAGE 1

| PEAK NO. | MEASURED MASS | NO. POINTS | ABSOLUTE INTENSITY | % INT. BASE | % INT. NREF | % TOT. ION |
|---|---|---|---|---|---|---|
| 1 | 473 | 21 | 1382. | 0.7 | 0.7 | 0.2 |
| 2 | 421 | 21 | 978. | 0.5 | 0.5 | 0.1 |
| 3 | 419 | 25 | 963. | 0.5 | 0.5 | 0.1 |
| 4 | 406 | 21 | 1083. | 0.6 | 0.6 | 0.1 |
| 5 | 405 | 25 | 2754. | 1.5 | 1.5 | 0.4 |
| 6 | 339 | 21 | 1816. | 1.0 | 1.0 | 0.2 |
| 7 | 338 | 21 | 1243. | 0.7 | 0.7 | 0.2 |
| 10 | 271 | 35 | 40566. | 21.8 | 21.8 | 5.2 |
| 15 | 204 | 35 | 19844. | 10.6 | 10.6 | 2.5 |
| 16 | 203 | 43 | 129824. | 69.7 | 69.7 | 16.6 |
| 17 | 202 | 35 | 13850. | 7.4 | 7.4 | 1.8 |
| 23 | 186 | 35 | 29898. | 16.0 | 16.0 | 3.8 |
| 24 | 185 | 35 | 10989. | 5.9 | 5.9 | 1.4 |
| 54 | 109 | 35 | 14559. | 7.8 | 7.8 | 1.9 |
| 70 | 89 | 35 | 9727. | 5.2 | 5.2 | 1.2 |
| 78 | 77 | 35 | 17709. | 9.5 | 9.5 | 2.3 |
| 82 | 70 | 35 | 9562. | 5.1 | 5.1 | 1.2* |
| 83 | 69 | 71 | 186384. | 100.0 | 100.0 | 23.8* |
| 88 | 63 | 35 | 10173. | 5.5 | 5.5 | 1.3 |
| 95 | 51 | 35 | 13194. | 7.1 | 7.1 | 1.7 |
| 101 | 39 | 35 | 15094. | 8.1 | 8.1 | 1.9 |

R

# FAB of (D)$ph_2SO$ complex, 1.26 in NBA(dry)

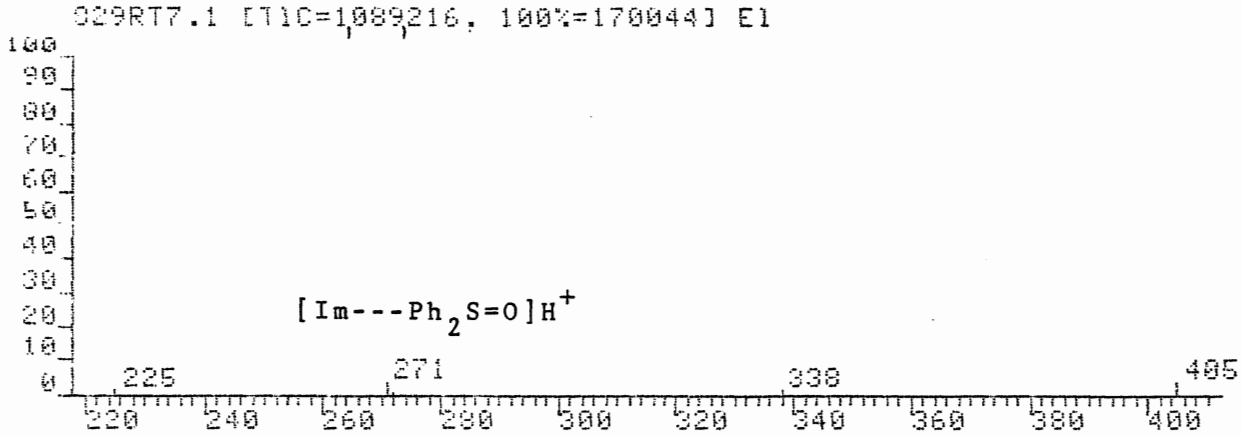


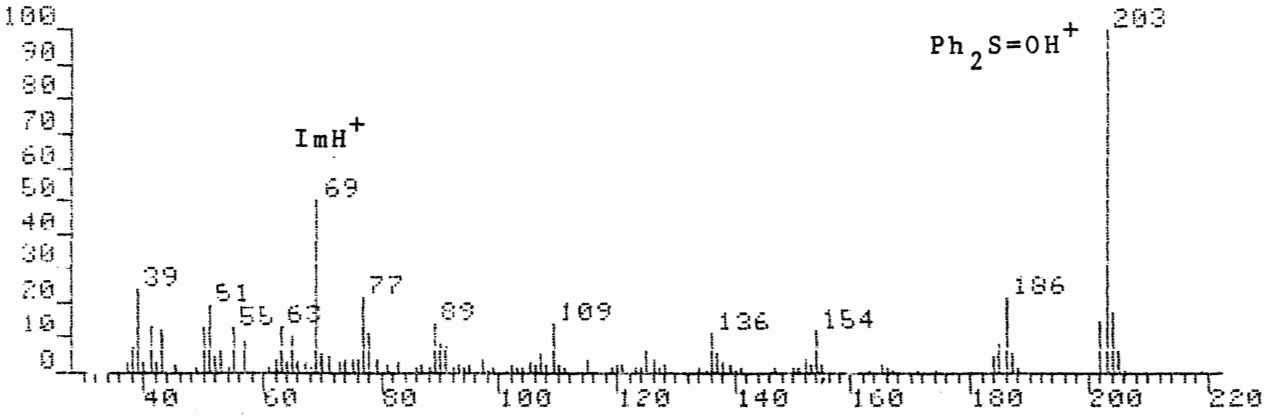


IONISATION: FAB (D)PH2SO-IM/NBA(DRY) 23MG/100MG
NO. PEAKS: 107
BASE/NREF INT: 170044./ 170044.
TIC: 1089216.
MASS RANGE: 37 - 405

| PEAK NO. | MEASURED MASS | NO. POINTS | ABSOLUTE INTENSITY | % INT. BASE | % INT. NREF | % TOT. ION |
|---|---|---|---|---|---|---|
| 1 | 405 | 35 | 6127. | 3.6 | 3.6 | 0.6% |
| 2 | 338 | 29 | 2596. | 1.5 | 1.5 | 0.2 |
| 3 | 272 | 25 | 1853. | 1.1 | 1.1 | 0.2 |
| 4 | 271 | 35 | 6056. | 3.6 | 3.6 | 0.6 |
| 9 | 204 | 43 | 28716. | 16.9 | 16.9 | 2.6% |
| 10 | 203 | 59 | 170044. | 100.0 | 100.0 | 15.6% |
| 11 | 202 | 43 | 24943. | 14.7 | 14.7 | 2.3% |
| 14 | 186 | 43 | 36539. | 21.5 | 21.5 | 3.4 |
| 24 | 154 | 43 | 20169. | 11.9 | 11.9 | 1.9 |
| 35 | 136 | 35 | 18295. | 10.8 | 10.8 | 1.7 |
| 50 | 109 | 51 | 24224. | 14.2 | 14.2 | 2.2% |
| 66 | 91 | 43 | 11287. | 6.6 | 6.6 | 1.0 |
| 67 | 90 | 35 | 13415. | 7.9 | 7.9 | 1.2 |
| 68 | 89 | 43 | 23802. | 14.0 | 14.0 | 2.2 |
| 75 | 78 | 43 | 17824. | 10.5 | 10.5 | 1.6 |
| 76 | 77 | 43 | 36767. | 21.6 | 21.6 | 3.4 |
| 82 | 70 | 43 | 9011. | 5.3 | 5.3 | 0.8 |
| 83 | 69 | 71 | 84668. | 49.8 | 49.8 | 7.8% |
| 87 | 65 | 43 | 16548. | 9.7 | 9.7 | 1.5 |
| 89 | 63 | 43 | 21451. | 12.6 | 12.6 | 2.0% |
| 92 | 57 | 43 | 14479. | 8.5 | 8.5 | 1.3 |
| 93 | 55 | 59 | 20593. | 12.1 | 12.1 | 1.9 |
| 95 | 53 | 51 | 10038. | 5.9 | 5.9 | 0.9% |
| 97 | 51 | 43 | 32971. | 19.4 | 19.4 | 3.0 |
| 98 | 50 | 43 | 20747. | 12.2 | 12.2 | 1.9 |
| 101 | 43 | 71 | 19065. | 11.2 | 11.2 | 1.8% |
| 103 | 41 | 43 | 22829. | 13.4 | 13.4 | 2.1 |
| 105 | 39 | 43 | 40626. | 23.9 | 23.9 | 3.7 |
| 106 | 38 | 43 | 12137. | 7.1 | 7.1 | 1.1% |

# FAB of (D)$ph_2SO$ complex, 1.26 in NBA(wet)

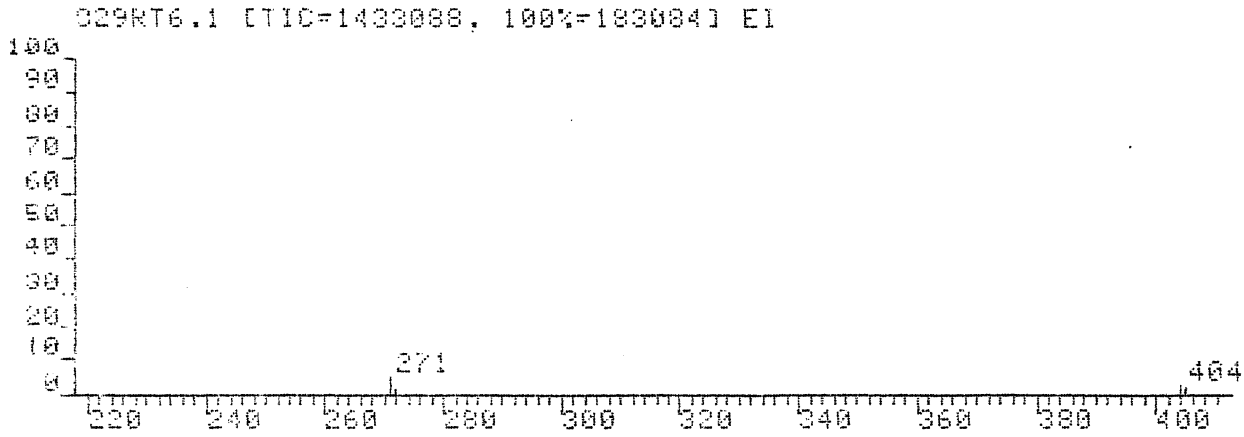


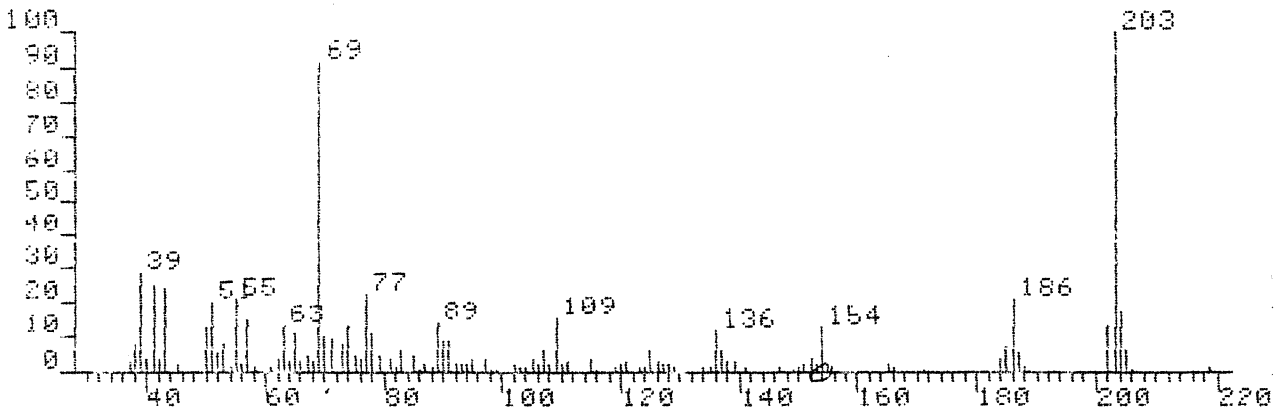


IONISATION: FAB D-PH2SO/IM/NBA (WET) 23MG/100MG
NO. PEAKS: 107
BASE/NREF INT: 183084./ 183084.
TIC: 1433088.
MASS RANGE: 37 - 405
RETN TIME/MISC: 0: 0/ 0/ 0/ 0
PAGE 1

| PEAK NO. | MEASURED MASS | NO. POINTS | ABSOLUTE INTENSITY | % INT. BASE | % INT. NREF | % TOT. ION |
|---|---|---|---|---|---|---|
| 1 | 405 | 25 | 3561. | 1.9 | 1.9 | 0.2 |
| 2 | 404 | 29 | 5548. | 3.0 | 3.0 | 0.4 |
| 3 | 272 | 29 | 2941. | 1.6 | 1.6 | 0.2 |
| 4 | 271 | 35 | 9982. | 5.4 | 5.4 | 0.7 |
| 8 | 204 | 43 | 30662. | 16.7 | 16.7 | 2.1 |
| 9 | 203 | 59 | 183084. | 100.0 | 100.0 | 12.8* |
| 10 | 202 | 43 | 24220. | 13.2 | 13.2 | 1.7 |
| 13 | 186 | 43 | 37694. | 20.6 | 20.6 | 2.6 |
| 20 | 154 | 43 | 21966. | 12.0 | 12.0 | 1.5 |
| 31 | 136 | 43 | 20622. | 11.3 | 11.3 | 1.4 |
| 48 | 109 | 71 | 28834. | 15.7 | 15.7 | 2.0 |
| 63 | 91 | 35 | 15057. | 8.2 | 8.2 | 1.1 |
| 64 | 90 | 35 | 14698. | 8.0 | 8.0 | 1.0 |
| 65 | 89 | 43 | 26289. | 14.4 | 14.4 | 1.8 |
| 70 | 83 | 43 | 10776. | 5.9 | 5.9 | 0.8 |
| 74 | 78 | 43 | 20049. | 11.0 | 11.0 | 1.4 |
| 75 | 77 | 43 | 41025. | 22.4 | 22.4 | 2.9 |
| 78 | 74 | 71 | 24475. | 13.4 | 13.4 | 1.7* |
| 79 | 73 | 43 | 13895. | 7.6 | 7.6 | 1.0 |
| 80 | 71 | 43 | 16973. | 9.3 | 9.3 | 1.2* |
| 81 | 70 | 51 | 17952. | 9.8 | 9.8 | 1.3* |
| 82 | 69 | 87 | 167800. | 91.7 | 91.7 | 11.7* |
| 86 | 65 | 35 | 19183. | 10.5 | 10.5 | 1.3 |
| 88 | 63 | 43 | 23460. | 12.8 | 12.8 | 1.6 |
| 92 | 57 | 43 | 27024. | 14.8 | 14.8 | 1.9 |
| 94 | 55 | 59 | 38369. | 21.0 | 21.0 | 2.7 |
| 96 | 53 | 59 | 13292. | 7.3 | 7.3 | 0.9* |
| 97 | 52 | 35 | 9493. | 5.2 | 5.2 | 0.7 |
| 98 | 51 | 43 | 36992. | 20.2 | 20.2 | 2.6 |
| 99 | 50 | 35 | 22405. | 12.2 | 12.2 | 1.6 |
| 101 | 43 | 71 | 43936. | 24.0 | 24.0 | 3.1* |
| 103 | 41 | 43 | 45297. | 24.7 | 24.7 | 3.2 |
| 105 | 39 | 43 | 53563. | 29.3 | 29.3 | 3.7 |
| 106 | 38 | 35 | 13900. | 7.6 | 7.6 | 1.0 |

FAB of $ph_2CO$ complex, 1.26 M in NBA

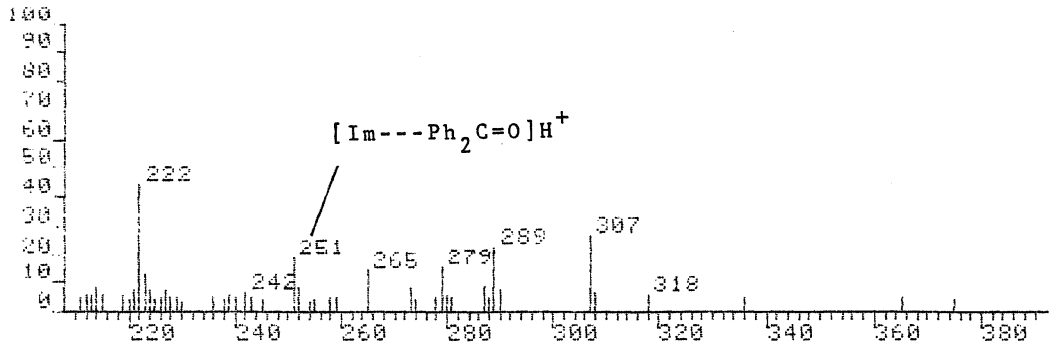


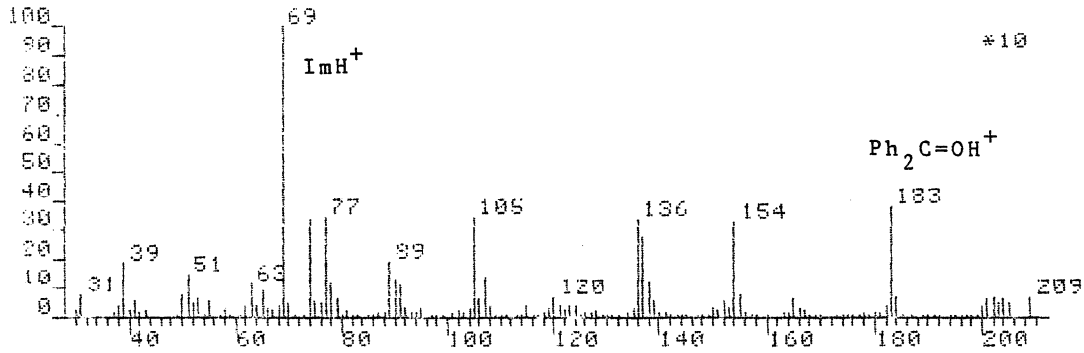


IONISATION:
NO. PEAKS: 197
BASE/NREF INT: 244872./ 244872.
TIC: 1871168.
MASS RANGE: 30 - 375
RETN TIME/MISC: 0: 0/ 0/ 0/ 0
PAGE 1

| PEAK NO. | MEASURED MASS | NO. POINTS | ABSOLUTE INTENSITY | % INT. BASE | % INT. NREF | % TOT. ION |
|---|---|---|---|---|---|---|
| 1 | 375 | 21 | 913. | 0.4 | 0.4 | 0.0 |
| 2 | 365 | 25 | 1265. | 0.5 | 0.5 | 0.1 |
| 3 | 336 | 21 | 1237. | 0.5 | 0.5 | 0.1 |
| 4 | 318 | 35 | 1383. | 0.6 | 0.6 | 0.1 |
| 5 | 308 | 35 | 1449. | 0.6 | 0.6 | 0.1 |
| 6 | 307 | 35 | 6524. | 2.7 | 2.7 | 0.3 |
| 7 | 290 | 25 | 1757. | 0.7 | 0.7 | 0.1 |
| 8 | 289 | 35 | 5612. | 2.3 | 2.3 | 0.3 |
| 9 | 288 | 29 | 1135. | 0.5 | 0.5 | 0.1 |
| 10 | 287 | 25 | 2159. | 0.9 | 0.9 | 0.1 |
| 11 | 281 | 21 | 1232. | 0.5 | 0.5 | 0.1 |
| 12 | 280 | 21 | 1372. | 0.6 | 0.6 | 0.1 |
| 13 | 279 | 35 | 3816. | 1.6 | 1.6 | 0.2 |
| 14 | 278 | 21 | 1118. | 0.5 | 0.5 | 0.1 |
| 15 | 274 | 21 | 932. | 0.4 | 0.4 | 0.0 |
| 16 | 273 | 25 | 1804. | 0.7 | 0.7 | 0.1 |
| 17 | 265 | 29 | 3541. | 1.4 | 1.4 | 0.2 |
| 18 | 259 | 21 | 1247. | 0.5 | 0.5 | 0.1 |
| 19 | 258 | 25 | 1150. | 0.5 | 0.5 | 0.1 |
| 20 | 255 | 21 | 835. | 0.3 | 0.3 | 0.0 |
| 21 | 254 | 21 | 712. | 0.3 | 0.3 | 0.0 |
| 22 | 253 | 29 | 1850. | 0.8 | 0.8 | 0.1 |
| 23 | 251 | 35 | 4593. | 1.9 | 1.9 | 0.2 |
| 38 | 223 | 29 | 3093. | 1.3 | 1.3 | 0.2 |
| 39 | 222 | 35 | 10935. | 4.4 | 4.4 | 0.6 |
| 40 | 221 | 25 | 1667. | 0.7 | 0.7 | 0.1 |
| 68 | 183 | 51 | 93824. | 38.3 | 38.3 | 5.0* |
| 69 | 182 | 35 | 8003. | 3.3 | 3.3 | 0.4 |
| 165 | 75 | 71 | 12829. | 5.2 | 5.2 | 0.7* |
| 166 | 74 | 71 | 82624. | 33.7 | 33.7 | 4.4* |
| 169 | 70 | 35 | 11468. | 4.7 | 4.7 | 0.6 |
| 170 | 69 | 71 | 244872. | 100.0 | 100.0 | 13.1* |

# Appendix III

Positive FAB mass spectra of multiple donor systems

FAB of 1,10-phenathroline-$Me_2NH_2^+Cl^-$ in NBA (0.6 M )

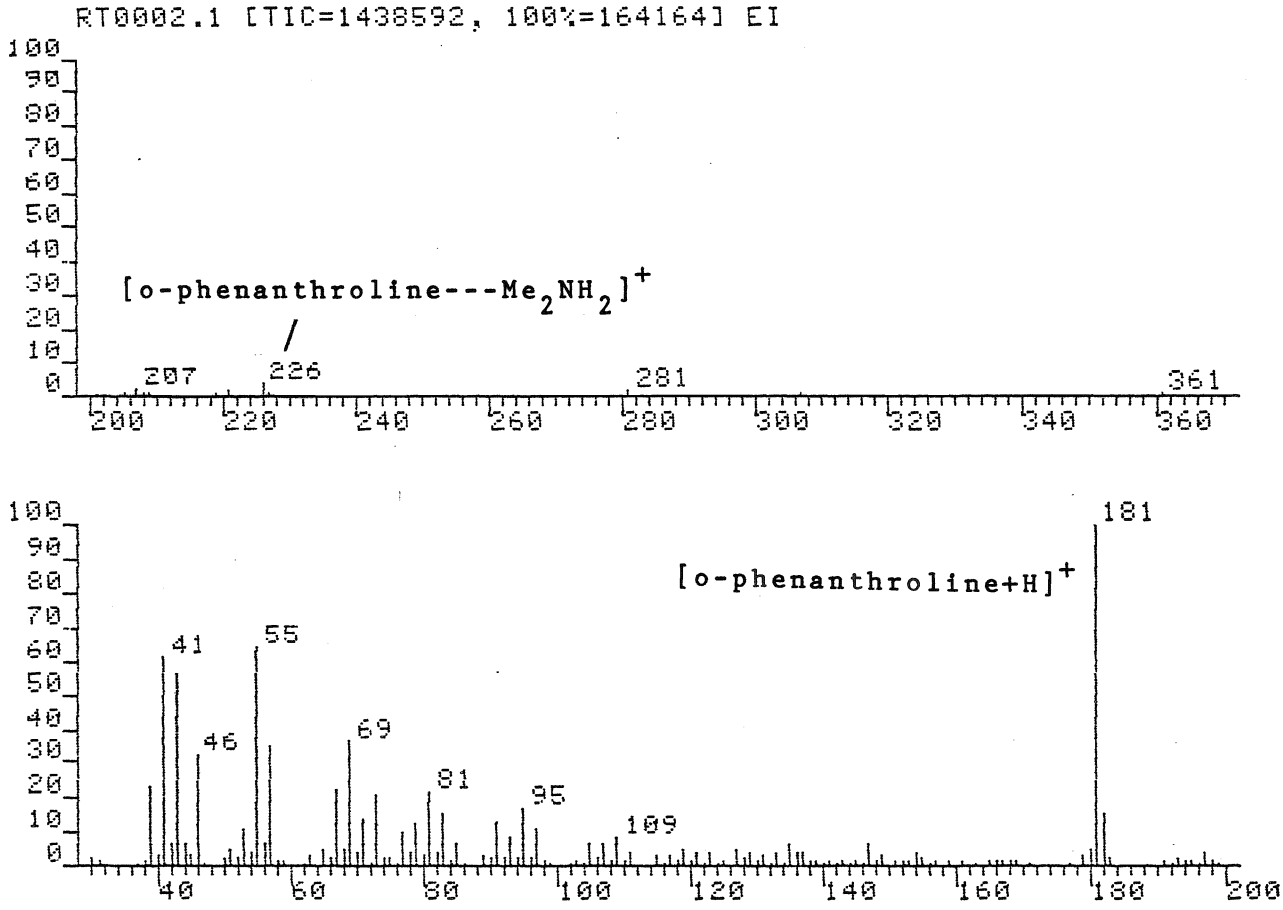


IONISATION: FAB
NO. PEAKS: 144
BASE/NREF INT: 164164./ 164164.
TIC: 1438592.
MASS RANGE: 30 - 361

| PEAK NO. | MEASURED MASS | NO. POINTS | ABSOLUTE INTENSITY | % INT. BASE | % INT. NREF | % TOT. ION |
|---|---|---|---|---|---|---|
| 1 | 361 | 25 | 1821. | 1.1 | 1.1 | 0.1 |
| 3 | 281 | 25 | 2171. | 1.3 | 1.3 | 0.2 |
| 4 | 227 | 25 | 1685. | 1.0 | 1.0 | 0.1 |
| 5 | 226 | 35 | 6780. | 4.1 | 4.1 | 0.5 |
| 6 | 221 | 25 | 2100. | 1.3 | 1.3 | 0.1 |
| 10 | 207 | 35 | 4064. | 2.5 | 2.5 | 0.3 |
| 23 | 181 | 51 | 164164. | 100.0 | 100.0 | 11.4* |
| 133 | 46 | 35 | 54302. | 33.1 | 33.1 | 3.8 |

FAB of $ph_2SO_2$-$Me_2NH_2^+Cl^-$ in NBA (0.06 M )

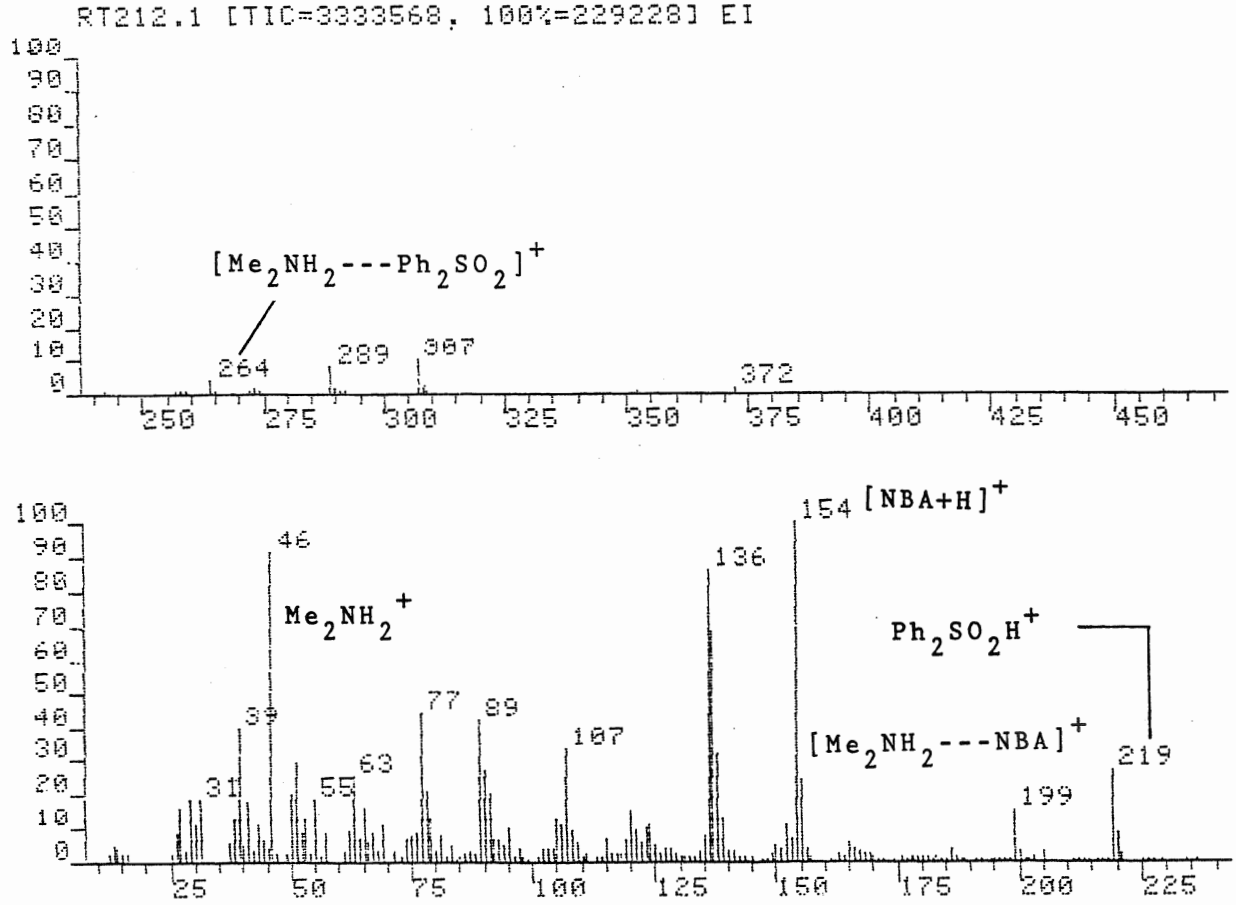


SCAN: 1, 6/25/87 23:12
IONISATION: FAB Ph2SO2*MeNH2+Cl- 0.06M in NBA
NO. PEAKS: 201
BASE/NREF INT: 229228./ 229228.
TIC: 3333568.
MASS RANGE: 12 - 460
RETN TIME/MISC: 0: 0/ 0/ 0/ 0
PAGE 1

| PEAK NO. | MEASURED MASS | NO. POINTS | ABSOLUTE INTENSITY | % INT. BASE | % INT. NREF | % TOT. ION |
|---|---|---|---|---|---|---|
| 2 | 372 | 25 | 2941. | 1.3 | 1.3 | 0.1 |
| 6 | 308 | 35 | 4921. | 2.1 | 2.1 | 0.1 |
| 7 | 307 | 43 | 23251. | 10.1 | 10.1 | 0.7 |
| 10 | 290 | 29 | 3837. | 1.7 | 1.7 | 0.1 |
| 11 | 289 | 35 | 17278. | 7.5 | 7.5 | 0.5 |
| 13 | 273 | 29 | 2906. | 1.3 | 1.3 | 0.1 |
| 17 | 264 | 35 | 9762. | 4.3 | 4.3 | 0.3 |
| 30 | 219 | 51 | 63709. | 27.8 | 27.8 | 1.9 |
| 44 | 199 | 43 | 35655. | 15.6 | 15.6 | 1.1 |
| 81 | 154 | 59 | 229228. | 100.0 | 100.0 | 6.9 |
| 96 | 138 | 43 | 72980. | 31.8 | 31.8 | 2.2* |
| 97 | 137 | 59 | 155988. | 68.0 | 68.0 | 4.7 |
| 98 | 136 | 59 | 197676. | 86.2 | 86.2 | 5.9 |
| 126 | 107 | 51 | 76928. | 33.6 | 33.6 | 2.3 |
| 143 | 89 | 43 | 97524. | 42.5 | 42.5 | 2.9 |
| 155 | 77 | 51 | 101340. | 44.2 | 44.2 | 3.0 |
| 180 | 46 | 51 | 211360. | 92.2 | 92.2 | 6.3* |
| 187 | 39 | 43 | 91692. | 40.0 | 40.0 | 2.8 |

FAB of $ph_2SO_2$-$Me_2NH_2^+Cl^-$ in NBA (0.16 M )

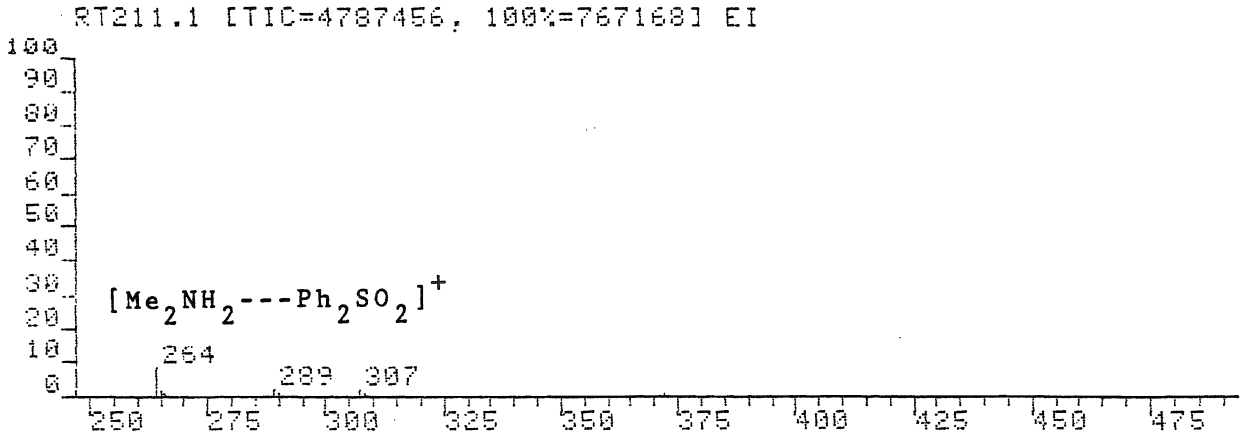


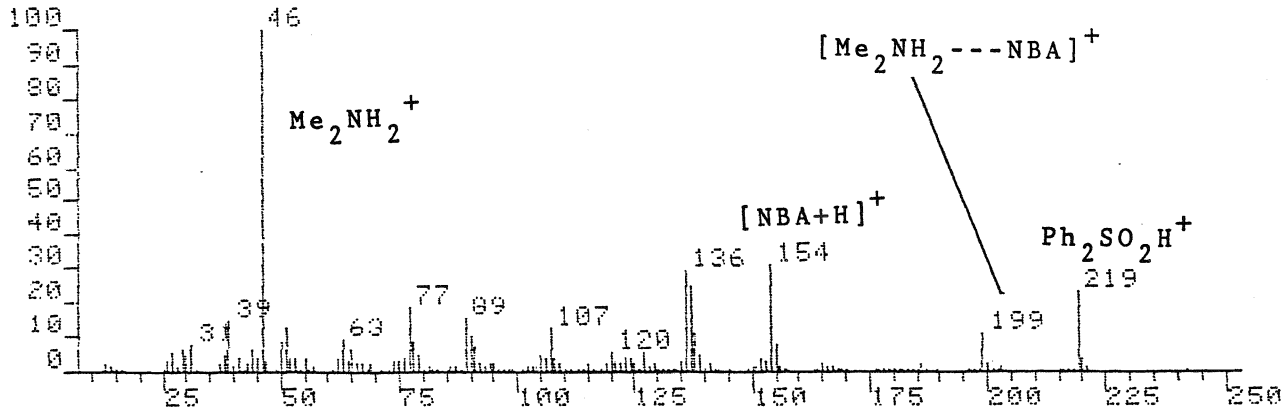


SCAN: 1, 6/25/87 22:51
IONISATION: FAB Ph2SO2*MeNH2+Cl- 0.16M in NBA
NO. PEAKS: 231
BASE/NREF INT: 767168./ 767168.
TIC: 4787456.
MASS RANGE: 12 - 482

| PEAK NO. | MEASURED MASS | NO. POINTS | ABSOLUTE INTENSITY | % INT. BASE | % INT. NREF | % TOT. ION |
|---|---|---|---|---|---|---|
| 24 | 264 | 51 | 68940. | 9.0 | 9.0 | 1.4 |
| 54 | 219 | 71 | 179596. | 23.4 | 23.4 | 3.8 |
| 70 | 199 | 43 | 80400. | 10.5 | 10.5 | 1.7 |
| 107 | 155 | 43 | 56206. | 7.3 | 7.3 | 1.2 |
| 108 | 154 | 71 | 242628. | 31.6 | 31.6 | 5.1 |
| 123 | 138 | 51 | 82068. | 10.7 | 10.7 | 1.7 |
| 124 | 137 | 59 | 192988. | 25.2 | 25.2 | 4.0 |
| 125 | 136 | 59 | 229468. | 29.9 | 29.9 | 4.8 |
| 134 | 127 | 51 | 39290. | 5.1 | 5.1 | 0.8 |
| 141 | 120 | 43 | 42343. | 5.5 | 5.5 | 0.9 |
| 153 | 107 | 51 | 91580. | 11.9 | 11.9 | 1.9 |
| 169 | 91 | 59 | 54478. | 7.1 | 7.1 | 1.1 |
| 170 | 90 | 51 | 77104. | 10.1 | 10.1 | 1.6 |
| 171 | 89 | 43 | 118916. | 15.5 | 15.5 | 2.5 |
| 182 | 78 | 43 | 60827. | 7.9 | 7.9 | 1.3 |
| 183 | 77 | 51 | 141412. | 18.4 | 18.4 | 3.0 |
| 194 | 65 | 43 | 48065. | 6.3 | 6.3 | 1.0 |
| 196 | 63 | 43 | 72380. | 9.4 | 9.4 | 1.5 |
| 205 | 51 | 43 | 91560. | 11.9 | 11.9 | 1.9 |
| 206 | 50 | 43 | 65016. | 8.5 | 8.5 | 1.4 |
| 209 | 46 | 103 | 767168. | 100.0 | 100.0 | 16.0* |

# FAB of $ph_2SO_2$-$Me_2NH_2^+Cl^-$ in NBA (0.60 M )

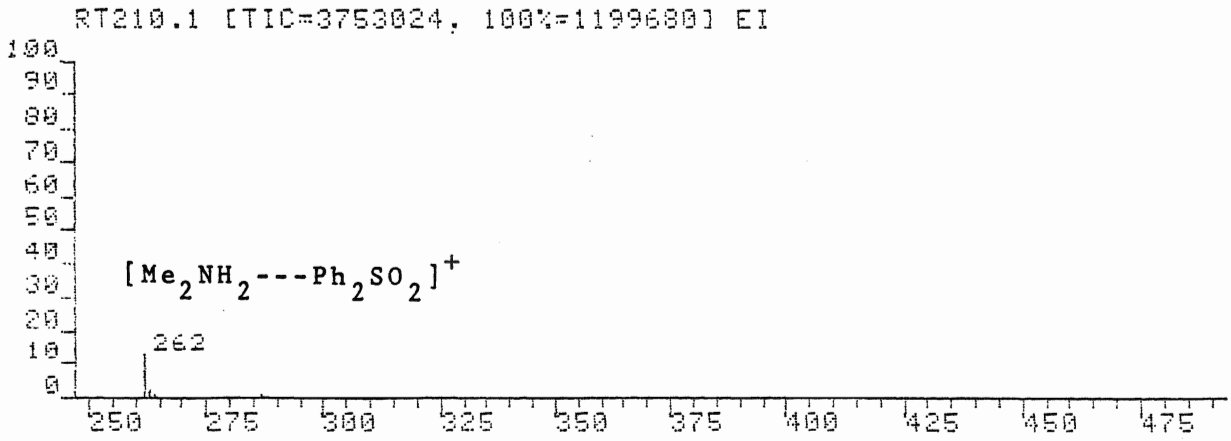


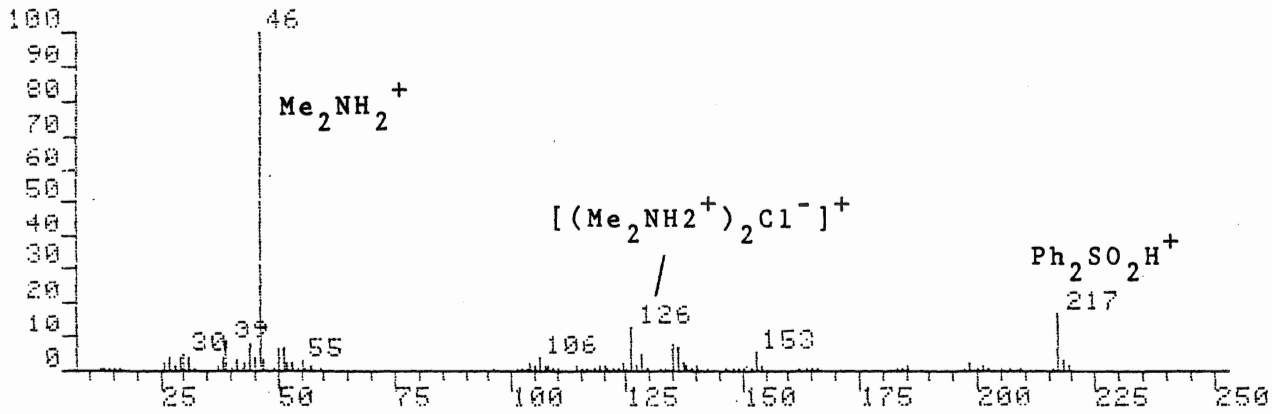


D:\...\RT210.MS
SCAN: 1, 6/25/87 22:41
IONISATION: FAB PH2SO2*MeNH2+Cl- 0.61M in NBA
NO. PEAKS: 148
BASE/NREF INT: 1199680./ 1199680.
TIC: 3753024.
MASS RANGE: 12 - 478
RETN TIME/MISC: 0: 0/ 0/ 0/ 0
PAGE 1

| PEAK NO. | MEASURED MASS | NO. POINTS | ABSOLUTE INTENSITY | % INT. BASE | % INT. NREF | % TOT. ION |
|---|---|---|---|---|---|---|
| 13 | 262 | 51 | 144856. | 12.1 | 12.1 | 3.9 |
| 21 | 217 | 71 | 202416. | 16.9 | 16.9 | 5.4 |
| 60 | 153 | 43 | 62317. | 5.2 | 5.2 | 1.7 |
| 74 | 136 | 51 | 78868. | 6.6 | 6.6 | 2.1 |
| 75 | 135 | 51 | 92896. | 7.7 | 7.7 | 2.5 |
| 82 | 128 | 43 | 54698. | 4.6 | 4.6 | 1.5 |
| 84 | 126 | 59 | 162436. | 13.5 | 13.5 | 4.3 |
| 122 | 51 | 43 | 85996. | 7.2 | 7.2 | 2.3 |
| 123 | 50 | 43 | 69696. | 5.8 | 5.8 | 1.9 |
| 126 | 46 | 119 | 1199680. | 100.0 | 100.0 | 32.0*^ |
| 127 | 45 | 87 | 50759. | 4.2 | 4.2 | 1.4* |
| 128 | 44 | 59 | 87776. | 7.3 | 7.3 | 2.3 |
| 133 | 39 | 43 | 96564. | 8.0 | 8.0 | 2.6 |
| 138 | 30 | 71 | 51440. | 4.3 | 4.3 | 1.4* |

R

FAB of $ph_2SO_2$-$Me_2NH_2^+Cl^-$ in NBA (1.07 M )

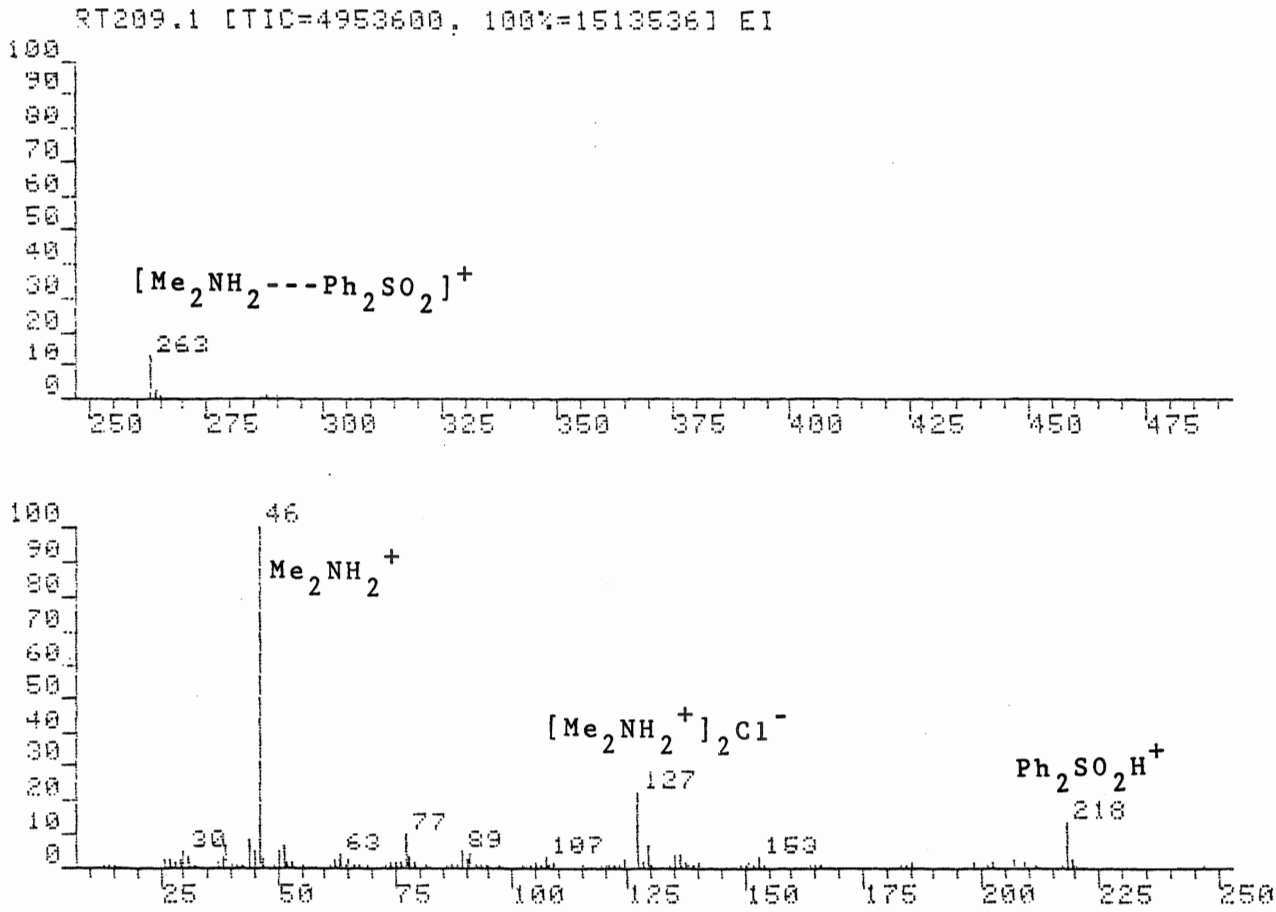


DRV:K12UY.MS
SCAN: 1, 6/25/87 22:30
IONISATION: FAB Ph2SO2%Me2NH2+Cl- 1.07M in NBA
NO. PEAKS: 173
BASE/NREF INT: 1513536./ 1513536.
TIC: 4953600.
MASS RANGE: 12 - 480
RETN TIME/MISC: 0: 0/ 0/ 0/ 0
PAGE 1

| PEAK NO. | MEASURED MASS | NO. POINTS | ABSOLUTE INTENSITY | % INT. BASE | % INT. NREF | % TOT. ION |
|---|---|---|---|---|---|---|
| 17 | 263 | 59 | 192660. | 12.7 | 12.7 | 3.9 |
| 28 | 218 | 71 | 213372. | 14.1 | 14.1 | 4.3 |
| 80 | 129 | 51 | 107052. | 7.1 | 7.1 | 2.2 |
| 82 | 127 | 71 | 345584. | 22.8 | 22.8 | 7.0 |
| 125 | 77 | 59 | 150824. | 10.0 | 10.0 | 3.0 |
| 146 | 51 | 43 | 90672. | 6.0 | 6.0 | 1.8 |
| 150 | 46 | 143 | 1513536. | 100.0 | 100.0 | 30.6^ |
| 152 | 44 | 51 | 122708. | 8.1 | 8.1 | 2.5 |
| 157 | 39 | 43 | 93204. | 6.2 | 6.2 | 1.9 |

FAB of $ph_2SO_2$-$Me_2NH_2^+Cl^-$ in sulfolane (0.9 M )

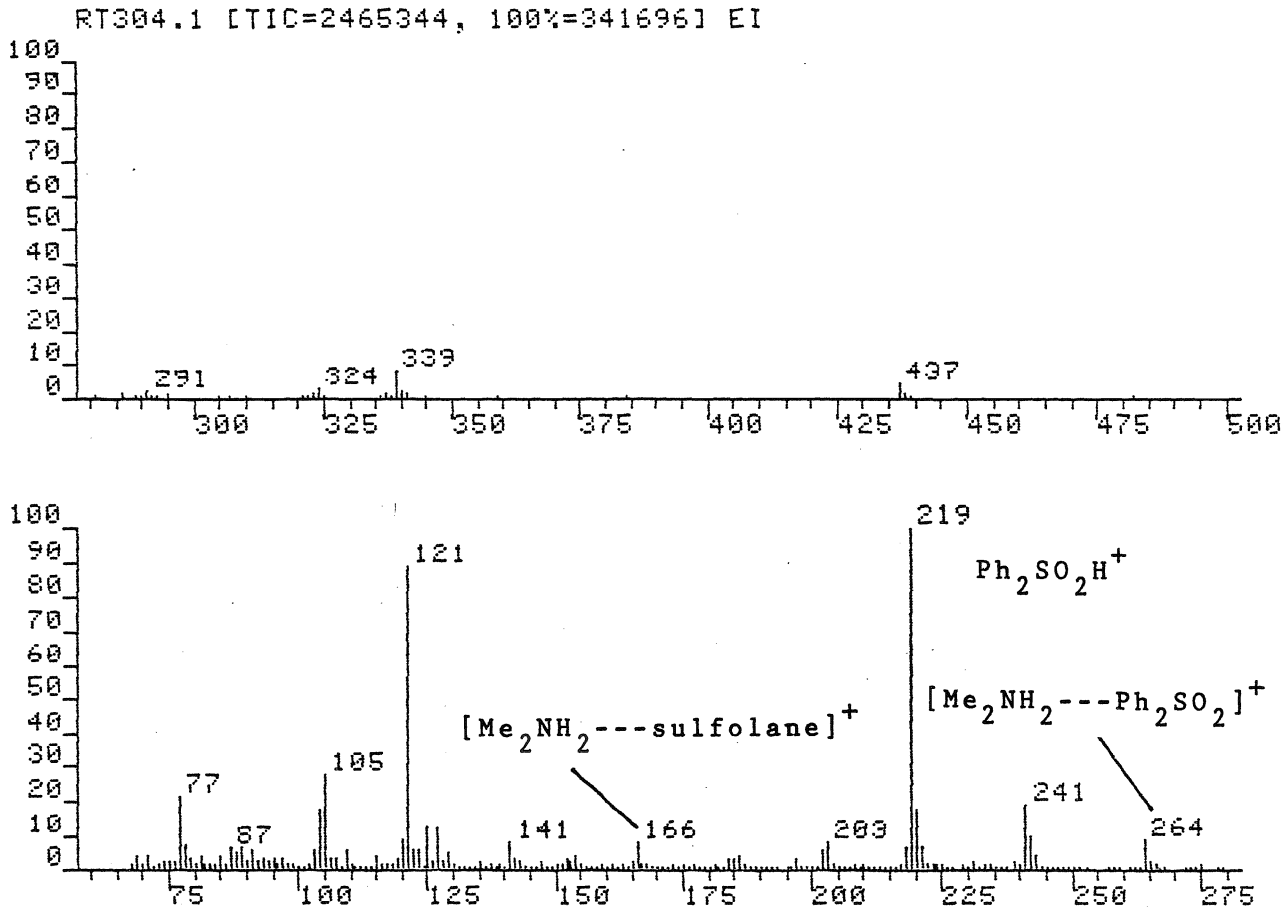


DPO:RT304.MS
IONISATION: FAB
NO. PEAKS: 300
BASE/NREF INT: 341696./ 341696.
TIC: 2465344.
MASS RANGE: 68 - 485

| PEAK NO. | MEASURED MASS | NO. POINTS | ABSOLUTE INTENSITY | % INT. BASE | % INT. NREF | % TOT. ION |
|---|---|---|---|---|---|---|
| 47 | 339 | 51 | 31293. | 9.2 | 9.2 | 1.3 |
| 106 | 264 | 43 | 31717. | 9.3 | 9.3 | 1.3 |
| 127 | 242 | 71 | 35557. | 10.4 | 10.4 | 1.4 |
| 128 | 241 | 59 | 65568. | 19.2 | 19.2 | 2.7 |
| 147 | 221 | 51 | 23550. | 6.9 | 6.9 | 1.0 |
| 148 | 220 | 71 | 62837. | 18.4 | 18.4 | 2.5 |
| 149 | 219 | 119 | 341696. | 100.0 | 100.0 | 13.9 |
| 150 | 218 | 71 | 22873. | 6.7 | 6.7 | 0.9 |
| 165 | 203 | 51 | 28340. | 8.3 | 8.3 | 1.1 |
| 166 | 202 | 43 | 17895. | 5.2 | 5.2 | 0.7 |
| 202 | 166 | 43 | 30535. | 8.9 | 8.9 | 1.2 |
| 247 | 121 | 87 | 305152. | 89.3 | 89.3 | 12.4 |

FAB of $ph_2SO_2$-$Me_2NH_2^+Cl^-$ in glycerol (0.9 M )

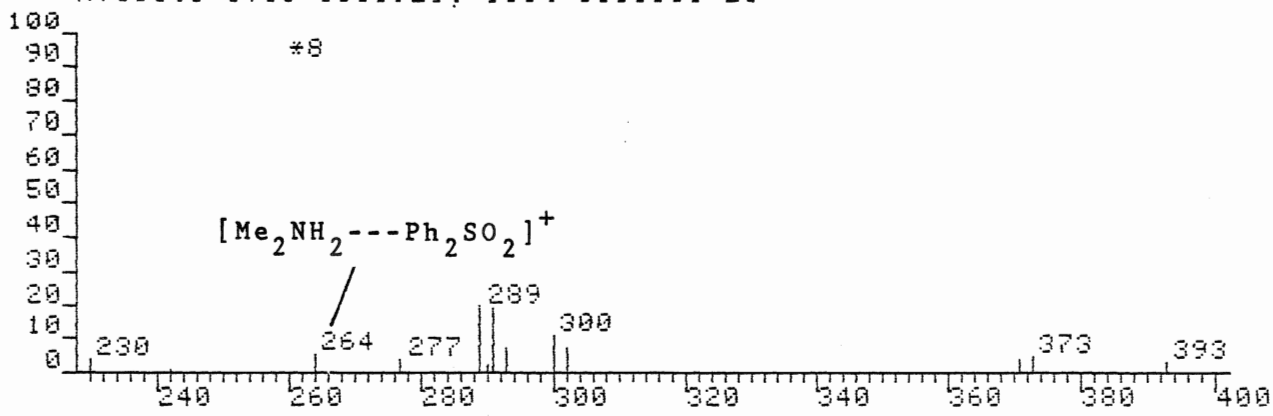


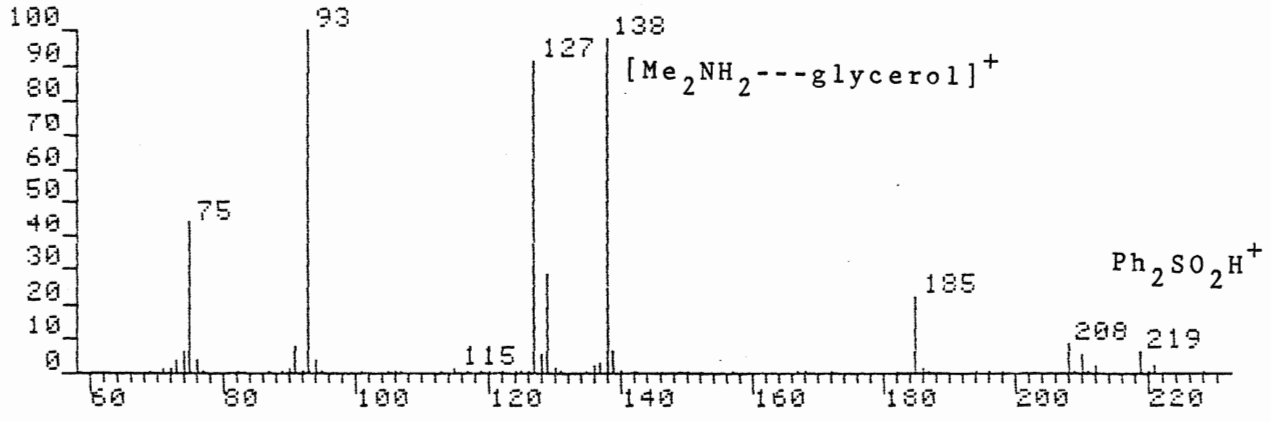


DP0:RT303.MS
IONISATION: FAB
NO. PEAKS: 80
BASE/NREF INT: 333168./ 333168.
TIC: 1660928.
MASS RANGE: 69 - 393

| PEAK NO. | MEASURED MASS | NO. POINTS | ABSOLUTE INTENSITY | % INT. BASE | % INT. NREF | % TOT. ION |
|---|---|---|---|---|---|---|
| 2 | 373 | 29 | 2005. | 0.6 | 0.6 | 0.1 |
| 4 | 302 | 29 | 2941. | 0.9 | 0.9 | 0.2 |
| 5 | 300 | 29 | 4659. | 1.4 | 1.4 | 0.3 |
| 6 | 293 | 29 | 3023. | 0.9 | 0.9 | 0.2 |
| 7 | 291 | 35 | 7836. | 2.4 | 2.4 | 0.5 |
| 9 | 289 | 35 | 8174. | 2.5 | 2.5 | 0.5 |
| 11 | 264 | 29 | 2373. | 0.7 | 0.7 | 0.1 |
| 18 | 219 | 43 | 20600. | 6.2 | 6.2 | 1.2 |
| 21 | 210 | 35 | 19016. | 5.7 | 5.7 | 1.1 |
| 23 | 208 | 43 | 29081. | 8.7 | 8.7 | 1.8 |
| 41 | 138 | 71 | 326560. | 98.0 | 98.0 | 19.7 |
| 49 | 127 | 87 | 307248. | 92.2 | 92.2 | 18.5* |
| 66 | 93 | 71 | 333168. | 100.0 | 100.0 | 20.1* |

FAB of $ph_2SO_2$-$Me_2NH_2^+I^-$ in NBA (0.6 M )

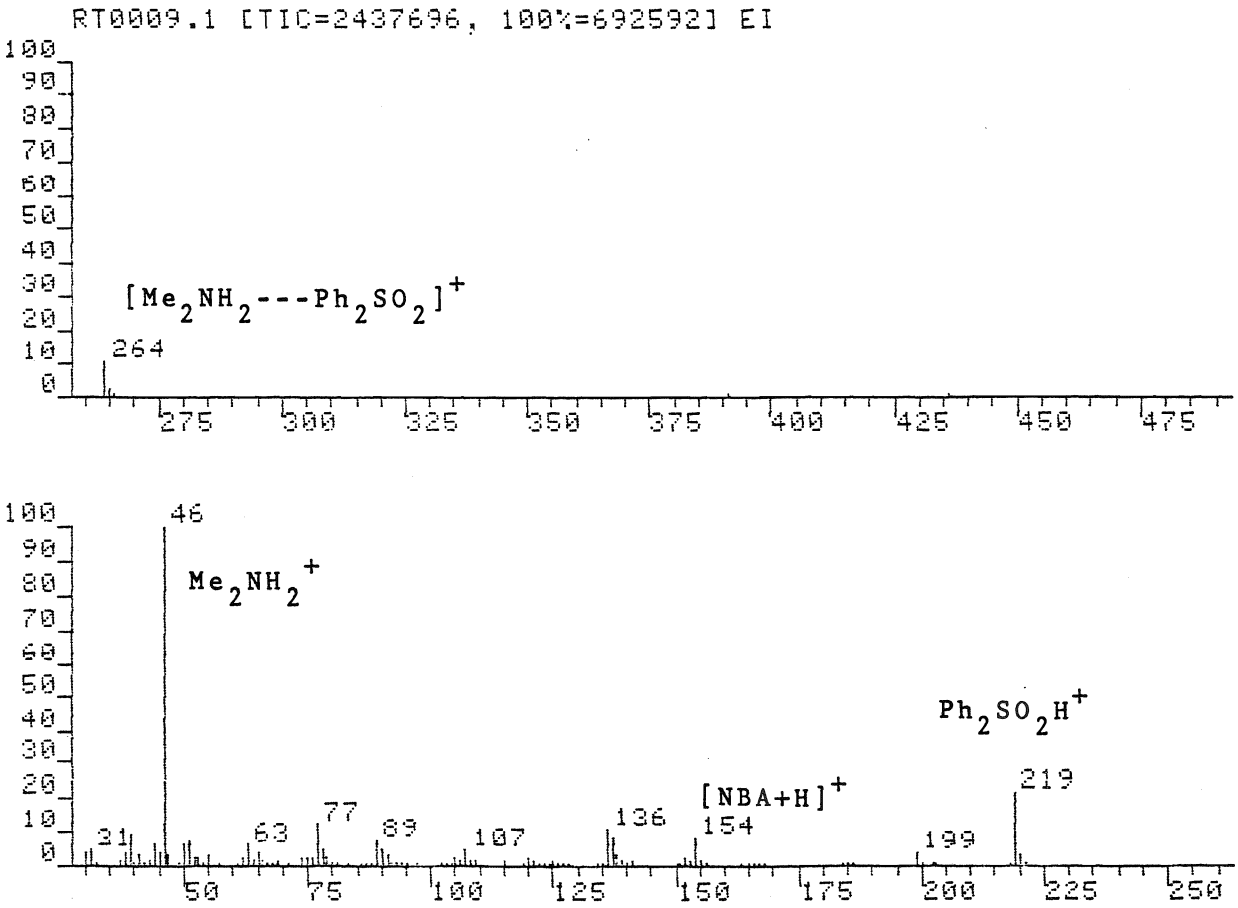


DPO:RT0009.MS
IONISATION: FAB
NO. PEAKS: 156
BASE/NREF INT: 692592./ 692592.
TIC: 2437696.
MASS RANGE: 30 - 485

| PEAK NO. | MEASURED MASS | NO. POINTS | ABSOLUTE INTENSITY | % INT. BASE | % INT. NREF | % TOT. ION |
|---|---|---|---|---|---|---|
| 10 | 265 | 35 | 14037. | 2.0 | 2.0 | 0.6 |
| 11 | 264 | 43 | 75056. | 10.8 | 10.8 | 3.1 |
| 19 | 220 | 35 | 17115. | 2.5 | 2.5 | 0.7 |
| 20 | 219 | 59 | 150524. | 21.7 | 21.7 | 6.2 |
| 28 | 199 | 43 | 28784. | 4.2 | 4.2 | 1.2 |
| 66 | 136 | 43 | 75672. | 10.9 | 10.9 | 3.1 |
| 118 | 77 | 43 | 82960. | 12.0 | 12.0 | 3.4 |
| 144 | 46 | 71 | 692592. | 100.0 | 100.0 | 28.4 |

FAB of $ph_2SO_2$-$Et_2NH_2^+Cl^-$ in NBA (0.6 M )

RT0005.1 [TIC=496240, 100%=196400] EI

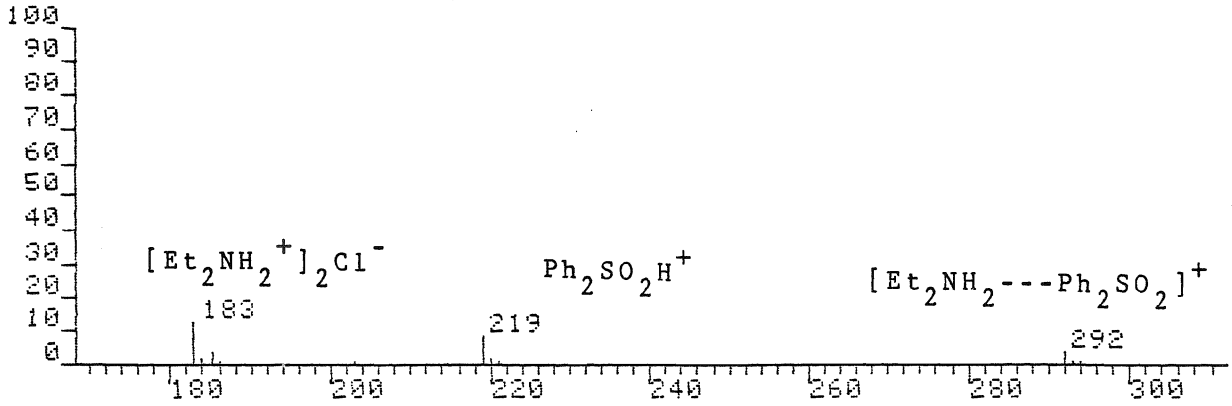


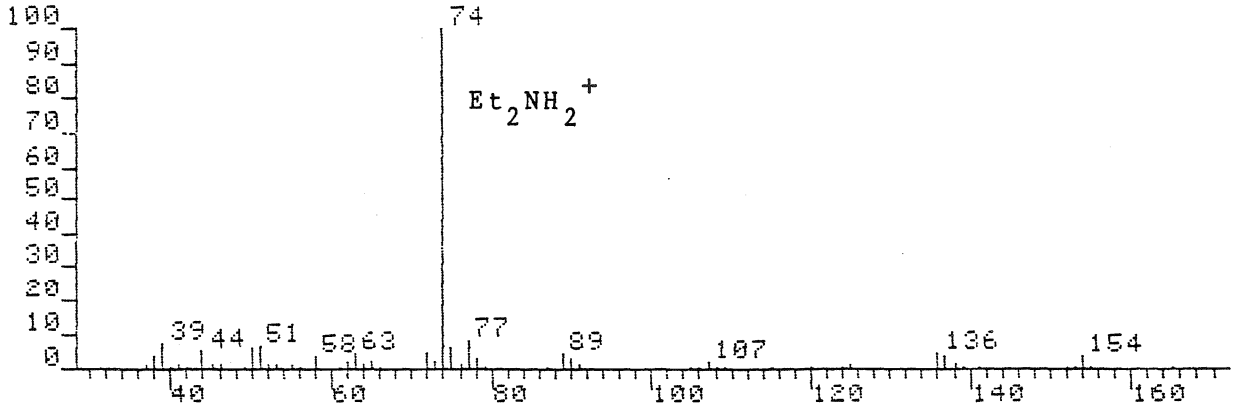


IONISATION: FAB
NO. PEAKS: 66
BASE/NREF INT: 196400./ 196400.
TIC: 496240.
MASS RANGE: 37 - 294

| PEAK NO. | MEASURED MASS | NO. POINTS | ABSOLUTE INTENSITY | % INT. BASE | % INT. NREF | % TOT. ION |
|---|---|---|---|---|---|---|
| 1 | 294 | 25 | 1160. | 0.6 | 0.6 | 0.2 |
| 2 | 293 | 25 | 1414. | 0.7 | 0.7 | 0.3 |
| 3 | 292 | 35 | 8206. | 4.2 | 4.2 | 1.7 |
| 6 | 219 | 35 | 16756. | 8.5 | 8.5 | 3.4 |
| 9 | 185 | 43 | 8294. | 4.2 | 4.2 | 1.7 |
| 10 | 184 | 35 | 2608. | 1.3 | 1.3 | 0.5 |
| 11 | 183 | 43 | 24540. | 12.5 | 12.5 | 4.9 |
| 40 | 74 | 71 | 196400. | 100.0 | 100.0 | 39.6 |

FAB of $ph_2SO_2$-i(pr)$_2NH_2^+I^-$ in NBA (0.6 M )

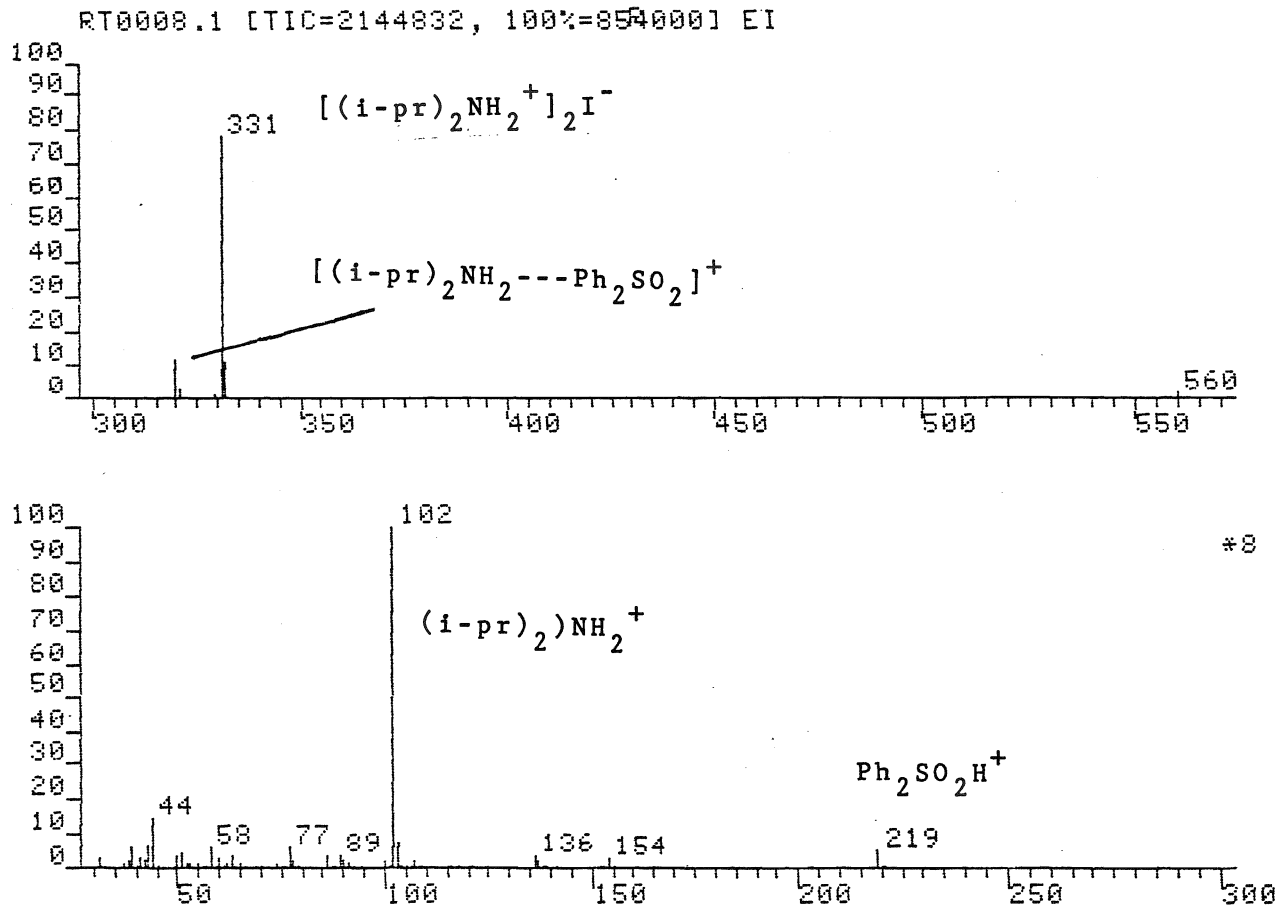


IONISATION: FAB
NO. PEAKS: 108
BASE/NREF INT: 854000./ 854000.
TIC: 2144832.
MASS RANGE: 31 - 560

| PEAK NO. | MEASURED MASS | NO. POINTS | ABSOLUTE INTENSITY | % INT. BASE | % INT. NREF | % TOT. ION |
|---|---|---|---|---|---|---|
| 2 | 332 | 35 | 11471. | 1.3 | 1.3 | 0.5 |
| 3 | 331 | 51 | 82976. | 9.7 | 9.7 | 3.9 |
| 6 | 320 | 35 | 12816. | 1.5 | 1.5 | 0.6 |
| 14 | 219 | 35 | 45556. | 5.3 | 5.3 | 2.1 |
| 23 | 154 | 35 | 22585. | 2.6 | 2.6 | 1.1 |
| 31 | 137 | 35 | 18785. | 2.2 | 2.2 | 0.9 |
| 32 | 136 | 35 | 30135. | 3.5 | 3.5 | 1.4 |
| 54 | 102 | 103 | 854000. | 100.0 | 100.0 | 39.8* |

FAB of $ph_2SO_2$-(imidazoleH)$^+I^-$ in NBA (0.6 M )

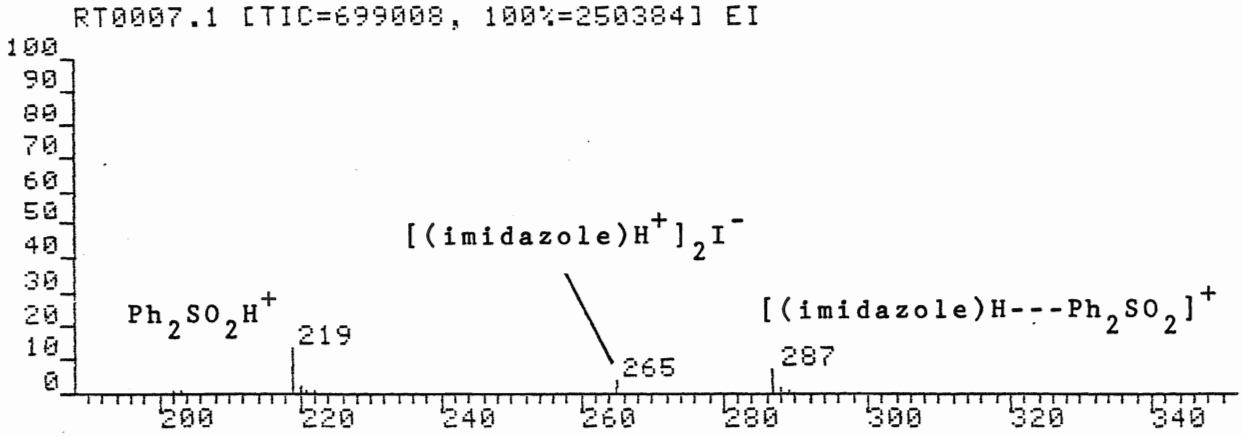


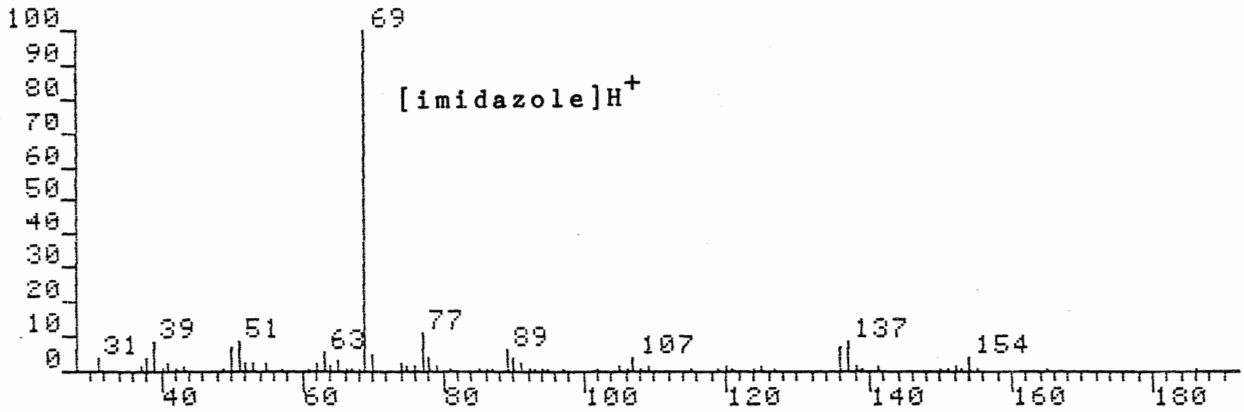


DRO:R10007.MS
IONISATION: EI
NO. PEAKS: 80
BASE/NREF INT: 250384./ 250384.
TIC: 699008.
MASS RANGE: 31 - 333

| PEAK NO. | MEASURED MASS | NO. POINTS | ABSOLUTE INTENSITY | % INT. BASE | % INT. NREF | % TOT. ION |
|---|---|---|---|---|---|---|
| 3 | 288 | 35 | 3360. | 1.3 | 1.3 | 0.5 |
| 4 | 287 | 35 | 18404. | 7.4 | 7.4 | 2.6 |
| 5 | 265 | 35 | 9002. | 3.6 | 3.6 | 1.3 |
| 9 | 219 | 43 | 32356. | 12.9 | 12.9 | 4.6 |
| 15 | 154 | 35 | 10643. | 4.3 | 4.3 | 1.5 |
| 23 | 137 | 43 | 21093. | 8.4 | 8.4 | 3.0 |
| 24 | 136 | 35 | 16667. | 6.7 | 6.7 | 2.4 |
| 52 | 77 | 43 | 27439. | 11.0 | 11.0 | 3.9 |
| 57 | 69 | 59 | 250384. | 100.0 | 100.0 | 35.8 |

FAB of $ph_2SO_2$-(pyridineH)$^+Br^-$ in NBA (0.6 M )